Discipline of Engineering and Energy

Various Approaches for Power Balancing in Grid-connected and Islanded Microgrids

Yuli Astriani

33234845

This thesis is presented for the Degree of

Master of Philosophy

of

Murdoch University

March 2020

Declaration

I declare that this thesis is my own account of my research and contains as its main content work which has not previously been submitted for a degree at any tertiary education institution.

Yuli Astriani

March 2020

Acknowledgment

I would like to express my deepest gratitude to my supervisors Dr. GM Shafiullah and Dr. Martin Anda. Thank you for the kind advice, support, and encouragement given to me throughout the course of my research work. I appreciate your time, your contribution of brilliant ideas, and your patience when teaching me how to prepare and write my research paper. Your feedback was always constructive and encouraging.

I wish to thank Bruna Pomella (B.A.Dip.Ed University of Melbourne) from http://scriboproofreading.com.au/ for proofreading and editing my thesis. She ensured that spelling, language, punctuation, syntax and grammar are correct, eliminated redundant words or phrases, and checked for clarity and fluency.

I sincerely thank my parents, sisters, brother, and nieces for their love, support, encouragement, prayers, and good wishes during my journey in completing my master's degree. Also, I thank Allah Swt. for His blessings.

I also thank my Head of Division, B2TKE in BPPT who gave me permission and encouragement to pursue my study for a Master's degree. I am grateful to my colleagues in B2TKE-BPPT who gave valuable feedback and motivation. Thanks to my "office friends" Sanggita, Shoeb, and Wayan who were always there to share and discuss the journey in pursuing our study. Thank you to all my friends in MUISA and KALAM for your help, caring, and sharing. I also thank the "angklung" team for many wonderful experiences.

Finally, I am grateful to the Ministry of Research and High Education of Republic Indonesia for giving me the opportunity to study abroad by providing the financial support through the Research and Innovation in Science and Technology Project (RISET-Pro) program.

Publications Arising from this Thesis

1. **Yuli Astriani**, G. Shafiullah, F. Shahnia,"Optimizing Demand Response and Determining Its Incentive in Microgrids", submitted to Applied Energy, ELSEVIER.
2. **Yuli Astriani**, G. Shafiullah, F. Shahnia, M. Anda"Determining a demand response incentive for microgrids", Proceedings in the 9th International Conference on Power and Energy Systems (ICPES), Perth, Australia, 2019.
3. **Yuli Astriani**, G. Shafiullah, F. Shahnia, "Optimising under-voltage load-shedding using genetic algorithm in microgrids", Proceedings in the 2nd International Conference on High Voltage Engineering and Power Systems (ICHVEPS), Bali, Indonesia, 2019.
4. **Yuli Astriani**, G. Shafiullah, F. Shahnia, "Demand response under renewable generation fluctuations considering customer discomfort", 2108 APWCE, pp. 253-258: IEEE.
5. **Yuli Astriani**, G. Shafiullah, F. Shahnia, and Riza, "Additional controls to enhance the active power management within islanded microgrids", *Energy Procedia,* ELSEVIER*,* vol. 158, pp. 2780-2786, 2019.
6. **Yuli Astriani**, G. Shafiullah, M. Anda, and H. Hilal, "Techno-economic evaluation of utilising a small-scale microgrid", *Energy Procedia,* ELSEVIER, vol. 158, pp. 3131-3137, 2019.

Abstract

One of the promising solutions to reduce power imbalance, an undesired impact of intermittent renewable energy sources, is to supply the loads by means of local distributed energy resources in the form of a microgrid. Microgrids offer several benefits such as reduction of line losses, increased system reliability, and maximum utilisation of local energy resources. A microgrid, during its islanded operation, is more susceptible to the frequency and voltage fluctuation caused by a sudden dispatch either from the generation or load. Therefore, additional control is required to manage either the output power from the generation side or the demand from the end-user side. Thus, appropriate and efficient control and monitoring systems need to be installed. However, the cost of such a system will reduce the rate of investment return on microgrid projects. This research has focused on developing various techniques to maintain the voltage and frequency within acceptable limits in microgrids, taking into account various influencing factors.

This study proposes an additional active power management technique through the use of inverters, that can maintain the microgrid's frequency when the generated power in the microgrid is much higher than its demand. Also, to facilitate the microgrid's transition from grid-connected to islanded mode, the inverters can be controlled with a soft starting ramp. Moreover, a control function employing a droop control method is proposed in order to reduce the output power of the renewable sources when the microgrid frequency is much higher than the nominal frequency.

On the other hand, when the demand is higher than the generated power, managing the demand under a demand response program is proposed as a means of maintaining the microgrid stability. This is an inexpensive solution which will not reduce the rate of investment return on the microgrid project. However, this requires the installation of appropriate enabling technologies at the utility and end-user sides. Moreover, the participation from demand response participants is influenced by the profit earned from engaging in the program. Therefore, in this research, the technical and economic benefits of demand response deployment are analysed in detail.

The execution of the demand response program through load-shifting, reducing the appliances' consumed power, and load-shedding causes customer discomfort. To minimise this

discomfort, in this thesis, suitable strategies are suggested for various groups of loads. Furthermore, each load profile contains information on its capacity, flexibility, and operating time. The proposed approach ensures that the loads with a larger capacity and flexibility are the most preferred ones to be controlled during demand response events so that customer discomfort and the number of affected loads can be minimised. Also, this study examines the load's economic value, power losses, emission factor, and cost of energy production to maximise the microgrid operator's profit as a result of deploying the demand response program.

Meanwhile, to encourage end-users' engagement in demand response programs, the microgrid operator should offer incentives to the customer as compensation for any incurred costs and discomfort felt. The given incentives should be such that both the microgrid operator and the end-user gain the maximum profit. Therefore, this study proposes an approach for calculating the level of incentives that should be given to the participants by comparing the differences between ongoing revenue and the cost of energy with and without demand response.

Table of Contents

List of Figures

List of Tables

List of Abbreviations

BES	Battery energy storage
BPPT	Agency for the assessment and research of technology, Indonesia
DER	Distributed energy resources
DG	Diesel generator
DLC	Direct load control
ESS	Energy storage system
IRR	Internal rate of return
LCOE	Levelised cost of energy
NDE	Non-delivered energy
NPV	Net present value
O&M	Operation and maintenance
PCC	Point of common coupling
PT. PLN	The Indonesian state-owned utility company
PV	Photovoltaic
RES	Renewable energy resources
SoC	State of charge

Chapter 1 Introduction

1.1 Background

Microgrids are referred to as localised electricity generation and distribution networks in which a high percentage of the energy is generated by renewable energy resource (RES)-based distributed energy resources (DERs). The deployment of microgrids is believed to provide both technical and economic benefits. Within a microgrid, the generators are located closer to the end-users; thus, the power loss in the network lines is reduced. Moreover, the microgrid can operate in either grid-connected or islanded modes, giving extra flexibility and improving the system's reliability and resiliency [1].

In the grid-connected mode, a microgrid is considered as a single controlled entity of its upstream grid. Hence, when a microgrid has excess power from its RES-based sources, it will act as a generating unit and injects the excess power to the upstream grid. Meanwhile, when the microgrid is facing power shortage, it resembles a load that absorbs power from the upstream grid to address its power deficiency. Therefore, it is expected that the balancing of power in a grid-connected microgrid can be achieved easily. A balanced state between generated and consumed power is a must either in any power system, including a microgrid, to maintain the frequency and voltage within the standard range of operation.

On the other hand, the power balancing of a microgrid during the islanded mode is a technical challenge that needs to be addressed carefully. This is more critical for microgrids with high RES-based sources because of the system's smaller inertia [2] and limited reserve capacity. Therefore, a sudden demand increase or generation loss can significantly affect microgrid stability.

A balance of supply and demand can be achieved by managing the amount of the power produced from the DERs or the power consumed by the loads. If the management on the generation side is applied, then the microgrid controller will send command signals to the

generation units to ramp up or ramp down their output power. On the other hand, demand-side management aims to decrease, increase, or shift the power consumed by the loads.

To ensure maximum benefits, a microgrid should be equipped with additional controllers. Various microgrid technologies and architectures have been reviewed in previous studies [3, 4]. The enabling technologies include local controllers and a central microgrid controller. The microgrid operator installs local controllers at each DER and controllable load to ensure stable performance. Voltage drops or short circuit faults must be detected locally so that the microgrid can immediately give a response, whether it be changing to the islanded mode if the problems come from the upstream grid, or isolating the faulty components within the microgrid. The microgrid's central controller has to supervise the microgrid to coordinate all of its DERs and load operations, and to exchange information with the upstream grid [5]. Fig. 1.1 shows a typical configuration of an ac microgrid. This microgrid network connects to the upstream grid through an interface point, known as the point of common coupling (PCC).

The costs related to establishing a microgrid project include the cost of DERs, microgrid controllers, the distribution network, information and communication infrastructure, metering components, as well as their installation and commissioning [6]. On the other hand, the value of a microgrid deployment depends on its projected rate of return on investment [7]. To obtain a positive net present value (NPV) of the microgrid return of investment, a microgrid may reduce its operational expenditure by minimising the cost of energy production. This is equal to maximising the utilisation of the embedded DERs or reducing its energy consumption. However, the microgrid's generated power may not be enough to supply all of the local demand. Moreover, if the main DERs in the microgrid are conventional power plants, such as diesel or gas-driven generators, maximising the power generated by the DERs will result in a higher cost of energy production. Therefore, effectively controlling the demand is one of the alternative solutions to ensure a balance between supply and demand while minimising the amount of energy imported from the upstream grid [8].

A demand-side management program aims to leverage the efficiency of energy consumption, and its implementation is expected to help the grid operator to achieve a balance between supply and demand [9, 10]. Demand-side management consists of two major tools: demand response and energy efficiency. Energy efficiency focuses on the long-term goals to

achieve energy sustainability, while demand response focuses on the short-term objectives of reducing peak load, valley filling and, finally balancing supply and demand.

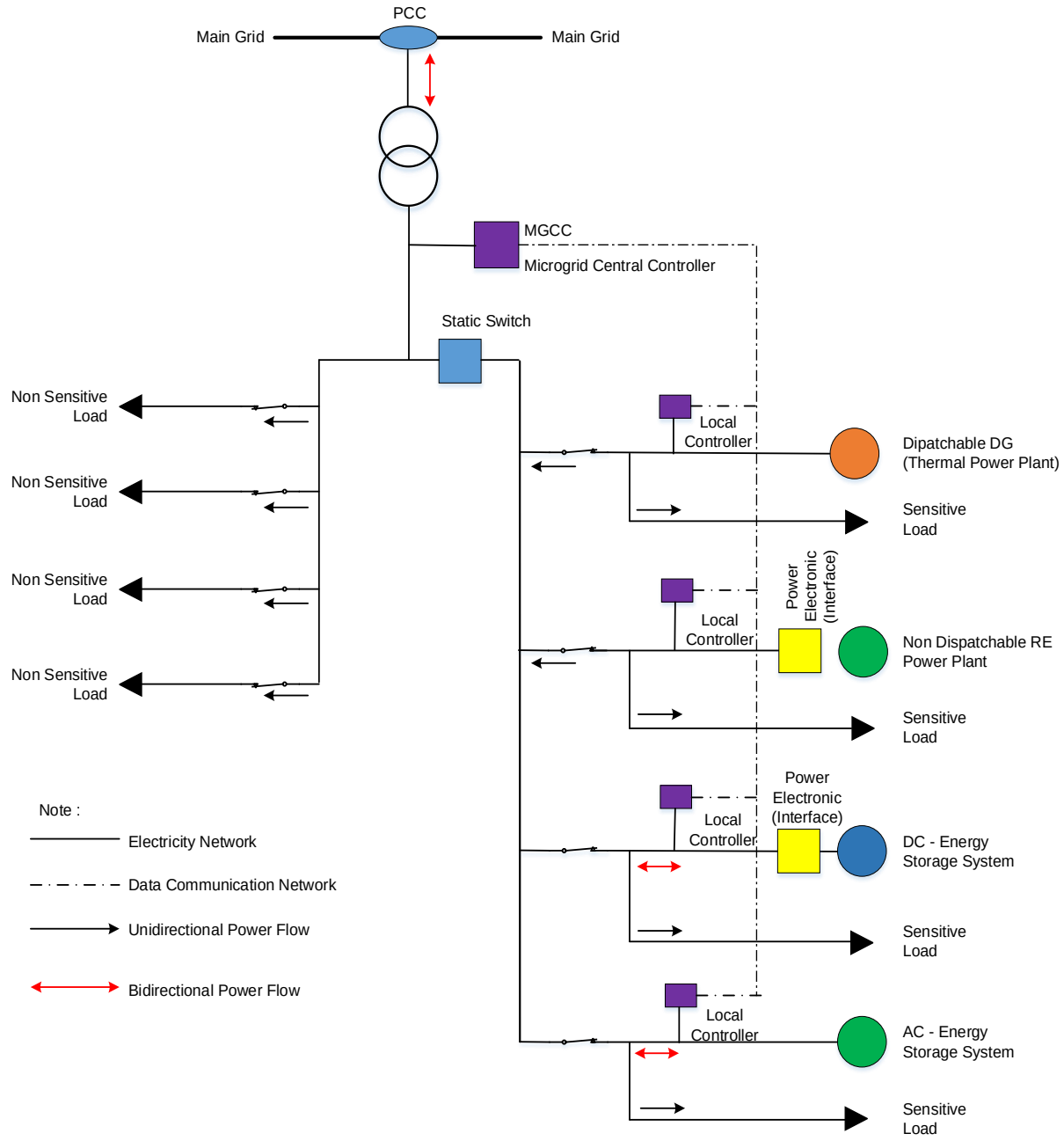

Figure 1.1 Typical configuration of an ac microgrid.

In this study, the adjusting of load consumption based on the changes of available power will be referred to as *demand response*. Thus, a demand response not only adjusts the amount of loads' consumed power but also manages their operation time to maintain the power balance [11, 12].

In the demand response program, the loads are classified into two types: critical and non-critical load. A critical load is defined as the load that needs uninterruptible supply, while a non-critical load may become the object of load-shedding, shaving, and scheduling. Moreover, the load dispatching method in a demand response has three classifications: manual, semi-automated, and fully-automated [13]. Manual demand response needs the customers or facility operators to be present to acknowledge the notification from the utility and then give a response by manually turning off or changing the setpoint of the switches or controllers. Therefore, upgrading into automated demand response is suggested to help customers systemise their participation in the demand response program. However, an automated demand response needs installation of additional components of information and communication technology infrastructure and modern control technology. Additional technologies either hardware or software are necessary for demand response enablement; this may include, dimmers for the lighting system, a thermostat for an air conditioning system, a dashboard interface, etc. It is reported in [14] that the use of technologies to enable demand response in conjunction with the time-of-used strategy resulted in a more significant reduction of peak demand. Fig. 1.2 shows an overview of the deployment of demand response in a microgrid.

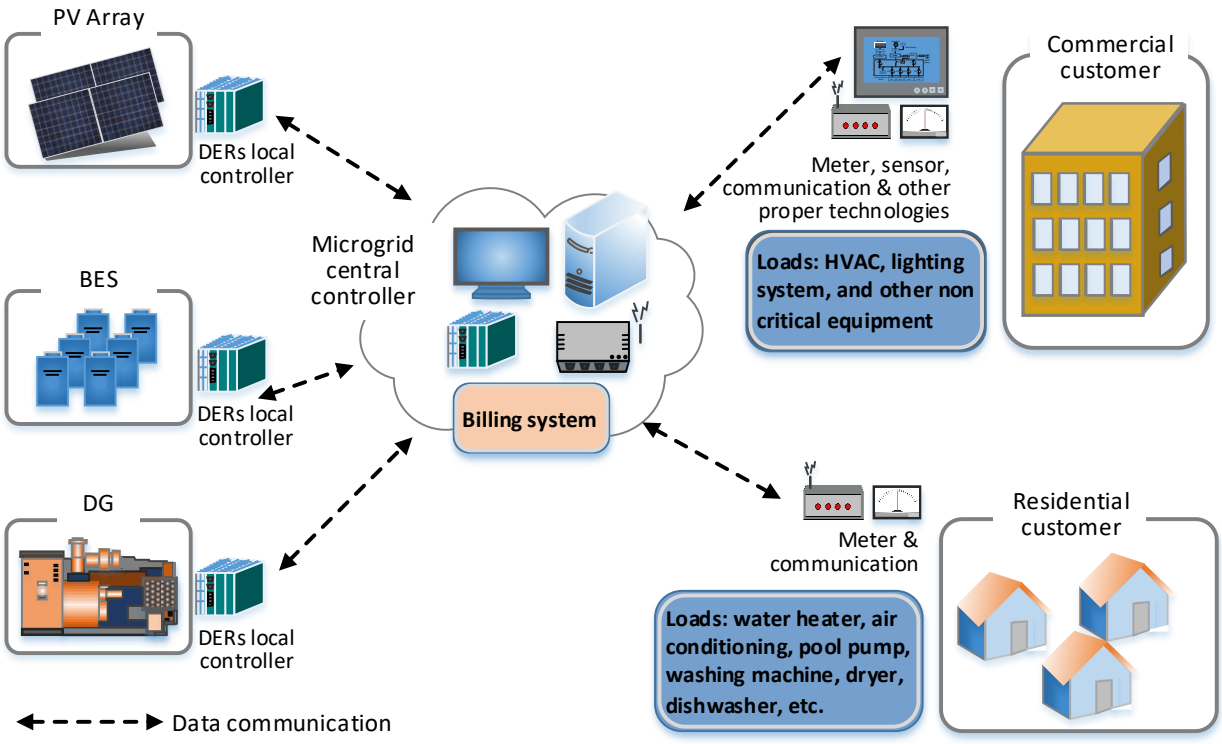

Figure 1.2 Overview of demand response deployment in a microgrid.

Nowadays, advanced technologies that enable a demand response program are available and have become more accessible; however, the investment cost incurred by both the utility and the participants discourages its adoption [15, 16]. On the other hand, as a microgrid is a small and localised power system, the implementation of demand response in a microgrid is expected to be easier and cheaper than its implementation in the broader grid. Moreover, most microgrids have a monitoring and control system. Thus, data communication infrastructure, metering, and system control may already have been partially installed in the microgrid.

As stated in [17, 18], the implementation of an effective demand response program is greatly affected by the customer's active participation. Varying electricity prices and the offering of incentives affect customers' energy consumption behaviour. However, the uncertainty of revenue return has made the customers reluctant to participate in the demand response program. Bill savings from a demand response program may not be enough to recover the initial investment costs and compensate the inconvenience to the participants who are required to constantly monitor the price changes and then execute the required demand response strategy [19]. Furthermore, [16] stated that opportunity and comfort loss-costs vary from one participant to another, although in many demand response programs, the incentive payments scheme is based on a fixed rate per kilowatt-hour. If the issues of financial benefit and inconvenience are not addressed, the participants may withdraw from the demand response program [20].

Therefore, in this thesis, we propose a demand response technique which takes customer discomfort into consideration and propose an approach for determining an appropriate demand response incentive. Applying the proposed methods, we conduct a techno-economic analysis of demand response implementation in a modelled microgrid. The demand response approach proposed in this thesis is intended to strike a balance between a microgrid's generated power and the consumed power in order to minimise the total amount of energy that needs to be imported from the upstream grid. The modelled microgrid's DERs consist of a diesel generator, photovoltaic (PV) system, and battery energy storage (BES); while the microgrid's end customers are individual households and commercial buildings. Moreover, in considering the effects of demand response on the customer discomfort, the loads are classified based on their priority and operating characteristics, and are weighted based on their capacity, flexibility, and economic value.

1.2 Aim and objectives

The main aim of this thesis is to propose suitable control techniques to manage the power balance in a microgrid. To this end, generation and demand-side control techniques have been chosen and studied as effective approaches. A techno-economic analysis is conducted to determine the effects of deploying such techniques in a microgrid project in term of RES fluctuation, customers discomfort, microgrid operator's profit and the project's payback period. To achieve this goal, specific objectives have been established:

- To develop additional generation side management in a real islanded microgrid following the fluctuation of its RES-based DERs.
- To develop demand response strategies for correcting any voltage deviation and prolonging the supply to the critical loads, and to formulate an optimisation method addressing the issues of customer discomfort and the microgrid operator's profits.
- To determine the incentives to be given to the demand response participants, taking into consideration the demand response payback period.

1.3 Significance of research

The deployment and integration of microgrids in distribution networks is an effective means of achieving reliable and resilient power grids. Thus, in this thesis, the focus is on various aspects of microgrid control to ensure a balance between the power generated by its DERs and the power consumed by its loads. The proposed techniques, when applied to a microgrid, will ensure that the microgrid's voltage and frequency are maintained within the acceptable range of operation, an essential factor for stabilising systems with significant variations in the output power of DERs.

1.4 Thesis structure

The remainder of the thesis is organised as follows:

Chapter 2 presents a comprehensive review of the importance of balancing supply in a microgrid, the technical and economic benefits of demand response deployment, the types of demand response programs, and the cost associated with demand response deployment.

Chapter 3 presents a techno-economic analysis of a small-scale microgrid. The analysis results show that a smart-small-scale microgrid is not economically feasible, one of the reasons being the cost of purchasing the advanced equipment and control technology.

Chapter 4 presents the effect of RESs intermittency on the frequency deviation within microgrids. In this chapter, a real microgrid test case is used to show the need for the proposed additional active power management to stabilise the microgrid frequency during its islanded operation.

Chapter 5 proposes a method to optimise demand response implementation in a microgrid. This chapter also presents two study cases of demand response deployment in a microgrid. First, a simple sequence demand-side management to prolong the supply to the real microgrid test case' critical loads is described. Second, a load adjustment method using active power-voltage droop control is proposed and evaluated.

Chapter 6 proposes a method to determine the incentive that should be given to the demand response participants by the microgrid owner. The chapter discusses the procedure for deriving the demand response profit from the differences in microgrid ongoing costs and revenues as well as the carbon tax reduction.

Chapter 7 summarises the key findings of the thesis and also offers suggestions for future research direction in this area of interest.

Chapter 2 Literature Review

In this chapter, the relevant literature is reviewed in order to evaluate the previous researches on managing the balance between the output power of the microgrid's DERs and its demand. The method of controlling the DERs' output power such as curtailment, droop control, and BES utilisation are examined. Meanwhile, the existing literature on demand response deployment is reviewed with particular focus on the importance of load classification, the currently available types of demand response, as well as the challenges, benefits, and the costs of deploying demand response.

2.1 Distributed Energy Resources (DERs) Management

One of the methods used to minimise energy cost production and CO_2 emission in a microgrid is to increase the percentage of RES-based DER penetration. However, without proper control of its dispatch management, this action may result in an unstable microgrid. The maximised deployment of RES-based DERs can cause a lack of spinning reserve in which is crucial in a microgrid as it used to maintain the voltage and frequency of microgrid by balancing supply and demand.

There are two types of reserve provision management in microgrid: grid-forming reserve and grid-following reserve. The grid-forming reserve determines the voltage magnitude and frequency of microgrid during its islanded mode. Generator units included in the grid-forming category are the dispatch-able power plants such as diesel generator and inverter-based BES. Grid-forming units often act as the master device in the "master-slave" control mode. If the grid-forming reserve is no longer sufficient to support the demand changes in active-reactive power control (grid supporting units), then microgrids must use their grid-following reserve. The grid-following reserve includes a microturbine and a fuel cell. Meanwhile, other uncontrollable or partially controllable micro power sources such as PVs and wind turbines are used to deliver their maximum power (grid feeding units).

There are various methods of controlling DERs in the power grid, described below.

2.1.1 Hard curtailment

Hard curtailment means reducing the amount of generated power by totally turning off one or more DERs. This method is executed when a power grid has surplus power or is facing transmission congestion [21, 22]. Inverter-based DERs which do not have additional control for ramping down their output power are more likely to encounter this curtailment method. However, an unintended hard curtailment might occur when excess power causing microgrid frequency exceeds the inverter operating frequency [23]. Moreover, curtailing RES-based DERs is contrary to the purpose of reducing CO_2 emission.

2.1.2 Droop control

Control methods such as maximum power point tracking and pulse width modulation are used to maximise the output power from the RES-converter-based DERs. However, the most widely-used control method for load sharing between generation units to maintain a grid's frequency is droop control. This method is commonly used to adjust the amount of fuel that goes into the governor of the dispatch-able unit [24]. Currently, an imitating droop control method has also been implemented in the converter of RES-based DERs [25-27].

The relationship between active power and frequency and the correlation between reactive power and voltage can be determined as [25]

$$f = f_0 + k_P(P - P_0) \tag{2.1}$$

$$V = V_0 + k_Q(Q - Q_0) \tag{2.2}$$

where f, V, P, Q are respectively the current value of frequency, voltage, active power, and reactive power; while subscript "$_0$" denote the previous correlated value; and k_P and k_Q respectively denote the active and reactive power droop constants. Fig. 2.1 is a diagram of the droop control slope. The slope depends on the droop constant. It shows the effect of the changes in active power on the critical frequency and reactive power on the voltage.

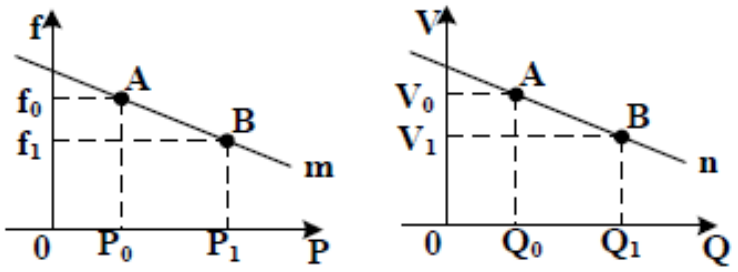

Figure 2.1 Schematic diagram of droop control.

The conventional droop control (*P-f* and *Q-V* droop) method will perform better with high-voltage transmission lines because the line impedance is mainly inductive so that in the conventional droop control formula, resistance is considered as zero. However, most of the microgrids operate at low or middle voltage where its line resistance to reactance ratio is quite high. Therefore some modified droop control such as P-V and Q-f droop control, and adaptive transient droop have been proposed [28, 29].

2.1.3 Energy storage utilisation

An energy storage system (ESS) is optional but may be required to balance the generation and the consumption of electricity in microgrids [30]. During peak load, an ESS will discharge its stored energy to supply the demand. With the current technologies that have enabled fast discharge, an ESS is suitable to be used as a compensator of RESs fluctuation. On the other hand, when RESs' electricity production is abundant and higher than the demand, the ESS in a microgrid can absorb and store the energy to be utilised later when needed. Mostly, the charging period of ESSs can be halted. Thus, ESSs can be considered as interruptible loads. Energy storage systems may consist of batteries bank, flywheel, compressed air, pumped storage, batteries from electric vehicle, and other energy storage technologies [31].

The sizing optimisation of ESS determines the effectiveness of its utilisation for power balancing in a microgrid. If the ESS capacity is too large, then the installation cost will not be economically feasible; if ESS capacity is too small, it will be challenging to run a stable microgrid. The optimum size of ESS depends on rated power capacity, initial cost, and the operating and maintenance cost [32, 33]. Battery Energy Storage (BES) is the most widely-used ESS. However, because it is expensive, batteries are deployed only in a small portion of the microgrid.

2.1.4 Other

Some studies have proposed algorithms such as predictive control [34, 35], stochastic [36, 37], and artificial intelligence algorithm [38, 39].

2.2 Demand Response

In a microgrid, managing its loads' power usage may inevitable, either to minimise the cost of energy production or to maintain microgrid stability. For example, in a microgrid that consists of a solar PV system which usually has surplus power during daytime, it is recommended that some of its load operation time be shifted from night to daytime. There are three techniques available for demand-side management: peak shaving, load-shifting, and valley filling. To be able to implement these methods, microgrids often divide their loads into sensitive, non-sensitive, and controllable loads [40, 41].

During peak load, the microgrid controller may shed the non-sensitive loads, thereby clipping the peak load. Meanwhile, the operation time of some loads may be shifted from their ordinary operation time depending on the available power. When the generated power is much higher than the demand, the shifted loads can fill in the valley [42]. Under the load-shifting program, the utility operator should consider whether it is cost-effective in terms of the cost of energy production, and ensure that another power deficiency does not occur after its execution. Moreover, the deferring of a load may affect the load performance or causing customer discomfort. Therefore, load classification is important so that the implemented demand management algorithm can contribute to maintaining optimal grid stability, while simultaneously considering the customers' convenience and the financial aspect.

2.2.1 Load Classification

The previous studies have suggested that loads that have the same profile should be put in the same group to determine the best demand response scheme for each group. In [43], the loads are classified based on their priority; for example, loads that provide public services will have higher priority. The common operating time profiles of loads were introduced in [44]. The demand response methods such as shifting, shedding and dimming are presented in [40, 45].

The allocation of a load to a particular group often differs from one company/institution to another. For example, the computer and lighting system may be the priority loads in an office building, while air conditioning may be the second priority. On the other hand, air conditioning systems may be the first priority in a test laboratory.

In this thesis, the loads are classified as follows:

- Critical load: Critical loads are the highest priority loads that serve crucial infrastructures such as hospitals, data centres, and other public service areas. Critical loads need uninterrupted supply, and their time of operation cannot be shifted.
- Controllable load: Controllable loads are loads that we can control electrically by varying the amount of power usage to operate the loads, such as dimming the lighting systems, adjusting the temperature for air conditioning units, and regulating the speed of induction or synchronous motor using variable-frequency devices, etc. A shimmy load is mentioned in [46]. This is a load that can give a fast response in increasing and decreasing the amount of its consumed power through a dispatch signal to ensure a real-time balance against the fluctuation from the generation side. This load supports the voltage and frequency control management; thus, it must react under a 5-minute or 4-second dispatch signal.
- Shiftable load: Shiftable loads are those whose operation time is flexible so that it can be delayed, or can be scheduled at any time within a time frame range but cannot be interrupted when these loads are run. As an example, the stages in washing machines are often programmed as sequential steps. Thus, it is not possible to interrupt its operation.
- Interruptible load: Interruptible loads are loads that can be interrupted during their operation. For example, the charging and discharging process of an ESS can be interrupted.

2.2.2 Type of Demand Response

Besides the stability issue, demand response implementations are often triggered by economic reasons such as price-based and incentive-based demand response. Therefore, the utilities must provide their customer with information on the electricity price. With this information, the utility tries to encourage its customers to reduce their electronic appliance

usage during higher electricity price or shift to a time when the electricity price is lower. Hence, demand response will reduce the customers' electricity bill.

There are two types of demand response program as mentioned in [47-50]. These are described below.

2.2.2.1 Load Response

In this program, to regulate a power system frequency, the utility operator will instigate the load control, primarily for load reduction. By participating in the demand response program, customers will receive an incentive [49, 50].

- Direct load control (DLC)

  In the DLC program, the utility will directly control (ON/OFF) the customer's load. This program usually applied to residential customers or small commercial building to control some appliances that will not affect customer activity if the appliances, such as an electric water heater and air conditioner, are turned off for a limited period [47, 48].

- Curtailable load

  This program is applied to industrial and large commercial building customers that possibly turn off some of their equipment for a specified time. The utility will send a curtailment request to the customer prior to load reduction. The notification may be given minutes, hours, or even a day ahead. The utility may directly control the loads, or the participants can perform the load adjustment themselves depending on the agreement between the utility and the operator [47,49].

- Interruptible load

  This program catered to the large industrial or commercial building customers that have backup power to supply some or even all of their load. The contract agreement between utility and customer include penalties if there is any non-performance. The notification should be given by considering the time required by the affected customers to prepare their backup power [47, 48].

- Scheduled load

  The utility and the customers pre-determine the scheduling. This program is inflexible because of the (usually monthly) scheduling agreement; therefore, if at a particular time,

the utility needs an urgent load reduction, its cannot ask the customer to reduce their power usage [47, 49].

2.2.2.2 Price Response

Price-based demand response is a voluntary action by customers who are prompted to adjust their energy usage for economic reasons. This program can be implemented when the already-established electricity market is liberalised, enabling the variation in electricity tariffs. The utility has to provide information on electricity pricing, such as the real-time, hourly, or time-of-use rate [49, 50].

- Real-time pricing

  The implementation of this program requires an advanced metering infrastructure that allows a customer in observe electricity prices in real-time, and support the energy management system that includes smart meter, billing scheme, price forecasting (usually on an hourly basis - a day ahead), etc. [47, 49].

- Time-of-use rate

  In this demand response program, electricity price is differentiated into peak, off-peak, intermediate, weekdays, weekend tariff, etc. However, the pricing rate and the operating time is fixed for each time frame so that customers know in advance when the price is going to be higher or lower. Therefore, after ascertaining the rate, customers tend to shift their power usage from the higher price time to the lower price time. Some smart meters have a feature that automatically calculates the electricity bill based on time-of-use rate [47, 49].

- Critical peak-pricing

  During a peak period, the load demand may reach a critical level. Therefore, the utility needs to operate all the generation units, including the power plants which have high production costs, to provide the critical peak demand. As a result, the utility will charge a higher-than-standard rate. The day and the exact times of the critical demand event may be unpredictable, but based on real-time load profile, the utility will know whether the critical peak load will occur. One hour or more before the event, the utility must inform the customers of the starting time and duration of the event [47, 49].

2.2.3 Challenges on the demand response Implementation

Many countries have deployed demand response programs, such as the United States, Singapore, China, Brazil, and most European countries. However, not all the planned demand response programs have successfully resulted in optimal benefits. These experiences have enabled researchers to determine the barriers to demand response deployment. Most of the studies that reviewed the demand response challenges have identified three significant types of challenges: technological, regulatory framework, and customers themselves [16, 20, 51, 52].

As mentioned, the cost of the demand response enabling technology and the uncertainty of the customers' demand response profit has made the customers reluctant to participate in this scheme; thus, it would be difficult to expect customers to participate actively. Moreover, the lack of an operational standard, the issue of meter privacy and risk of cybersecurity attack have also discouraged the adoption of a demand response program [53, 54]. In addition to the cost of the system-enabling technologies, the utility also needs to pay for customer education, the development of demand response strategies, and the compensation costs for customers' inconvenience comfort reduction.

The lack of market experiences and of a regulatory framework for demand response scheme will lead to an unsuitable demand response mechanism. For example, [20] stated that a smart meter is one of the most crucial devices in a demand response program. However, due to utility's operator lack of experiences, the demand response implementation is unsuccessful. For example, because Brazil had no smart meter rollout, the Tariff Flags and White Tariff scheme implementation did not produce optimal benefits [51].

As mentioned above, in the load response (incentive) demand response program, the utility sends a request to instigate load reduction one hour or more before the execution; some scheme requires a day ahead notification. This scheme is reducing the flexibility of demand response in maintaining grid reliability and participating in the power market. Furthermore, many demand response schemes require the participants to be able to reduce a specific amount of their loads, such as 1 MW or more in a demand bidding program [12]. Therefore, research and innovation are needed to formulate appropriate policies and establish an effective market framework. For example, for residential customers who were negligible before [55] because of

their small capacity and flexibility, nowadays the demand response aggregator allows their untapped potential to be utilised.

Other barriers are related to tariff elasticity, structure, and the ease with which participants can obtain real-time electricity pricing. For example, the tariff structure in the UK is more favourable than in Denmark for demand response. Around 70% of the electricity tariff's component in the UK comes from the energy cost both for the residential and industrial customers. However, in Denmark, the share of energy costs in the electricity price component is only around 30% for residential customers and about 50% for industrial customers [56].

A demand response program is usually executed according to the predicted and actual amount of the generated power and demand; therefore, it is crucial to perform load profiling to define the baseline when choosing a suitable demand response strategy [55, 57] and its incentives [58, 59]. The customers' energy usage patterns change over time; therefore, it is not easy to determine an accurate baseline. Achieving optimal load reduction is also difficult because, naturally, customers who are accustomed to operating their appliances during non-peak load period are more likely to join a demand response program compared to those customers who frequently consume electrical energy during peak periods. Moreover, a gaming possibility that exists in the bidding program adds further uncertainty to baseline calculation.

2.2.3 Technical Benefits of demand response implementation

Besides providing the benefit of supply and demand balancing, the implementation of demand response also produces other technical benefits in the grid operation as explained below.

2.2.3.1 Frequency and voltage regulation

Grid frequency and voltage deviate from their nominal value when the capacity of supply and demand is unbalanced. If the deviation exceeds the allowed range of operation, it may threaten the grid's reliability. When a grid is facing under-frequency or under-voltage, this indicates that the grid is encountering power shortage. On the other hand, over frequency and voltage occurs when the demand is lower than the generated power. During this event, with the

demand response program, the utility may reduce the total demand by disconnecting some of the shedable loads or shifting the shiftable loads to the off-peak period hours. In [60], it is shown that the utilisation of demand response, combined with an energy storage system, can counter the intermittent effect of RES on frequency fluctuation. Moreover, [61] describes the potential of autonomous demand response for primary frequency control. It is indicated in [62] that, with the demand flexibility, the DERs curtailment can be reduced for voltage control in the medium voltage distribution. Also, the utilisation of residential demand response together with on-load tap changers can regulate voltage in an unbalance low-voltage grid [63].

2.2.3.2 Ancillary power

As stated in [64], a utility needs to provide a predefined capacity to be reserved for ensuring its network reliability, such as frequency control, network support and control, and system restart. Ancillary power should be available throughout the whole year. Because the changing of load consumption gives a faster response than ramping up conventional power plants, demand response is more powerful as a means of providing ancillary power during unforeseen or emergency events [65]. The potential of demand response program to provide ancillary power by controlling the controllable and deferrable loads are discussed in [66]. Meanwhile, [67] explained the utilisation of residential loads and electric vehicles in providing ancillary power.

2.2.3.3 Contingency mitigation

Contingency occurs when one or more components within the grid such as a generator, transmission line, or transformer fail so that power flows in the grid lead to an overload situation or exceed other operational limits such as thermal limit, voltage, etc. To recover from this overload, the utility may utilise the demand response program to curtail the loads. Ref. [68] simulates the flexibility of thermostatically-controlled loads to be used as contingency reserve provision. Meanwhile, an optimisation approach curtailing the loads and transferring them to the adjacent substation during contingency is proposed in [69].

2.2.3.4 Load shaping

Knowing the load pattern or being able to forecast the capacity of the next demand is crucial in helping the utilities to manage the dispatching schedule of their generation units. With a demand response program, either the DLC or price-based demand response, a utility will have more control over shaping the loads following the available generation or minimising the cost of energy production. Refs. [70, 71] have presented a grid's load shaping using electric vehicles. Meanwhile, [72] proposed a new approach to load shaping by utilising energy storage combined with dynamic pricing. Also, [73] found that scheduling the consumed energy of the household loads can successfully leverage the ratio between peak and peak-off period.

2.2.3.5 Black-start smoothing

Once a power grid encounters a total or partial blackout, the grid needs to again turn on the affected generation units. Mostly, utilities use a small diesel generator as the line charging for starting up the big-central power plant. During blackout recovery, a huge surge of current may occur, especially if the loads consist of a lot of inductive loads. Therefore, some of the loads need to be released at the start of the recovery process. The importance of load management after a blackout in terms of the restoration time is presented in [74]. It is also concluded in [75] that the previously captured data which contain the historical generation and load profile are important to speed up the grid restoration.

2.2.4 Economic benefits of demand response implementation

The benefits of a demand response program go directly to the participants; other customers who do not participate in the demand response program will also acquire indirect benefits from a demand response program [12]. In [76], the benefits of demand response implementation in a power system are classified into four main categories: participant, market-wide, reliability, and market performance benefits.

The varying electricity prices and the offering incentives are two factors that affect customers' energy consumption behaviour. Customers tend to reduce their load when the electricity tariff is high. Therefore, demand response participants will save on the electricity bill

or receive incentive payments. Also, the application of load-shedding, shifting, and valley filling will improve grid reliability, thereby avoiding further forced outage and saving customers from financial loss.

Curtailing of the load during peak periods will also flatten the load shape of the overall market [77]; this means that utilities can avoid or delay the need to build additional high-cost power plants to be utilised during peak periods. Moreover, demand response will create a more price-competitive electricity market and encourage the utilisation and innovation of smart technologies in the power system. As a demand response program leads to lower wholesale market prices, all customers will save on their electricity bill.

The NERA report for the Ministerial Council on Energy Smart Meter Working Group [78] has shown that one of the benefits of the smart meter rollout is the enablement of the demand response program. [79] discussed the installation of the advanced metering infrastructure in a microgrid which has enabled the implementation of price-response demand response program by providing the price changes information. The study shows that adjusting load consumptions based on market pricing led to higher cost savings for the flexible microgrid customer. Moreover, in the broader grid, a microgrid is considered as a single entity so that the benefits of demand response in a microgrid can be easily quantified mainly from the ratio of purchased energy before and after implementing the demand response program which can be calculated from the smart meter measurements.

In the study conducted by [80], several houses with their appliances (consumers) and houses with PV system (prosumers) are coordinated through a central controller to incorporate a demand response program. These aggregated houses were considered as a flexible entity (microgrid). In this paper, the modelled microgrid consists of real data from 201 households in Austin. This microgrid can buy and sell energy from the upstream grid. It implements the demand response program based on a mixed-integer linear programming algorithm. The proposed model shows that by incorporating the demand response program, the microgrid can reduce energy costs by 6.8%.

In [81], a stochastic model is presented to forecast load demand and market price based on a time-of-use tariff to minimise the cost of energy in a microgrid. The DERs in the proposed model comprise wind turbine, PV system, fuel cell, and diesel generator. The main objective of the proposed method is to optimise the scheduling DERs to meet forecasted demand while

reducing cost. The study result shows that the total cost of energy production can be decreased by increasing the amount of energy generated by the clean and low-cost DERs, and selling the surplus power to the upstream grid. In addition, system reliability and customer satisfaction increase load-shedding is avoided.

More comprehensive benefits that may arise from demand response implementation in power system are presented in [14, 82, 83]. The papers have reviewed eight demand response benefits and distinguished which benefits can be quantified as listed in Table 2.1. This table shows that only the benefits of demand response to the interconnecting DERs cannot be quantified.

Table 2.1 Demand response benefits [14, 56, 82, 83].

Type of benefits	**Quantification**
Because the total energy demand is reduced, the utility's energy production costs are decreased. Thus, the utility's customers will benefit from the reduction of their electricity bill.	Yes
Benefits from shift peak demand strategy: during the peak period, to fulfil the demand, a utility needs to operate a high-cost peaking power plant; therefore, shifting some of the load during peak demand to the non-peak period results in a short-run marginal cost saving.	Yes
Benefits in terms of delaying/avoiding investment in a new plant by using demand response to reduce or shift the peak demand or respond to emergencies.	Yes
Benefits of using demand response in providing reserve power by curtailing or postponing some of the loads for emergencies/unforeseen events, for example, avoiding overload during the black-start process after a blackout.	Partial
Benefits of demand response combine with ESS to mitigate the effect of RESs fluctuation resulting in the saving of fuel cost, reducing CO_2 emission, providing standby reserve, and avoiding RES curtailment.	Yes
Benefits from balancing the system by interconnecting the DERs.	No
Benefits of congestion reduction in the transmission line resulting in delaying/avoiding investment to expand or build new lines and avoiding transmission network re-enforcement.	Yes
Benefits from using demand response to reduce or shift peak demand improving distribution network efficiency and reduce losses by, for example, relieving voltage constraint and congestion in the distribution system.	Yes

2.2.5 Cost of demand response implementation

The execution of the demand response program is done by connecting, disconnecting, interrupting, shifting, or controlling the loads. The load dispatching methods applied in demand response scheme are classified as: manual, semi-automated, and fully-automated [84]. The manual demand response needs the customers or facility operators to be present to acknowledge the notification from the utility and then respond by manually turning off or changing the set point for the switches or controllers. Therefore, it is suggested that customers upgrade to automated demand response to institutionalise their demand response program.

Previous studies have shown that more savings can be had from the automated demand response as the decision to shift or shed customer loads would not be dependent on the customer's preference but would be determined by a preprogrammed algorithm. The demand response algorithm is intended to exploit loads' flexibility, either to minimise energy production or to maintain grid stability. However, automated demand response may violate customers' comfort level; therefore, customer preferences in terms of how they will control their energy consumption need to be pre-determined. An application of automated residential demand response was simulated by [85, 86], and showed that the automated demand response could reduce customers' electricity bill without compromising customer comfort.

2.2.5.1 Enabling technologies of demand response implementations

An automated demand response requires the installation of an additional modern control and data communication infrastructure because, as mentioned in [87], smart grid and demand response are intrinsically linked. The enabling technologies include smart metering, sensing, control, and data communication infrastructure, which need to be installed at both the utility and the end-user side. The utility deploys the communication network to retrieve data from the metering device, send billing information to the customer, or send a request signal to inform the customer prior to the execution of a demand response event. Data exchange between devices or between the end-user and the utility require different bandwidth, latency, and security depending on application requirements. A comprehensive review of the requirement of the data communication network for the major smart grid application that includes a demand response feature, meter reading, home and building automatic network are presented in [88].

Meanwhile, for the end-user, the need for enabling technologies varies based on the automated level of the demand response program they want to implement. For example, a fully automated demand response program for the residential customers will need advanced software and hardware for its control mechanism, and customers will need to change their conventional load to a smart load. Lawrence Berkeley National Laboratory has assessed the enabling technologies that are needed by the end-user for implementing demand response program as listed in Table 2.2. The listed enabling technologies make the load dispatch-able, so that shed, shift and shimmy services become applicable.

Table 2.2 End-user enabling technologies for demand response program [46].

Sector	End-Use	Enabling Technology Summary
Commercial and Residential	Battery-electric & plug-in hybrid vehicles	Automated demand response
All	Behind-the-meter batteries	Automated demand response
Residential	Air conditioning	DLC, programmable communicating thermostat
	Electric water heater	DLC or Automated demand response
	Pool pumps	DLC
Commercial	HVAC	Depending on site size: energy management system, automated demand response, DLC, and programmable communicating thermostat
	Lighting	A range of luminaire, zonal & standard control options
	Electric water heater	Automated demand response
	Refrigerated warehouse	Automated demand response
Industrial	Process & large facilities	Automated load-shedding & process interruption
	Agricultural pumping	Base switch & automated demand response
	Wastewater treatment	Automated demand response

2.2.5.2 Cost of enabling technologies

As mentioned above, the incurring of additional costs for the purchase of enabling technologies is one of the hindrances to the adoption of demand response program. Moreover, monthly bill reduction might not be sufficient enough to compensate for the costs of additional required equipment if only a small portion of the customer's loads can be listed in the demand response program [19]. Therefore, to encourage customers to participate in a demand response program, it is necessary to educate them. The utility has to explain the system and provide to the customer an estimation of the total costs and benefits of demand response implementation. The microgrid's operator should perform a comparative study of the demand response deployment costs and the incentive or bill reduction given to e customers who can then estimate their return on investment.

The costs of demand response program implementation have been classified in [12, 14, 76] into initial costs and running costs that are incurred by both the participants and the demand response implementor. Some of the costs, such as the investment in the enabling technology, can be easily quantified. However, other costs are difficult or impossible to quantify, such as the costs of reducing the customer's comfort level or the loss of a business opportunity. These demand response costs are listed in Table 2.3.

There are three types of demand response costs that can be quantified: initial investment, fixed-ongoing, and variable costs. When establishing a demand response program, the utility or demand response aggregator needs to invest in the development of a demand response strategy and the installation of measurement, control, software, and data communication technologies. The fixed and variable costs are those incurred when the demand response program is running. Fixed costs are all the costs, aside from the capital investment, associated with the operation and maintenance of the demand response program. As an example, the cost of third-party data communication services is considered to be a fixed cost. On the other hand, variable costs are those resulting from the reduction of loads, where revenue is lost because less electricity has been sold to the customers [89]. A modelled microgrid that incorporates a demand response program that takes into account the costs of load-shedding, has been presented in [90]. Another cost that may occur as a result of enabling demand response strategy is the cost of ESS utilisation [91, 92], which involves ESSs purchasing and wear costs.

Table 2.3 The incurred demand response costs [14].

Type of costs		**Cost**	**Quantification**
Participant costs	Initial costs	Procuring the enabling technology	Yes
		Developing a demand response program strategy	No
	Event-specific costs	Comfort reduction/inconvenience costs	No
		Reduced amenity/business opportunity losses	No
		Rescheduling costs (e.g., overtime pay)	No
		Large industrial or commercial customers that engaged in the interruptible load program need to provide their onsite generator; therefore, they need to spend fund for generator fuel and its operation and maintenance costs	No
System costs	Initial costs	Upgrading/retrofitting metering and communication system	Yes
		Upgrading the billing system, purchasing the software license and developing the program, and procuring additional equipment related to demand response program	Partial
		Customer education	Partial
	Ongoing program costs	Program administration/management	Partial
		Marketing to recruit customer in engaging demand response program	Partial
		Payments to the participating customers	Partial
		Program evaluation	No
		Metering & data communication infrastructure	Yes

2.3 Discussion

It can be concluded that one of the solutions that could improve the reliability of the current traditional grid and contribute to the reduction of CO_2 emission is the deployment of any distributed power system that uses renewable energy sources using microgrid concepts. However, the appropriate technologies needed to incorporate a control and monitoring system in a microgrid makes the rate of return on investment in a microgrid relatively slow. Moreover, maintaining microgrid stability is not a small task due to the uncertainty of the output power from renewable energy sources and the lack of inertia in a microgrid. In situations when demand

is higher than supply, maximising the utilization of fossil fuel-based DERs results in higher energy production costs. Whereas, when demand is much smaller than the supply, performing hard curtailment of the RES-based DERs are contradictory to the purpose of reducing CO_2 emission.

Therefore, the balancing of supply and demand in the microgrid whilst achieving higher penetration of renewable energy sources is impossible without implementing a demand response program. Even though many papers have simulated the utilisation of demand response programs, and shown that demand response programs could improve microgrid stability and reduce the costs of energy, not many of the proposed demand response programs have performed optimally by considering customer discomfort and the project's feasibility for both the microgrid owner and the demand response participants.

The literature review revealed several research gaps. Firstly, some of the demand response deployment costs cannot be easily quantified. Secondly, the main benefit mentioned in the modelled demand response programs is the reduction in the participants' electricity bill; however, this financial benefit has not been compared with the investment and other associated costs. The one and only open modelling framework that compares the cost-benefit ratio of a demand response program is based only on the price-response program, whereas future demand response programs are expected to take into consideration the variations in renewable output power. Lastly, to the best of this author's knowledge, no study has ever been conducted to determine the appropriate demand response incentive which considers customer discomfort and the profits earned by the microgrid's owner.

Chapter 3 Feasibility of Deploying a Small-scale Microgrid

This chapter presents an evaluation of the techno-economic analysis of utilising a real small-scale microgrid. The analysis is performed by considering the possible business models, i.e., net metering for the electricity bill, the feed-in tariff for utilising renewable energy, and demand response implementation by exploiting the BES roles. These are in response to the price variation during peak and off-peak periods. Also, it is assumed that compensation is given every time the microgrid is in an islanded mode. The feasibility of each model is determined by the microgrid's net present value (NPV) and internal rate of return (IRR).

3.1 Approaches for calculating cost and benefits ratio

The microgrid test case in this study is a 10kW PV integrated microgrid located at the office of Agency for The Assessment and Research of Technology (BPPT)'s office in Serpong, Indonesia. The microgrid is connected to 380VAC three-phase system and consists of a 10kWp PV array with a grid-tied inverter, SCADA and PLC system as microgrid controller, weather station, and 10kWh lithium BES connected to three bidirectional BES inverters to form three-phase AC system as shown in Fig.3.1. The BES inverter can be operated in on-grid and off-grid system and provides voltage reference for the grid-tied PV inverter during the islanded mode. The loads consist of the lighting system and the wall sockets for supplying electrical equipment as well as microgrid controller instrumentation.

The feasibility of the microgrid test case is measured by calculating its NPV and IRR value with the assumption that the microgrid lifetime is 25 years considering the PV module lifetime. Note that the term 'net present value' means that the value estimated for the following years is converted to the value of the current years; as such, the interest and discount rate are taken into consideration in the NPV calculation method (discount method). The correlation between NPV and IRR is defined as

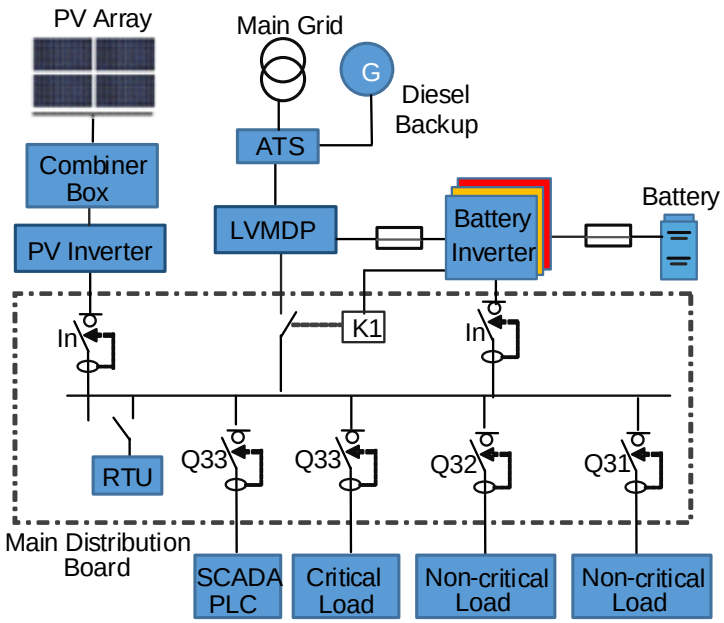

Figure 3.1 Single line diagram of the study case microgrid.

$$NPV_{\text{microgrid}} = \sum_{i=0}^{N_{year}-1} \frac{CF_n}{(1+IRR)^n} \tag{3.1}$$

where CF_n is the cash flow for the year-n, which is the difference between the microgrid received revenue and cost including the investment and periodic costs.

$$CF_n = Revenue_n - Cost_n \tag{3.2}$$

The following sections describe the approaches for calculating the NPV of the microgrid's revenues and costs throughout the microgrid's lifetime.

3.1.1 Estimation of PV Power

The PV system's output power is computed based on [93] and uses a yearly solar irradiations data of the studied location. Output power from a PV system is affected mainly by the intensity of solar insolation and PV module temperature. The common equation for calculating a PV system's output power (P_{PV}) is:

$$P_{\text{PV}}^{h,y} = RC_{\text{PV}} \times Der_{\text{PV}}^{y} \times \left(\frac{\bar{G}_h}{G_{\text{STC}}}\right) \times \left(1 + \alpha_P\left(Temp_{\text{PV}}^{h} - Temp_{\text{STC}}\right)\right) \tag{3.3}$$

where RC_{PV} is the PV array rated capacity (kW) under the STC (standard test condition), Der_{PV}^{y} is the PV derating factor at current year y (%), $\bar{G}_h$ is the average intensity of solar radiation in the

current time step h (kW/m^2), G_{STC} is the insolation intensity under STC (1 kW/m^2), α_P is the PV module temperature coefficient of power (%/^{o}C), $Temp_{PV}$ is the PV module temperature in the current time step (^{o}C), and $Temp_{STC}$ is the PV cell temperature under STC. In this study, the available data is the hourly insolation profile. Thus, the effect of PV module temperature changes is ignored.

The performance efficiency of PV modules decreases throughout its operation lifetime, mainly because the module is exposed to direct sunlight and may encounter extreme ambient temperature changes. Thus, referring to the PV module's derating factor shown in its datasheet, i.e., 2.5% in the first year and 0.5% for the following years [94], the produced energy for the following years can be predicted.

3.1.2 Estimation of microgrid total cost and revenues

The deployment costs consist of the initial, operation and maintenance, and replacement costs. The initial cost comprises the total price of the purchased equipment, installation, and software development costs. As the value of money changes over time, the calculation of the predicted operation and maintenance costs and the electricity price takes into consideration the rate of inflation, i.e., 3.53% [95]. The replacement cost is calculated by assuming that the equipment price decreases by an average of 15% per year, according to the report in [96]. Meanwhile, the salvage value is ignored because most of the equipment components are used until the end of their lifespan. On the other hand, the microgrid revenues are defined as follows:

- Two approaches are used to calculate the income from the PV system, i.e., net metering and feed-in tariff. In the net metering method, the electricity generated from the PV system will be rated the same as the customer's electricity price, i.e., $0.08 per kWh [97] for the BPPT building. Meanwhile, the feed-in tariff method is used to simulate if the utility gives incentives to the microgrid for producing electricity from the RESs. To generalise the solar energy tariff, this study uses regulation as in [98] which stated that feed-in tariff for the solar power plant located in Java Island is 14.5 cents/kWh.
- The revenue from a BES system is calculated by assuming that the demand response program is implemented based on the price variation. A BES system is assumed to be charged during off-peak periods and discharged during peak periods. The Indonesian state-

owned utility company applies a higher tariff during peak period with a multiplication factor of K = 1.5 [97]. The peak period is from 5 PM to 10 PM.

- The reliability improvement revenue is calculated by assuming that compensation is provided to the customer who faced supply interruption. Based on [99], the Indonesian state-owned utility company (PT. PLN) is obliged to give a 35% reduction on the consumer's minimum electricity bill if the realisation of power service quality level exceeds 10% above the level of standardised electricity service quality. However, as the microgrid capacity is much smaller compared to the total loads of one of the BPPT buildings where the microgrid is installed, the microgrid cannot be considered to represent the BPPT customer class; therefore, the compensation refers to [100], i.e., the value of service $2.5/kWh non-delivered energy (NDE). This reliability revenue is then calculated based on the average interruption occurrence [101], i.e., five interruptions with a total duration of five hours per month.
- The last revenue is derived by assuming that the carbon tax is also implemented. It is suggested that for the initial implementation of carbon tax in Indonesia is $10/ton CO2 [102]. Based on [103], the emission factor for electricity generation in the studied location is 0.877 ton CO_2/MWh.

3.2 Results and Discussions

Based on the predicted cash flow for 25 years, the microgrid's NPV and IRR are calculated with the considered discounted rate, i.e., 7.5% [104]. The NPV and IRR will be calculated following the variation of the determined costs and benefits given in Section 3.1.2.

3.2.1 Energy from the PV system

The total generated energy is accumulated for 25 years based on the lifetime of the PV module. The output energy from the PV system is calculated based on the solar irradiation data extracted from the BPPT's pyranometer in 2016. The output power from the PV system of the microgrid is shown in Fig. 3.2. The generated energy from the PV system is 16,232 kWh in the

first year of operation. The total amount of energy produced by the PV system over the 25-year lifespan is presented in Fig. 3.3, assuming the same solar irradiation.

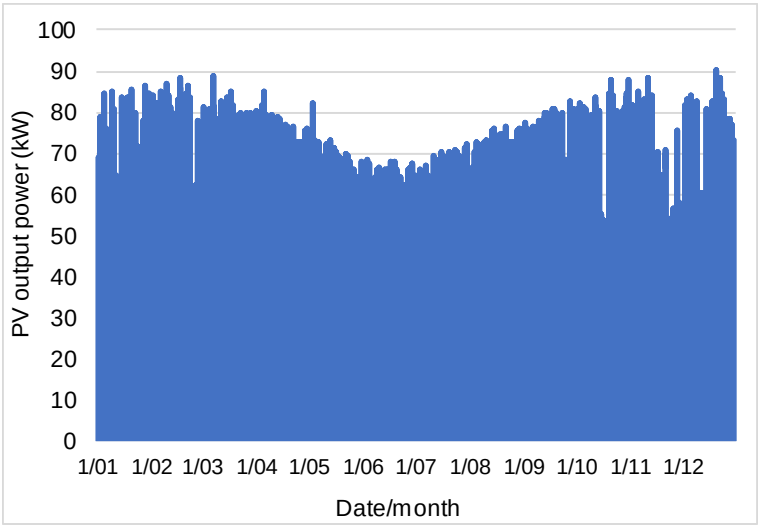

Figure 3.2 The output energy from the 10kWp PV array in 2016.

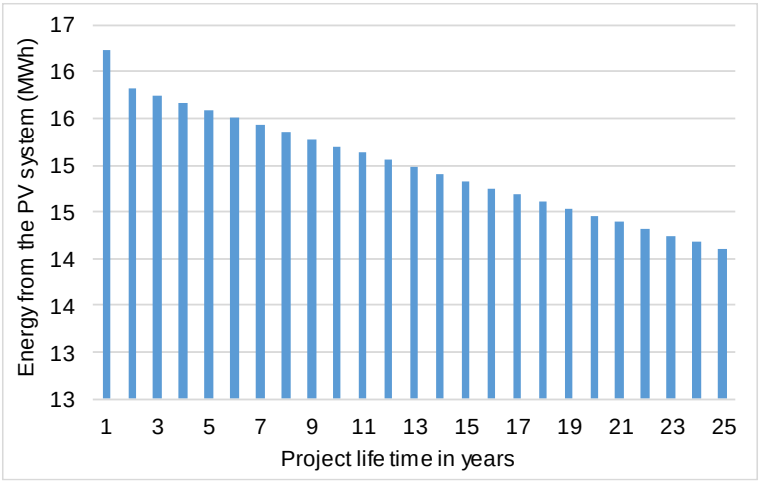

Figure 3.3 The PV system energy through the microgrid lifetime considering PV module derating factor.

3.2.2 Microgrid Costs and Revenues

Table 3.1 shows the microgrid deployment costs, noting that the installation cost of the studied microgrid is $46,803. The cost of BES utilisation accounts for almost 40% of the total deployment cost. It is mentioned in [105] that a bigger BES capacity may reduce customer dissatisfaction rate, but also incurs a higher upfront cost which is not economically feasible. In this microgrid, a BES system is needed to enable the islanding mode and could contribute to

improving microgrid's income by exploiting price deviations between peak and off-peak periods. Table 3.1 shows only the initial costs of the microgrid project deployment. Fig. 3.4 shows the microgrid cash flow which depicts the microgrid revenues and the assumed ongoing costs for the microgrid operation and maintenance and its component replacement over 25 years.

Table 3.1 Microgrid deployment costs.

Item	Price	Lifetime	Item	Price	Lifetime
PV module	$8,160	25 years	MDB panel, combiner box, support module, etc.	$1,848	20 years
PV inverter	$2,789	12.5 years	SCADA system	$2,414	-
$LiFePO_4$ BES	$11,734	20 years	PLC system	$814	12 years
3 BES inverter	$7,059	12.5 years	Additional uninterruptible power system	$450	5 years
PC server and monitor	$2,444	5 years	Installation cost & software development	$7,235	
Weather station	$1,856	5 years	**Total Cost**	**$46,803**	

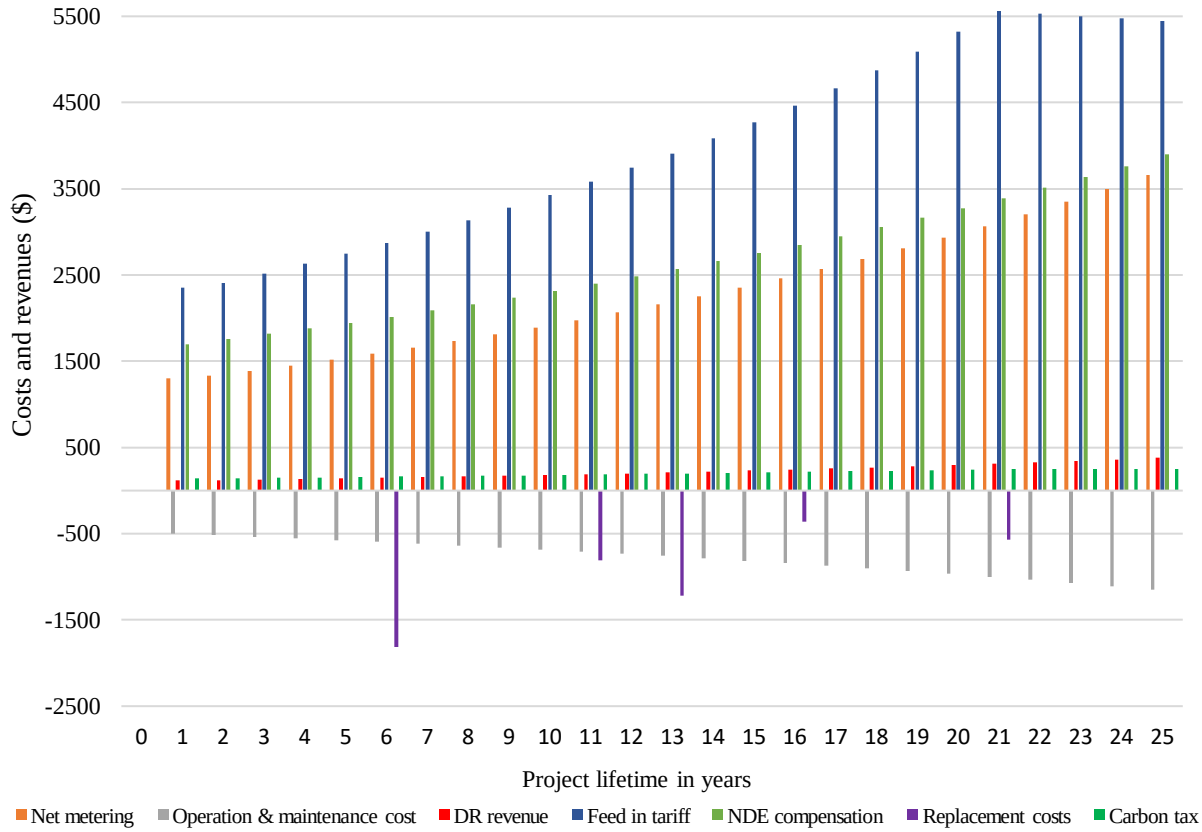

Figure 3.4 Cash flow diagram for microgrid running costs and revenues.

It can be seen from Fig. 3.4 that the revenue from carbon tax implementation is the smallest of the microgrid revenues. The revenue from a BES system in a demand response program is also very small. This happens because the peak price period is applicable only in once allocated time per day; thus, BES utilisation as a response of price deviation between peak and off-peak period can also be done once a day and resulted in the small BES's revenue. On the other hand, the biggest amount of revenue is obtained with the feed-in tariff model.

3.2.3 Microgrid Feasibility

A comparison of the NPV and IRR between the different business cases is presented in Table 3.2.

Table 3.2 Comparison of NPV and IRR based on available business cases.

Indicator	Net Metering	Net metering + demand response	Net metering + carbon tax	Net metering + NDE	Net metering + demand response + carbon tax	Net metering + demand response + NDE	Net metering + NDE + carbon tax	Net metering + demand response + NDE + carbon tax
NPV	-$34,979.5	-$32,897.2	-$32,953.1	-$8,954.2	-$30,870.7	-$6,871.8	-$6,927.8	-$4,845.4
IRR	-2.1%	-1.2%	-1.3%	5.6%	-0.4%	6.1%	6.0%	6.5%
Indicator	Feed in tariff	Feed in tariff + demand response	Feed in tariff + carbon tax	Feed in tariff + NDE	Feed in tariff + demand response + carbon tax	Feed in tariff + demand response + NDE	Feed in tariff + NDE + carbon tax	Feed in tariff + demand response + NDE + carbon tax
NPV	-$17,996.5	-$15,914.1	-$15,970.1	$8,028.9	-$13,887.7	$11,236.8	$10,055.3	$12,137.7
IRR	3.4%	4.0%	3.9%	9.1%	4.5%	9.6%	9.4%	9.8%

It can be seen from Table 3.2 that if the revenue from the PV system is based on a net metering model, this results in a negative NPV value, meaning that the project is not feasible. Moreover, most of the business models with the net metering model face losses as indicated by the negative IRR. On the other hand, a positive IRR observed for the feed-in tariff model which indicates that this microgrid will acquire profits. Meanwhile, a positive NPV indicating that the microgrid is economically feasible is obtained when both the feed-in tariff and reliability options

were considered. The contribution of a BES in the demand response program is insignificant as well as is the revenue from the reduced carbon tax. The demand response revenue increased only by IRR 0.5% on average.

3.3 Summary

The results of the techno-economic analysis show that the deployment of a small scale microgrid equipped with modern control technologies for enabling microgrid services is not economically viable if only the net metering business model is considered. On the other hand, providing incentives for utilising renewable sources such as in the feed-in tariff has significantly increased microgrid's NPV and IRR. Meanwhile, the absence of price variation reduces the opportunity of demand response implementation so that installing a large BES for the purpose of participating in a demand response program may causing losses to the microgrid. Therefore, in evaluating microgrid feasibility, adding other microgrid revenues obtained by quantifying reliability improvement as the result of installing energy storage and microgrid controller or including carbon tax revenue, will increase microgrid viability. In the future work, sensitivity analysis needs to be carried out by varying the technologies and size of DERs and exploring other benefits of the microgrid such as the provision of frequency or voltage restoration to its upstream grid by forcing the BES system to charge or discharge according to variations in the system.

Chapter 4 Active Power Management of Distributed Energy Resources (DERs)

This chapter describes the effects of the intermittency of the non-dispatchable RESs such as solar and wind energy in islanded microgrids. This chapter shows the utilisation of generation-side management to enhance the active power management within a microgrid when the microgrid is operated in an islanded mode. To get a seamless transition from the grid-connected mode to islanded mode, a soft start ramping function is proposed and applied to the PV inverter. Meanwhile, to avoid the RESs curtailment, an active power reduction at over frequency conditions also been proposed and applied to the PV inverters. Both additional controls are implemented in a real microgrid test case and the results from the experimental measurements are presented in this chapter.

4.1 Effect of RES Fluctuations to the Microgrid Frequency

Increasing the percentage of the RES-based DERs in the microgrid reduces the microgrid's inertia, because of the intermittency of RES-based DERs or the use of power electronic interfaces [106, 107]; thus the grid stability is concerned [108]. Another problem that may arise is the repeated of the DERs connection or disconnection, as the DERs try to connect to the microgrid but fail because of the over-voltage or over-frequency situations. The RES-based DERs curtailment is contrary to the purpose of reducing CO_2 emission. A promising solution to address this intermittency effect is to utilise ESSs. With the ESS's energy management system, ESSs can be controlled to absorb the excess power generated by the RES-based DERs or discharge its stored energy when the microgrid faces a power shortage. However, the use of large ESSs has been limited due to cost [109].

The following sections present the effects of RESs fluctuation on the microgrid's frequency deviation and its countermeasure when an inverter-based microgrid is operated in the islanded mode.

4.1.1 The Microgrid Test Case

In this chapter, the microgrid being considered is again the BPPT microgrid test case. In this microgrid, the BES can be operated either ON or OFF-grid mode, while the PV inverter is the grid-tied type. When the microgrid disconnects from its upstream grid and starts operating in the islanded mode, the BES's inverter changes its operation mode from grid-connected to off-grid. This process takes three to seven seconds. Meanwhile, the PV's inverter shuts down because there is no voltage and frequency reference during this period. Therefore, except for the essential ones, no other loads will be supplied. After a few seconds, the BES's inverter will act as the grid-forming unit and supply the loads and, subsequently, the PV's inverter will start to operate in the grid-following mode.

According to the Indonesian grid code, in normal conditions, a DER must work at its nominal capacity within the frequency range of 49 to 51 Hz; whereas during disturbances, it is permitted to drop down to 47.5 Hz or rise to 52 Hz [110]. Therefore, to comply with the Indonesian grid code, the operating frequency for a BES inverter is set from 47.5 to 51.5 Hz, and from 47.5 to 51 Hz for the PV inverter as the PV system is the secondary reserve during islanded operation so that its maximum frequency is set lower than that for BES's inverter.

The microgrid islanding mode in this study is realised by disconnecting the microgrid from its upstream grid (i.e., by opening the switch at the point of common coupling). However, when the solar irradiation is high (e.g., during middays) but the load is low, the PV inverter starts switching on and off repeatedly, as it tries to connect to the microgrid but fails because the microgrid frequency exceeds its allowed range.

4.1.2 Study Case

First, let us evaluate the real microgrid test case shown in Fig.3.1 where the microgrid is connected to its upstream grid. During the testing, the average solar insolation was 841 W/m2, and the module temperature was 49.5^{o}C. Therefore, the average of the measured PV system output power was approximately 7.57 kW (based on the datasheet of the used PV module and inverter [93, 94, 111]), while the total load was 1.5 kW. Fig. 4.1 shows the injected active power from the PV inverter along with the frequency when operated in connected mode. It can be seen

that the system frequency was in a stable condition even when the PV output power decreased. The network frequency remains around the nominal operating frequency of 50 Hz.

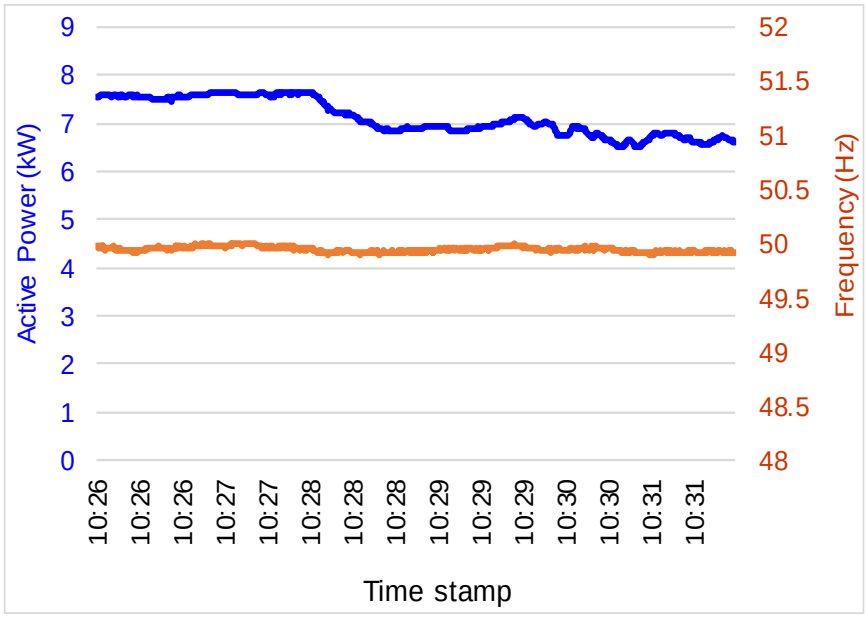

Figure 4.1 The output power of the PV system in grid-connected mode, along with the system's frequency.

Now, let us assume that the test case microgrid is in the islanded mode. Fig. 4.2 shows that the microgrid's frequency increases with the increment of PV output power.

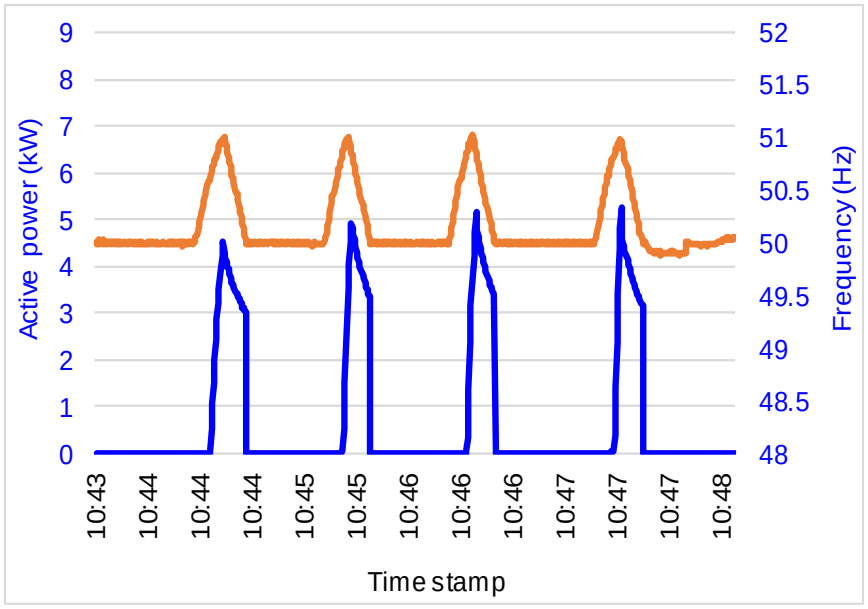

Figure 4.2 The output power of the PV system under the islanded mode, along with the microgrid's frequency.

It takes around four seconds for the PV inverter to ramp up its output power from 0 to 3.6 kW as the default output power ramp-up is 10% of its nominal capacity per second. When the PV inverter ramps up, subsequently, the BES inverter decreases its output power. However, the PV inverter automatically shuts down when the microgrid's frequency reaches 51 Hz, as the operating frequency of the PV inverter has been set in the range of 47.5 to 51 Hz. After approximately 40 seconds, the PV inverter starts to synchronise again and tries to inject its produced power. However, it shuts down again because of over-frequency.

4.2 Additional Active Power Management

Because the BPPT microgrid is an inverter-based microgrid, it has a small amount of inertia, so that a sudden dispatch from the uncontrollable DERs significantly affects the microgrid's stability when the microgrid is operated in an islanded mode. Without proper control, the PV system was curtailed. With this hard curtailment of the PV system, all the connected loads in this microgrid are supplied only from the energy stored in the BES. Thus, the energy within the BES is probably not enough to support the microgrid loads if the off-grid mode persists for a long time. Therefore, the PV system's active power output needs to be managed.

4.2.1 Employing a soft start ramp after microgrid isolation

Fig. 4.2 shows that the PV inverter shuts down when the microgrid's frequency reaches its maximum operating frequency. Therefore, additional active power management, i.e., a soft starting ramp is applied to the PV inverter to smooth the starting sequence after the microgrid begins operating in islanded mode. A soft-starting ramp method has been employed for grid-connected PV systems in [112] to mitigate the effects of sudden changes of solar irradiation or ambient temperature, and shows an improvement when compared with the conventional maximum power point tracking algorithm.

During normal operation, the PV inverter is set to have an output power ramp-up of 10% (i.e., the output power of increases by 10% of its nominal value per second). The active output power (P) is a function of the current (I) following the maximum power point tracking algorithm. On the other hand, with a soft-starting ramp function, two ramp-up gradients will affect the PV

inverter output power, during the starting up after the microgrid has been isolated from the grid [113]. Thus, the output current of the PV inverter will be determined by

$$I_t = I_{t-1} + \left(k_{soft} \times k_{inc} \times I_{nom}\right) \tag{4.1}$$

where I_t is the current at time t; I_{t-1} is the current at the previous time sample, and I_{nom} is the nominal current value while k_{soft} is the power gradient for starting up and k_{inc} is the gradient for increasing active power.

Now let us consider the same microgrid is employing the proposed controllers. First, a power gradient of 1.2% is set for the soft-starting ramp of PV inverter at the reconnection time, as well as a gradient of 20% for the active power increment. It can be seen from Fig. 4.3 that the slope of the active power rise and fall is not as steep as the slope before soft starting function is applied. Thus, it takes 80 seconds for the PV inverter to ramp up its output power from 0 to 2.5 kW. However, as the PV system's output power is much higher than the loads, it again shuts down before reaching its maximal output power due to over-frequency.

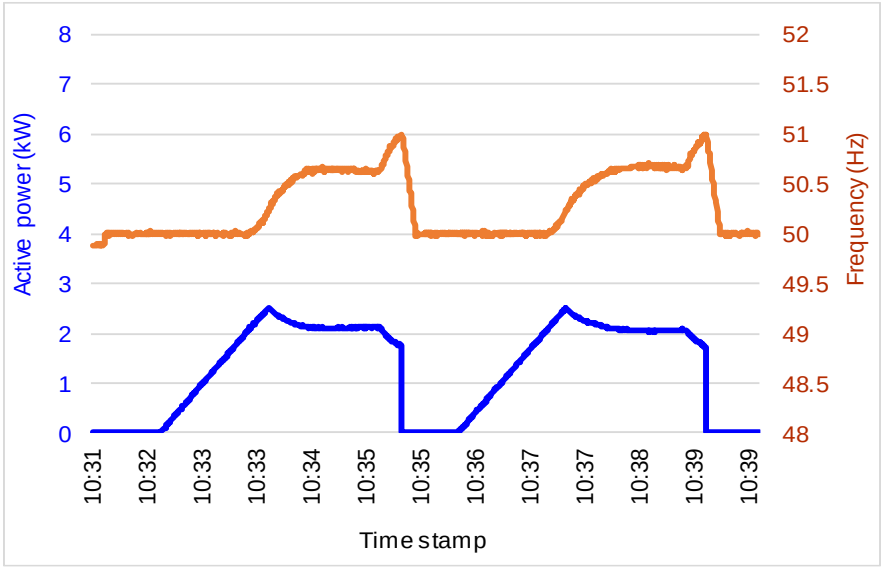

Figure 4.3 Output power of the PV system with the employed soft-starting ramp.

4.2.2 Implementing an active power reduction at over-frequency

As a microgrid is a localised power system, during the islanded mode, the DERs output power must match its load. Therefore, if the generated power is higher than the consumed power, the output power of the DER needs to be clipped. Fig. 4.3 shows that a hard curtailment

of the PV system can still be avoided. Therefore, the output power from the PV system needs to be reduced so that microgrid runs in the allowed range of frequency. In this study, the function of the active power reduction uses a droop algorithm:

$$P_t = \begin{cases} P_{t-1} \times k_{Pdec} \times (f - f_{start}) & , f \geq f_{start} \\ P_{t-1} + (P_{nom} \times k_{Pinc}) & , f_{rst} \leq f \leq f_{start} \end{cases} \quad (4.2)$$

The active power reduction when over-frequency occurs is illustrated in Fig. 4.4.

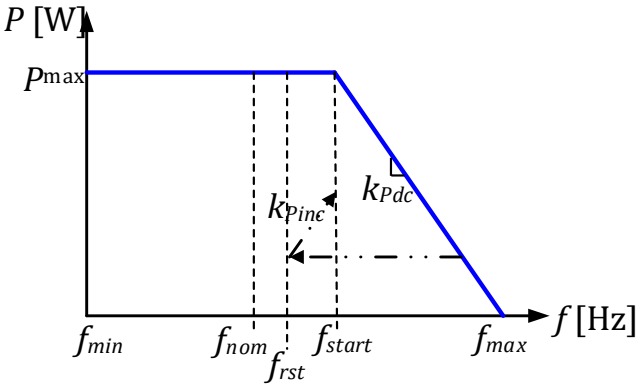

Figure 4.4 Active power-frequency illustration control of PV inverter.

The PV system through its inverter will inject all its produced power into the microgrid as long as the frequency (*f*) is lower than the predefined starting frequency (f_{start}). When the frequency is higher than f_{start}, the droop controller will reduce the PV inverter's output power with a ramping slope of k_{Pdec}; however, when the frequency decreases to the predefined resetting frequency of f_{rst}, the PV inverter again increases its output power by a gradient of k_{Pinc}. The values of f_{start}, and f_{rst}, are assumed higher than the nominal value to minimise the curtailment of PV, especially during the grid-connected mode of the microgrid [114]. k_{Pdec} is set to 90% per Hz based on the ratio of the predicted output power of the PV system and the load capacity during the tests, while k_{Pinc} is 10% per second.

Finally, an active power reduction at over-frequency is implemented assuming f_{start} is 50.2 Hz while f_{rst} is 50.05 Hz while the above-mentioned soft starting ramp function is active. When the microgrid's frequency is higher than 50.2 Hz, the PV inverter reduces its active power output. Hence, the frequency also decreases. When the frequency falls to 50.05 Hz, the PV inverter again ramps up its active power. It can be seen from Fig. 4.5 that after two risings and fallings, the system reaches its stable point at a frequency of approximately 50.5 Hz, while the PV inverter's

output power is around 1.5 kW. Based on the testing result, it takes seven minutes for the inverter to reach the desired value, which satisfies the 5-15 minute range specified in [2].

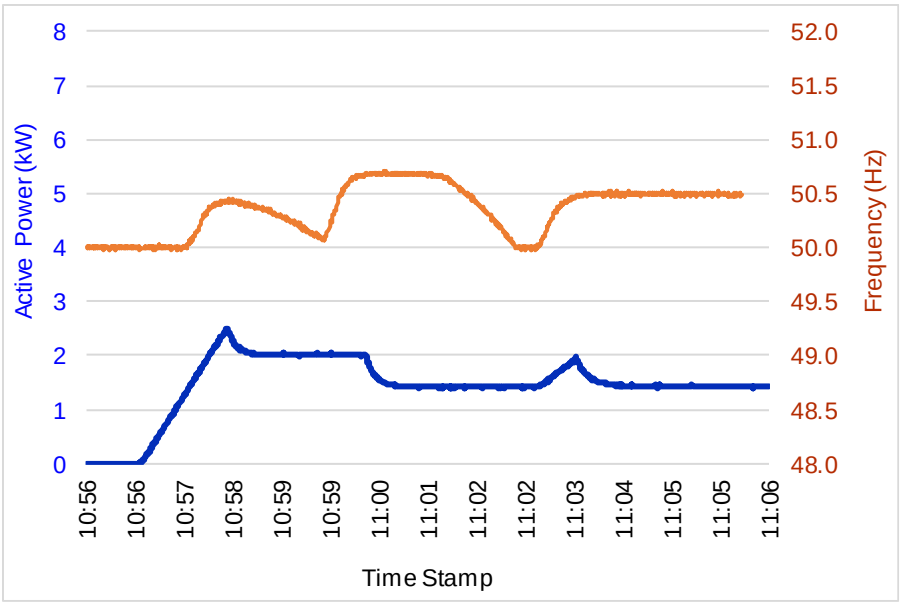

Figure 4.5 Output power of the PV system with the employed soft starting ramp and power reduction at over-frequency

4.3 Summary

This chapter has found that an islanded microgrid is prone to frequency deviations caused by RES fluctuations. The studies show that the proposed active power management has improved the microgrid frequency regulation. Through practical measurements, it is shown that employing a soft-starting ramp for the PV inverter can smooth the power delivered by the inverter when the microgrid starts operating in islanded mode. It is also demonstrated that reducing the active power output of the inverter against the deviation in the microgrid's frequency, by imitating the P-f droop control method, has avoided the hard curtailment of the inverter.

Chapter 5 Utilising Demand Response in Microgrid

This chapter proposes a load management scheme in lieu of controlling the microgrid's DERs as a means of maintaining the microgrid stability. The proposed demand response aims to optimize customer comfort and microgrid profits. The case study section in this chapter presents a simple demand-side management based on BES SoC in the real microgrid test case which is applied in a real microgrid test case. Also proposed is an active power-voltage droop control to restore the load bus which encounters under-voltage condition. To evaluate this proposed method, a simulation has disturbing out, the results of which are presented in this chapter.

5.1 Demand Response Optimisation

It has been confirmed that it is crucial to maintain the power balance between supply and demand in order to maintain the microgrid voltage and frequency deviation. This indicates that to prevent the microgrid voltage and frequency from deviating from the acceptable range, either the supply or the demand needs to be increased or decreased. This section presents two examples of demand response utilisation. A load-shedding scheme used to restore voltage deviation is studied within a modelled microgrid. Meanwhile, in the real-case microgrid, to improve its reliability during the islanded mode, a simple load-shedding scheme based on the microgrid BES's state of charge (SoC) is evaluated.

This section presents the proposed demand response optimisation so that the demand response deployment will not violate customer discomfort level, minimising the number of affected loads, and maximising the microgrid operator's profits. The objectives function in this study are formulated as:

- OF_1: The first consideration when implementing the demand response program is the project's profitability to the microgrid operator. The microgrid operator can earn an additional profit by shifting some of its loads from peak periods to off-peak periods or shaving some of them when the network consumption is relatively higher than the total

generation capacity. This is equal to minimising the cost of energy supply $Cost_{\mathrm{ES}}^{h}$. Therefore, the first objective is formulated as

$$OF_1 = \sum_{\mathrm{h}=1}^{N_{hours}} Cost_{ES}^{\mathrm{h}} \tag{5.1}$$

where $Cost_{ES}$ is the microgrid cost of energy supply and h is the time index (e.g., an hourly basis).

- OF_2; The second consideration is that the demand response implementation should not affect the microgrid's stability. To achieve this, the amount of the deferred load must be higher than and as close as possible to the amount of the deviation between the generated and consumed power before the demand response is executed; i.e.,

$$OF_2 = \sum_{h=1}^{N_{hour}} \left(P_{\mathrm{load}}^{DR,h} - P_{\mathrm{load}}^{h}\right) \geq P_{\mathrm{DCG}}^{h} \tag{5.2}$$

where P_{load} and P_{load}^{DR} are respectively the power supplied to the microgrid load before and after implementing the demand response program; while P_{DCG}^{h} is the difference between the consumed and generated power within a microgrid.

- OF_3: Third, it is better to minimise the number of the affected loads when executing the demand response; i.e.,

$$OF_3 = \sum_{n=1}^{N_{\mathrm{load}}} DRS_{\mathrm{load}}^{n} \tag{5.3}$$

where DRS_{load} is the loads' state, "1" means the loads are controlled under demand response program, whereas "0" indicates that the executed demand response does not affect the loads.

- OF_4: Finally, the algorithm of the demand response program should minimise the discomfort felt by the participants. Therefore, in this study, the demand response is executed sequentially by scheduling the shiftable loads, utilising the BES by discharging its stored energy, reducing the power usage from the controllable loads and in the final step, disconnecting the shedable loads if the MG still faces a power shortage problem.

$$OF_4 = \sum_{n=1}^{N_{\mathrm{load}}} Dis_{\mathrm{load}}^{n} \tag{5.4}$$

To achieve the optimisation objectives, the loads are classified based on their operational profile and economic value. Also, this chapter presents the optimisation solver tool used in this study, i.e., the Genetic Algorithm (GA).

5.1.1 Load and Customer Classification

In chapter 2, the four load classifications were presented: critical (uninterruptible), shiftable, controllable, and shedable loads. The demand response program implementation should consider the effects of its execution on the customer's discomfort. For example, the DLC under the demand response program is usually applied to residential customers or small commercial building. Controlling some of these customers' appliances might not significantly affect their activities if the appliances, such as an electric water heater or air conditioner, are turned off for a limited period [40, 43, 45, 115].

However, the DLC method is still has a higher probability of violating customer comfort level. Previous studies have suggested that in order to reduce the customers' discomfort, the loads that have the same character should be classified into one group, so as to determine the best demand response scheme for each group. In [43], the loads are classified based on their group priority. In [44], load scheduling is based on the loads' common operating time profiles. However, even for the loads that have the same characteristics and are in the same group, the customers usually have different preferences in terms of which load(s) should be uncontrolled or be allowed to continue operating. Also, many studies have investigated demand response applications for thermal loads such as air conditioner and water heater [116-118], taking into account the flexibility of their thermal inertia characteristic. Moreover, the available appliances may not be as flexible as thermal loads.

Therefore, to ensure that the algorithm of the demand response program is able to minimise the discomfort felt by the demand response participants, in this study it is proposed that the demand response program be executed sequentially, taking into account the following considerations:

- By assuming that load-shifting in a demand response program will cause the least discomfort to customers as the load's performance/function will still be fulfilled, the load-shifting strategy will be executed first before reducing the demand. Because the modelled

microgrid consist of a PV system and the modelled shift-able loads have their preferred time to be shifted when choosing the neighbourhood load's operating time, the predicted PV output power is taken into consideration.

- If, after the load-shifting process, the microgrid is still encountering power deficiency, then the next demand response strategy is to utilise the BES system. If the microgrid is facing a power shortage, the BES will discharge its stored energy. Whereas, if the microgrid has surplus power, then BES will absorb this excess power to be stored for later use.

- If, after BES storage has been utilised, the microgrid is still facing power deficiency, then, to balance the power flow, the microgrid will reduce its demand by reducing the power being consumed by the group of controllable loads. It is assumed that reducing the performance of an appliance is preferable to totally disconnecting it from the grid.

- If the microgrid is still encountering power deficiency although all the available controllable loads have been deferred but, the microgrid will disconnect some of its shedable loads as a last resort to balance the flow of electricity in the microgrid.

In order to solve an optimisation problem with multiple objectives, weighting criteria can be attributed to the input parameter so that the chosen solution is the fair judgement of those available. As an example, multi-objective decision-making has been proposed in [119-122] while [123] presents score-based decision-making.

To minimize the number of affected loads, it is preferable to control those loads that have a bigger capacity and flexibility and smaller economic value. Therefore, in this study, the loads will be indexed with a weighting value based on the load's power usage (W), the flexibility to withstand the demand response control command, and the load's economic value. Meanwhile, the discomfort level (Dis) felt by customers caused by their affected loads also related to the load's flexibility. Loads with higher flexibility will encounter a smaller comfort reduction per each demand response event.

5.1.1.1 Shiftable loads

Shiftable loads are the loads whose working time can be scheduled for other operation

times. If a shiftable load is operated, it should not be disconnected. Each customer has individual preferences in terms of when loads are to be shifted. The shifting flexibility will be different when the preferred shifting time overlap or not overlap with the load's original operating time. Overlap means that the original load operation time without the load-shifting program is within the time frame of the predefined preferred shifting time as shown in Fig. 5.1. The shifting flexibility of the overlap and non-overlap shifting time is defined as

$$Flex_{\text{Shift}} = \begin{cases} h_{\text{shift}}^{\text{DR,end}} - h_{\text{shift}}^{\text{DR,start}} - ST + 1, & \text{if overlap} \\ h_{\text{shift}}^{\text{DR,end}} - h_{\text{shift}}^{\text{DR,start}} - ST + 2, & \text{if not overlap} \end{cases} \tag{5.5}$$

where

$$ST = 1 - \Delta T \tag{5.6}$$

in which $h_{\text{shift}}^{\text{DR,start}}$ and $h_{\text{shift}}^{\text{DR,end}}$ are respectively the start and the end of the preferred shifting time. When the time frame overlap, the number "1" in (5.5) is retrieved as the $h_{\text{shift}}^{\text{DR,end}}$ included in the time frame (e.g., "7" indicates the time between 7:00 and 7:59), ST is the shiftable loads sliding time frame which is defined as the difference between the shortest sliding time (i.e., 1 hour) toward the loads operating duration (ΔT).

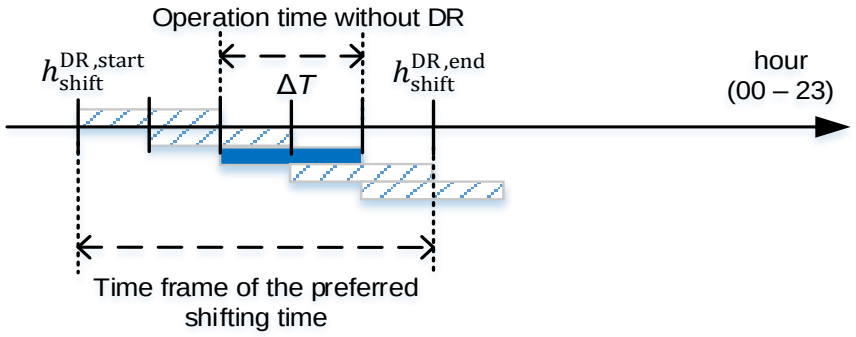

(a)

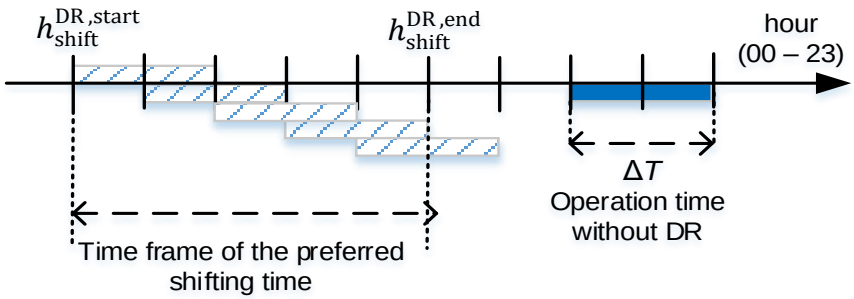

(b)

Figure 5.1 Time frame between the allowed shifting time and the original operation time, (a) when overlap, (b) not overlap.

The capacity weighting of shiftable loads is related to the load nominal capacity (P_{load}). In this study, the load's weighting capacity (ω_{cap}) is normalised within a range of $[1 \cdots 2]$ from

$$\omega_{\text{cap}} = 1 + \frac{P_{\text{load}} - P_{\text{load}}^{\min}}{P_{\text{load}}^{\max} - P_{\text{load}}^{\min}} \tag{5.7}$$

where superscript $^{\min}$ and $^{\max}$ indicate the smallest and the biggest load capacity.

In this study, the customer discomfort level is normalised within a range of $[0 \cdots 1]$. For example, for the shiftable loads, when a load is shifted to the farthest shifting time, it has "1' discomfort and has "0" discomfort if it is operated during its original operating time. The discomfort level felt by a shiftable load (Dis_{Shift}) is

$$Dis_{\text{shift}} = \frac{|\Delta h|}{h_{\text{shift}}^{\text{DR}} - h_{\text{shift}} + ST} \tag{5.8}$$

where $|\ |$ denotes the absolute function; h_{shift} and $h_{\text{shift}}^{\text{DR}}$ are respectively the shiftable loads' original starting operation time and that after applying for the demand response program, and Δh is the difference between its original time and the executed start of the shifting time.

5.1.1.2 Controllable loads

The utilisation of controllable loads in a demand response program means that when the loads are being operated, their performance is decreased by reducing their power usage. For example, by increasing the temperature setpoint of an air conditioning system by 1°C, this will reduce its power consumption by around 6% [124]. Most demand response programs use the thermal loads, such as air conditioners and water heaters, as the controllable loads. The function of a thermal load is dynamically affected by other factors, such as the number of occupants and the room's dimensions. However, in this proposed method, the profile of controllable loads is simplified with only two pieces of information: the controllable load's flexibility ($Flex_{\text{cont}}$) and the controllable load's capacity. $Flex_{\text{cont}}$ refers to how many times a load can be controlled to reduce its power usage under a predefined comfort setting. For example, a lighting system, if the intensity of a lighting system can be reduced to 30% of its normal operation, and if each command control reduces 10% of the intensity, then this lighting system has three-order flexibility. Meanwhile, the controllable load's capacity weighting is related to the total of power

that can be reduced (ΔP_{load}) according to the predifined load's flexibility. Again, the flexibility weighting (ω_{flex}) and ω_{cap} is normalised.

With the load's flexibility weighting, the proposed algorithm is intended to reduce the discomfort for the controllable loads by considering the standard deviation of discomfort level among the affected loads. For example, there are two loads with the 1st load allowed to reduce its power four times while it is twice for the 2nd load. In this case, the first step in the power reduction of the 2nd load will be carried out if the 1st load has been subject to power reduction twice so that the discomfort level for both loads become the same (i.e., each is 50%).

In this study, the demand response program is intended only for reducing the power consumption when the system faces a power shortage; therefore, only two conditions of controllable load discomfort level have been considered: the normal situation when there is no power reduction (discomfort level is 0%) and the situation when the power is reduced, as shown in Fig. 5.2. A 100% discomfort level means that the amount of power reduction is equal to the maximum allowed reduction steps. Therefore, the discomfort felt by the controllable loads (Dis_{cont}) is the ratio between the number of loads' power reduction steps that have been sent and the maximal reduction steps that are allowed to control the controllable loads per hour.

$$Dis_{\text{cont}}^{n,h} = \frac{\sum_{n=1}^{Flex_{\text{cont}}} 1 \times DRS_{\text{load}}^{n}}{Flex_{\text{cont}}} \tag{5.9}$$

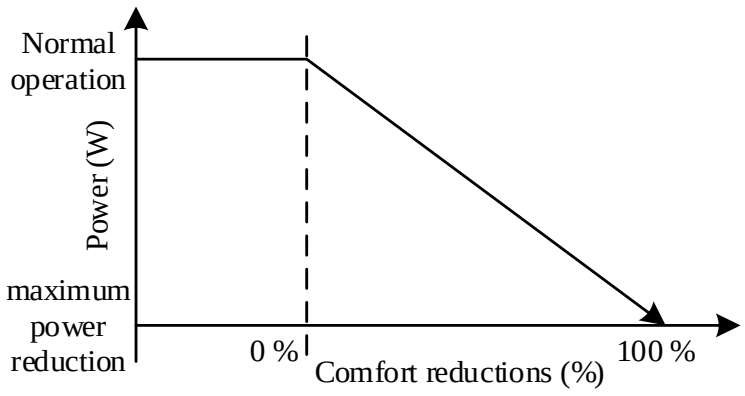

Figure 5.2 Illustration of the controllable loads' discomfort level.

5.1.1.2 Shedable loads

Each demand response command sent to the shedable loads means that the loads will be disconnected during operation. Meanwhile, the flexibility of a shedable load ($Flex_{\text{shed}}$) is related to the number of hours that the load can be disconnected in order to achieve minimum performance. For example, to ensure the water quality of a swimming pool, the pump should run for a minimum of four hours a day, although the pool pump in normal condition runs for eight hours a day; thus, this pump can be disconnected for four hours (controlled four times) in a day. Again, refer to equation (5.9), the shedable loads' capacity and flexibility weighting are normalised.

Unlike the controllable loads which are controlled on an hourly basis, the shedable load discomfort (Dis_{shed}) is defined with the same formula as that of controllable loads discomfort but on a daily basis (d).

$$Dis_{\text{shed}}^{n,d} = \frac{\sum_{n=1}^{24} 1 \times DRS_{\text{load}}^{n}}{Flex_{\text{shed}}} \tag{5.10}$$

Fig. 5.3 illustrates the discomfort level that will be encountered by the demand response participants based on load types.

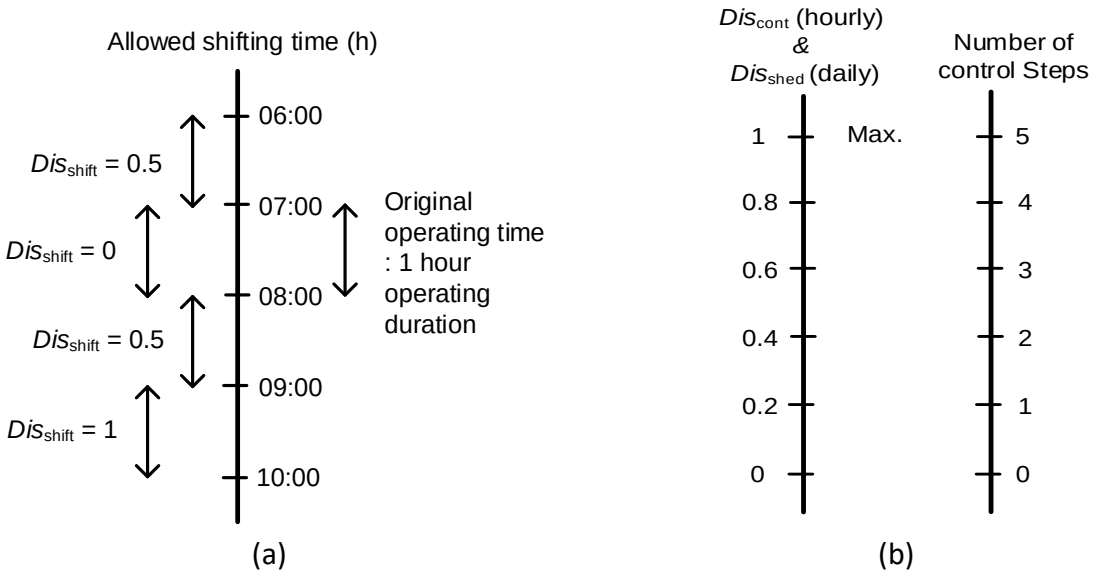

Figure 5.3 Illustration of customer discomfort level (a). shiftable loads (b). controllable and shedable loads.

5.1.1.2 Customer Types

As mentioned before, disturbing to a load's performance has different effects in terms of financial consideration of the customer. Hence, in this study, by considering that reducing the performance of commercial loads may affect the business process to the customer, commercial customers are assumed to have a higher economic value than residential customers (i.e., $EV_{\mathrm{com}} > EV_{\mathrm{res}}$). This economic value is assumed to be the same for all residential customer but can be different for various commercial customers.

With the weighting of each load and the economic value to the customer, the OF_3 can be rewritten as

$$OF_3 = \frac{\sum_{n=1}^{N_{\mathrm{load}}} \omega_{\mathrm{cap}}^n \times \omega_{\mathrm{flex}}^n}{\sum_{n=1}^{N_{\mathrm{load}}} EV_{x_2}^n} \tag{5.11}$$

where $x_2 \in \{\mathrm{res}, \mathrm{com}\}$ denotes the customer's types.

Table 5.1 summarises the load's parameters used in the GA solver when employing the optimisation of the loads' control under the demand response program.

Table 5.1 Load' parameters.

Shiftable	Controllable	Shedable
capacity	capacity (W)	capacity (W)
allowed shifting time (start and end time)	power reduction per control command	operating time
original start time	maximal command (hourly)	maximal shed (daily)
operation duration	Operating time	

5.1.2 Genetic Algorithm

With the above classification, each load will have information regarding its capacity, flexibility, and economic value. These values are discrete; thus, this study uses the Genetic Algorithm (GA) as the optimisation solver. GA is one of the nature-inspired algorithms that has been widely used in solving discrete value optimisation problems. In the GA application, at first, a space of random solutions called chromosome is generated. After that, using the feature of

evolution theory, the chromosomes are crossed over and mutated in order to obtain better generations [125].

Ref. [126] has stated that the size of the chromosome population has a significant impact on obtaining feasible solutions other than crossover and mutation rate. On the other hand, [127] mentioned the importance of the crossover and mutation rate. Usually, crossover probability has a higher rate, i.e., in the range of 0.5 – 0.95. Meanwhile, the mutation rate has a small value, i.e., lies from 0.001 to 0.05. The tutorial of solving multi-objective optimisation using GA in [128] explained that one of the general methodologies that can be applied is by determining entire Pareto optimal. The population must consist of a set of solutions which respect each other objectives function.

The steps for GA implementation in this study are:

- Define the population size of the Pareto optimal. Then, create an empty matrix with the defined size.
- Determine how many chromosomes which satisfy one of the objective function will be generated. For example, for the load-shifting demand response program, the Pareto optimal will consist of a set of possible solutions with 30% of them intended to satisfy the objective of minimising the number of affected loads, another 30% for maximising the microgrid owner's profits, 20% for minimising discomfort, 10% for maximising the weighting flexibility, and the last 10% for maximising the weighting value of a load's capacity.
- Generate a population consisting of random chromosomes, then check the fitness value and sorting them based on one of the objective functions. With the given percentage above, *N* best solutions are copied to the empty matrix of the Pareto optimal. Repeat this step based on the next objective function.
- The chromosomes in this Pareto optimal are then crossed over and mutated, with the crossover point being randomly determined. Meanwhile, only the mutation points for shiftable loads are selected randomly. The mutation points for controllable and shedable loads are chosen based on a predetermined function that a load with a small value of OF_3/OF_4 will be changed from '1' (controlled) to '0' (uncontrolled). On the other hand, a load which have a high value of OF_3/OF_4 will be changed from '0' to '1'.

- In each iteration of the GA process, *N* best solutions are chosen as the elite chromosome. Once the iteration has finished, the final solution is retrieved by comparing the fitness value of all the elite chromosomes, and then choosing the chromosomes which have at least three better values in terms of the objective functions.

In this study, instead of binary "1" and "0", the chromosomes consist of the integer (decimal) numbers which represent the load parameter. The steps described below are used to generate the Pareto optimal, check the fitness value, and the chromosomes crossing-over and mutation using an example, i.e., the GA optimisation for the controllable loads.

5.1.2.1 Generating chromosomes

The first step in the GA process is generating the chromosomes as

- Note that the demand response program in this study is considered on an hourly basis. Thus, the first step in creating chromosomes is to check and calculate the number of available loads (N_{load}) for a particular hour. This N_{load} is then used as the matrix size of the chromosomes.

- Then, for each of the available loads, a random number is generated in the range from 0 to $Flex_{\text{cont}}$ (the maximal number of command control can be applied to the loads).

$$GAC_{\text{cont}}^{m} = [\text{Rand}(R)^{m,1},\ \text{Rand}(R)^{m,2}, \cdots, \text{Rand}(R)^{m,N_{\text{load}}}] \tag{5.12}$$

where Rand denotes the random function, while $R \in \{0, 1, 2, \cdots Flex_{\text{cont}}\}$, and m denotes the index of the chromosomes in the population.

The next step is to generate a random population ($GAPop_{\text{cont}}$) from a set of chromosomes as

$$GAPop_{\text{cont}} = \begin{bmatrix} \text{Rand}(R)^{1,1} & \cdots & \text{Rand}(R)^{1,N} \\ \vdots & \ddots & \vdots \\ \text{Rand}(R)^{M,1} & \cdots & \text{Rand}(R)^{M,N} \end{bmatrix} \tag{5.13}$$
$$\forall M \in \{1, 2, \cdots Flex_{cont}^{max} \times 6\}$$
$$\forall N \in \{1, 2, \cdots N_{\text{load}}\}$$

Also, an empty matrix is generated for the Pareto optimal with the same size of $GAPop_{\text{cont}}$.

5.1.2.2 Checking fitness value

As mentioned, the chromosomes in the Pareto optimal should satisfy at least one of the objective functions; then, after generating a random population $GAPop_{\text{cont}}$, the fitness value for each chromosome will be calculated according to the first objective function; these fitness values are then sorted out. After that, the best "N" chromosomes are chosen to be copied to the Pareto optimal. For the controllable loads, N is equal to the $Flex_{cont}^{max}$. This step is repeated by again generating a random population, then checking the fitness function according to the next objective function, and the best N chromosomes are copied to the Pareto matrix in the next adjacent index. These steps are performed for all the objective functions until the Pareto optimal is completely occupied.

The checking of fitness values is formulated as

- Checking the fitness value for the total power (GAP_{cont}) from each chromosome, i.e.,

$$GAP_{\text{cont}}^{m} = \left[\text{Rand}(R)^{m,1} \times \Delta P_{\text{load}}^{m,1},\ \text{Rand}(R)^{m,2} \times \Delta P_{\text{load}}^{m,2}, \cdots, \text{Rand}(R)^{m,N_{\text{load}}} \times \Delta P_{\text{load}}^{m,N_{\text{load}}}\right] \tag{5.14}$$

  Refer to OF_2, this GAP_{cont}^{m} should be higher than and as close as the required power to be reduced $\left(P_{\text{DCG}}^{h}\right)$.

- Checking the number of the affected loads in each chromosome $(GANload_{cont}^{m})$ as

$$GAN_{\text{load}}{}_{\text{cont}}^{m} = \sum_{n=1}^{N_{\text{load}}} DRS_{\text{load}}^{m,n} \tag{5.15}$$

  where DRS_{load}^{n} is the loads' state, "1" means the loads are controlled under the demand response program, whereas "0" indicates that the executed demand response does not affect the loads. For the controllable loads, if $\text{Rand}(R)^{n} > 0$, the load is controlled under the demand response program, thus the $DRS_{\text{load}}^{n} = 1$.

  Refer to OF_3, this DRS_{load}^{n} should be minimised as much as possible. Moreover, as OF_3 has been rewritten in the equation (5.16), then the checking of the two other fitness values are performed, i.e., the total weighting $(GA\omega_{cont}^{m})$ and the total economic value $(GAEV_{\text{cont}})$.

- checking the total weighting for each chromosome as

$$GA\omega_{cont}^{m} = \sum_{n=1}^{N_{load}} DRS_{\text{load}}^{n} \times \omega_{\text{flex,cont}}^{n} \times \omega_{\text{cap,cont}}^{n} \tag{5.16}$$

- checking the total economic value for each chromosome as

$$GAEV_{cont}^{m} = \sum_{n=1}^{N_{load}} DRS_{\text{load}}^{n} \times EV_{x_2,\text{cont}}^{n} \tag{5.17}$$

- Checking the total discomfort ($GADis_{\text{cont}}$) for each chromosome as

$$GADis_{\text{cont}} = \sum_{n=1}^{N_{load}} \frac{R^{n}}{Flex_{\text{cont}}^{n}} \tag{5.18}$$

- Checking the additional profit. As mentioned, the controlling of loads under the demand response program is carried out to reduce the loads' power usage when the power generated by the microgrid-owned DERs is not enough to supply all the demand. In other words, the demand response program reduces the amount of imported power. Therefore, the additional profit from each chromosome is defined as

$$GAProfit_{cont}^{m,h} = \sum_{n=1}^{N_{load}} GAP_{cont}^{m,h} \times \left(Tariff_{\text{imp}}^{h} - Tariff_{\text{cus}}^{h}\right) \times T \tag{5.19}$$

where $Tariff_{\text{imp}}^{h}$ is the rate for importing power from the upstream grid, while $Tariff_{\text{cus}}^{h}$ is the energy tariff within the microgrid, and T denote the duration of the supply.

5.1.2.3 Chromosomes cross-over and mutation

Once the Pareto optimal has been generated, the chromosomes in the Pareto optimal are crossed over and mutated. The chromosome's index $\left(Cross_{\text{cont}}^{\text{id}}\right)$ and the load's index or the crossover point $\left(Cross_{\text{cont}}^{\text{pt}}\right)$ are determined randomly. In this study, the mutation rate is 80% of the chromosomes population (M). To avoid a chromosome crossing over more than one time, the first process is generated with the function of random permutation ($\text{Rand}_{\text{perm}}$).

$$\left[Cross_{\text{cont}}^{\text{id}}\right] = \sum_{1}^{0.8\times M} \text{Rand}_{\text{perm}}(M) \tag{5.20}$$

$$Cross_{\text{cont}}^{\text{pt}} = \text{Rand}(N) \tag{5.21}$$

Once the $Cross_{\mathrm{cont}}^{\mathrm{id}}$ and $Cross_{\mathrm{cont}}^{\mathrm{pt}}$ have been retrieved, then, the chromosomes are crossed over so that

$$GAC_{\mathrm{cont}}^{Cross_{\mathrm{cont}}^{\mathrm{id}}} = \begin{bmatrix} \mathrm{Rand}(R)^{Cross_{\mathrm{cont}}^{\mathrm{id}},1}, \mathrm{Rand}(R)^{Cross_{\mathrm{cont}}^{\mathrm{id}},2} \cdots \mathrm{Rand}(R)^{Cross_{\mathrm{cont}}^{\mathrm{id}},Cross_{\mathrm{cont}}^{\mathrm{pt}}}, \\ \mathrm{Rand}(R)^{Cross_{\mathrm{cont}}^{\mathrm{id+1}},Cross_{\mathrm{cont}}^{\mathrm{pt}}+1}, \mathrm{Rand}(R)^{Cross_{\mathrm{cont}}^{\mathrm{id+1}},Cross_{\mathrm{cont}}^{\mathrm{pt}}+2} \cdots, \mathrm{Rand}(R)^{Cross_{\mathrm{cont}}^{\mathrm{id+1}},N_{\mathrm{load}}} \end{bmatrix} \quad (5.22)$$

$$GAC_{\mathrm{cont}}^{Cross_{\mathrm{cont}}^{\mathrm{id+1}}} = \begin{bmatrix} \mathrm{Rand}(R)^{Cross_{\mathrm{cont}}^{\mathrm{id+1}},1}, \mathrm{Rand}(R)^{Cross_{\mathrm{cont}}^{\mathrm{id+1}},2} \cdots \mathrm{Rand}(R)^{Cross_{\mathrm{cont}}^{\mathrm{id+1}},Cross_{\mathrm{cont}}^{\mathrm{pt}}}, \\ \mathrm{Rand}(R)^{Cross_{\mathrm{cont}}^{\mathrm{id}},Cross_{\mathrm{cont}}^{\mathrm{pt}}+1}, \mathrm{Rand}(R)^{Cross_{\mathrm{cont}}^{\mathrm{id}},Cross_{\mathrm{cont}}^{\mathrm{pt}}+2} \cdots, \mathrm{Rand}(R)^{Cross_{\mathrm{cont}}^{\mathrm{id}},N_{\mathrm{load}}} \end{bmatrix} \quad (5.23)$$

As well as the chromosomes crossover index, the chromosomes mutation index ($Mut_{\mathrm{cont}}^{\mathrm{id}}$) is also chosen randomly using $\mathrm{Rand}_{\mathrm{perm}}$ function to avoid a repeating mutation, the mutation index in this study is 0.1.

$$\left[Mut_{\mathrm{cont}}^{\mathrm{id}}\right] = \sum_{1}^{0.1\times M} \mathrm{Rand}_{\mathrm{perm}}(M) \quad (5.24)$$

The load mutation index ($Mut_{\mathrm{cont}}^{\mathrm{pt}}$) is chosen by considering the load's weighting and the objective function. The $Mut_{\mathrm{cont}}^{\mathrm{pt}}$ are constrained with an upper and lower limit which determines whether the chosen load (point) will be changed to "0" or "1". A 5% deviation from the amount of the targeted power to be reduced defines those limits. Therefore, if the chromosome's active power is 5% higher or 5% lower than the targeted power to be reduced, then a load in this chromosome which previously was chosen to be controlled, is mutated.

- If the $GAP_{\mathrm{cont}}^{Mut_{\mathrm{cont}}^{\mathrm{id}}} > 1.05 \times P_{\mathrm{DCG}}^{h}$, then, to decrease the amount of power that will be reduced, the controllable loads with the smallest value of OF_3/OF_4, its value of $\mathrm{Rand}(R)^{Mut_{\mathrm{cont}}^{\mathrm{id}},Mut_{\mathrm{cont}}^{\mathrm{pt}}}$ will be changed to "0", which means the load will not be controlled to reduce its power usage.
- If the $GAP_{\mathrm{cont}}^{Mut_{\mathrm{cont}}^{\mathrm{id}}} < 0.95 \times P_{\mathrm{DCG}}^{h}$, then increase the amount of power that will be reduced from the related solution. A controllable load with a big value of ΔP_{load} but encountering less discomfort, its value of $\mathrm{Rand}(R)^{Mut_{\mathrm{cont}}^{\mathrm{id}},Mut_{\mathrm{cont}}^{\mathrm{pt}}}$ will be changed with "1", which means the power reduced from the nominal controllable loads became higher as well as its discomfort. The choosing of $Mut_{\mathrm{cont}}^{\mathrm{pt}}$ is done by checking the value of

($\omega_{\mathrm{cap}}^{n}/\mathrm{Dis}_{\mathrm{cont}}^{n}$) and sorting them out in a descending manner. The index of the loads with the biggest value of $\omega_{\mathrm{cap}}^{n}/\mathrm{Dis}_{\mathrm{cont}}^{n}$ is the chosen one.

The process of crossover and mutation chromosomes is then repeated within the predefined maximal iteration step.

5.2 Study Case

This section presents two case studies involving demand response implementation. First, a simple demand-side management to prolong the supply to the microgrid critical loads is implemented in a real microgrid test case. Second, an optimizing load-shedding scheme for correcting the voltage of a load bus is proposed.

5.2.1 Demand response to Prolong Supply to the Microgrid Loads

As mentioned in the previous section, in the BPPT microgrid, during its islanded mode, the BES is the primary unit for grid-forming, so that during the islanded mode the BES continuously discharges its stored energy. If there is no available energy in the BES, the microgrid will not be able to operate in islanded mode. To prolong the microgrid's service to its loads, the energy in the BES needs to preserve as long as possible.

Accurate information about a BES's SoC is important to determine its remaining capacity so that the microgrid controller can predict how long the BES can supply its loads. Moreover, by monitoring the SoC's level, the BES's over-charge and over-drain can be avoided. Thus, its lifetime will be prolonged [129].

Therefore, in this BPPT microgrid, a simple sequence-based method has been implemented for load-shedding, taking into consideration the BES's SoC level. In the microgrid under consideration, the assumed non-critical loads, i.e., some lighting and air conditioning loads are subject to the demand response program where they are classified based on priority. The group with the lowest priority is the one most likely to be disconnected. The load's classification and the shedding sequences are as follows:

- a group of lighting loads (through Q32) in Fig. 3.1 which was considered as the least prioritised load will be disconnected when the BES's SoC decreases to 80%; and

- another group of lighting and air-conditioning loads (through Q31 in Fig. 3.1) which was considered as the second least priority will be disconnected when the BES's SoC decreases to 50%
- the critical loads which include the microgrid controller will not be disconnected until the BES's SoC is 20%; this 20% limitation is taken as a precaution to prevent the BES from being over-drained, thereby prolonging its lifetime.

During the testing of this proposed demand response scheme, the total load during the testing varies from 2.5 to 4 kW. Fig. 5.4 compares the BES's SoC with and without the implemented demand-side management. As seen from this figure, by implementing the demand-side management, switch Q32 opens at 0:43:16 when the BES's SoC drops to 80% while Q31 opens at 3:07:19 when the SoC drops to 50%. On the other hand, as seen from this figure, before applying this demand-side management, Q31 would have opened at 1:39:35. This shows that the microgrid which implements load-shedding can supply its essential loads for a longer time.

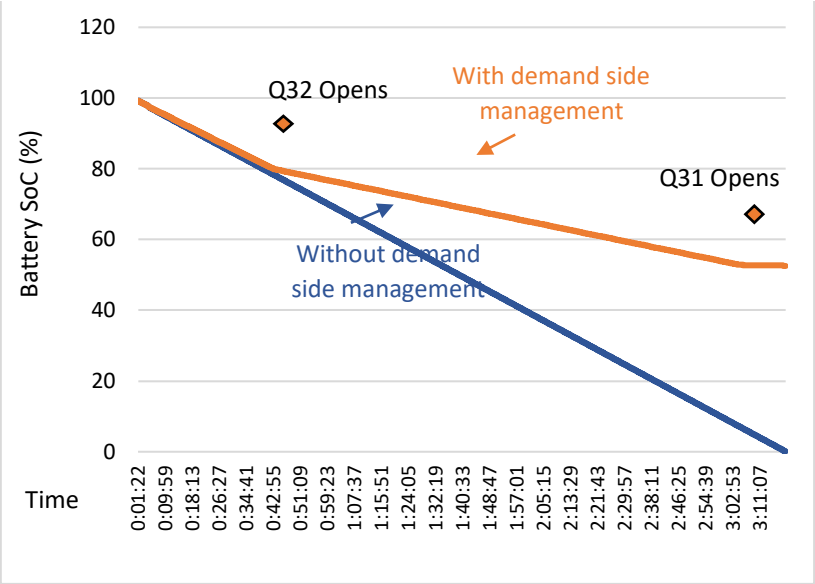

Figure 5.4 The BES's SoC before and after implementing the SoC-based load-shedding of non-essential loads.

5.2.2 Demand response for voltage correction

A power grid needs to maintain its voltage magnitude as over-voltage may damage the connected appliance while under-voltage can stop appliances from working. Appliance voltage

sensitivity tests have been conducted and published in [130-133]. The capability to withstand under-voltage condition varies among the electronic devices. The method used to measure appliances voltage immunity is standardised in [130]. In a power system, a voltage dip/sag is defined as the 10% reduction in voltage magnitude from its nominal voltage in 2 cycles until 1-minute duration. Most of the existing grid code mentioned that the lower bound of the standard operating voltage is -5% of the nominal voltage.

A power grid is regularly performing power flow analysis to optimise the network's utilisation of its distribution system. Power flow analysis, such as steady-state and short circuit analysis in a power system, is basically used to identify problems within an electricity network. The results of power flow analysis can be used to determine unit commitment optimisation, to avoid system collapse due to overloading, and to estimate the best position of the DERs to reduce power losses [134]. In a steady-state power flow analysis, it is assumed that the injected and consumed power are equal [135].

Suppose there are K buses in the grid, ac power flow analysis formulates power balance as

$$P_j = \sum_{k=1}^{K} |V_j|\,|V_k|\,|Y_{jk}| \cos(\theta_{jk} - \delta_j + \delta_k) \tag{5.25}$$

$$Q_j = \sum_{k=1}^{K} |V_j|\,|V_k|\,|Y_{jk}| \sin(\theta_{jk} - \delta_j + \delta_k) \tag{5.26}$$

where P_L and Q_L are the load's active and reactive power, j and k are the indexes for the buses, $|V|$ is the voltage magnitude, and δ is the angle. Using (5.25) and (5.26), the effect of RESs fluctuation to the microgrid frequency or voltage deviation can be analysed by varying the injected power from the RESs-based DERs.

Power flow analysis deals with the unknown states which include the term of the complex number (trigonometric function) so that it becomes nonlinear and non-convex [136]. Therefore, solving an optimal power flow problem requires a big number of iteration steps. The two most popular conventional methods are Gauss-Seidel and Newton Raphson method. The Newton Raphson method outperformed the former method in terms of convergence rate [137].

5.2.2.1 Newton Raphson power flow analysis

The functional constraints given in equations (5.25) and (5.26) are the objective function of power flow analysis, i.e., a balanced state between the loads' and generations' active and reactive power within a power system. Usually, the load's active and reactive power are known and fixed, while the generator's active and reactive power are unknown and have an upper and lower bond. In achieving the objective of the power flow analysis, at least the power system has one slack (swing) bus as the reference where it voltage magnitude and phase angle are defined. This bus should inject the differences between the total power generated from other generators and the total demand which includes loads' consumed power and the power loss in the system network. The buses where the active and reactive power are specified but the voltage and phase angle are unknown, are termed as the load (P-Q) busses. On the other hand, on the generator (regulated) busses, the voltage and active power are known, while the voltage phase angle and the buses' reactive power are the parameters that will be calculated by conducting a load flow analysis [138, 139].

Both the Gauss-Seidel and Newton Raphson method use the iterative technique. It is assumed that the solution of a one-dimensional function is equal to its initial value plus its partial derivative (the small differences per iteration step) of the unknown parameter. The Newton Raphson method uses the Jacobian ($\underline{J}$) matrix, an element of which is the partial derivative of the known to the unknown states. The Jacobian ($\underline{J}$) matrix is defined as

$$\underline{J} = \left[\begin{array}{ccc|ccc} \frac{\partial f(P_1)}{\partial \delta_1} & \cdots & \frac{\partial f(P_1)}{\partial \delta_k} & \frac{\partial f(P_1)}{\partial |V_1|} & \cdots & \frac{\partial f(P_1)}{\partial |V_k|} \\ \vdots & \ddots & \cdots & \vdots & \ddots & \cdots \\ \frac{\partial f(P_k)}{\partial \delta_1} & \cdots & \frac{\partial f(P_k)}{\partial \delta_k} & \frac{\partial f(P_k)}{\partial |V_1|} & \cdots & \frac{\partial f(P_k)}{\partial |V_k|} \\ \hline \frac{\partial f(Q_1)}{\partial \delta_1} & \cdots & \frac{\partial f(Q_1)}{\partial \delta_k} & \frac{\partial f(Q_1)}{\partial |V_1|} & \cdots & \frac{\partial f(Q_1)}{\partial |V_k|} \\ \vdots & \ddots & \cdots & \vdots & \ddots & \cdots \\ \frac{\partial f(Q_k)}{\partial \delta_1} & \cdots & \frac{\partial f(Q_k)}{\partial \delta_k} & \frac{\partial f(Q_k)}{\partial |V_1|} & \cdots & \frac{\partial f(Q_k)}{\partial |V_k|} \end{array}\right] \tag{5.27}$$

where $\frac{\partial f(P_1)}{\partial \delta_1}$ denotes the partial derivative of the bus's active power toward its phase angle.

In this study, the known states are the voltage angle and magnitude of the slack bus, the injected active power, voltage magnitude at the generator bus, load's active and reactive power,

and the impedance of the lines. With these given known states, the angle and voltage magnitude at all the buses can be calculated as

$$\begin{bmatrix} \delta_k \\ |V_k| \end{bmatrix}^{t+1} = \begin{bmatrix} \delta_k \\ |V_k| \end{bmatrix}^{t} - \left[\underline{J}^{-1} \right] \begin{bmatrix} P_k \\ Q_k \end{bmatrix} \tag{5.29}$$

where t is the index for the iteration steps.

5.2.2.2 Active power – voltage droop control

In a power system which consists of induction or synchronous generators, the network will have an inertia response. Therefore, an accurate load share is important to prevent over-shedding. The voltage magnitude per node drops proportionally alongside the distance between the correlated node and the generation or feeder bus. Therefore, each node will have different voltage droop constant which varies following the rise and fall of its active and reactive power. Focussing on the voltage correction, in this paper, the *P-V* droop control method is used to calculate the amount of active power that should be reduced in a node that is facing under-voltage.

The *P-V* droop constant is calculated by repeating the Newton-Raphson power flow analysis process, whereby with each repetition, the amount of active and reactive power of the affected node is reduced. Then, the droop constant is calculated by linearising the power flow analysis results using a simple linear regression as

$$P_k^{\text{adjusted}} = a + \left(b \times \left| V_k^{\text{adjusted}} \right| \right) \tag{5.30}$$

where P^{adjusted} denotes the adjusted active power of the affected load bus when the magnitude voltage is adjusted to $\left| V^{\text{adjusted}} \right|$, a is the intercept, and b is the droop gain.

If there is "*N*" OPF repetition, then a and b are defined as

$$a = \frac{\sum_{n=1}^{N} P_k^n \times \sum_{n=1}^{N} (|V_k|^n)^2 - \sum_{n=1}^{N} |V_k|^n \times \sum_{n=1}^{N} |V_k|^n \times P_k^n}{N \times \sum_{n=1}^{N} (|V_k|^n)^2 - \left(\sum_{n=1}^{N} |V_k|^n\right)^2} \tag{5.31}$$

$$b = \frac{N \times \sum_{n=1}^{N} |V_k|^n \times P_{\text{j}}^n - \sum_{n=1}^{N} |V_k|^n \times \sum_{n=1}^{N} P_k^n}{N \times \sum_{n=1}^{N} (|V_k|^n)^2 - \left(\sum_{n=1}^{N} |V_k|^n\right)^2} \tag{5.32}$$

Referring to the result from (5.1), the amount of active power to be reduced (ΔP_k) is defined as

$$\Delta P_k = P_k^{\text{adjusted}} - P_k \tag{5.33}$$

The amount of reactive power to be deferred is calculated by assuming that the power factor at the affected bus remains unchanged.

$$\Delta Q_k = \Delta P_k \frac{\sin \theta_k}{\cos \theta_k} \tag{5.34}$$

where ΔQ is the targeted load's reactive power to be reduced.

5.2.2.3 Load adjustment

From this section onwards, the methods described above are developed and evaluated in MATLAB. Now, let us consider a small-radial microgrid which is shown in Fig. 5.5 as the modelled microgrid to simulate the effect of RESs fluctuation on the voltage deviation in the microgrid. This microgrid consists of a diesel generator (DG), and it is assumed as the slack unit, a PV system, four load busses, and the 6 kV distribution line.

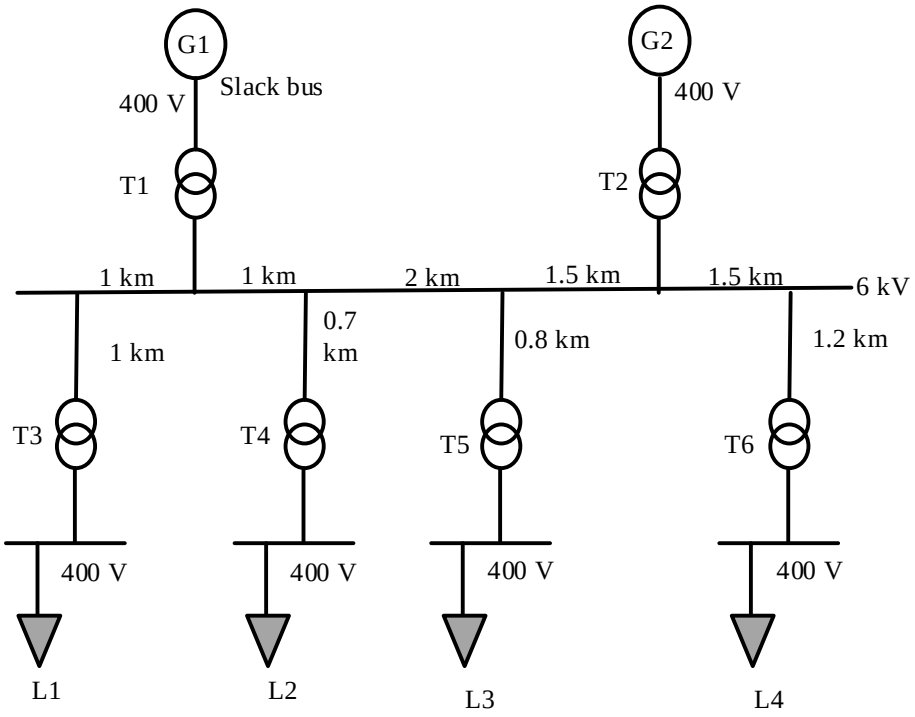

Figure 5.5 The modelled microgrid.

A specific line length between buses is established to simulate the effects of the distance between the load and generator buses on the load bus voltage. The microgrid lines' impedance is (1.0697 + *i* 1.666) ohm/km. The grid's S_{base} is 200kVA while its transformers impedance is 4% of its capacity. The total load capacity of each bus is listed in Table. 5.2. By representing the proposed grid in the per unit (pu) system, there will be 10 nodes (buses) as shown in Fig. 5.6.

Table 5.2 The capacity of each load bus.

Load bus	Active power (W)	Reactive power (VAr)
L1	35740	17800
L2	27240	12240
L3	92570	37690
L4	72530	33260

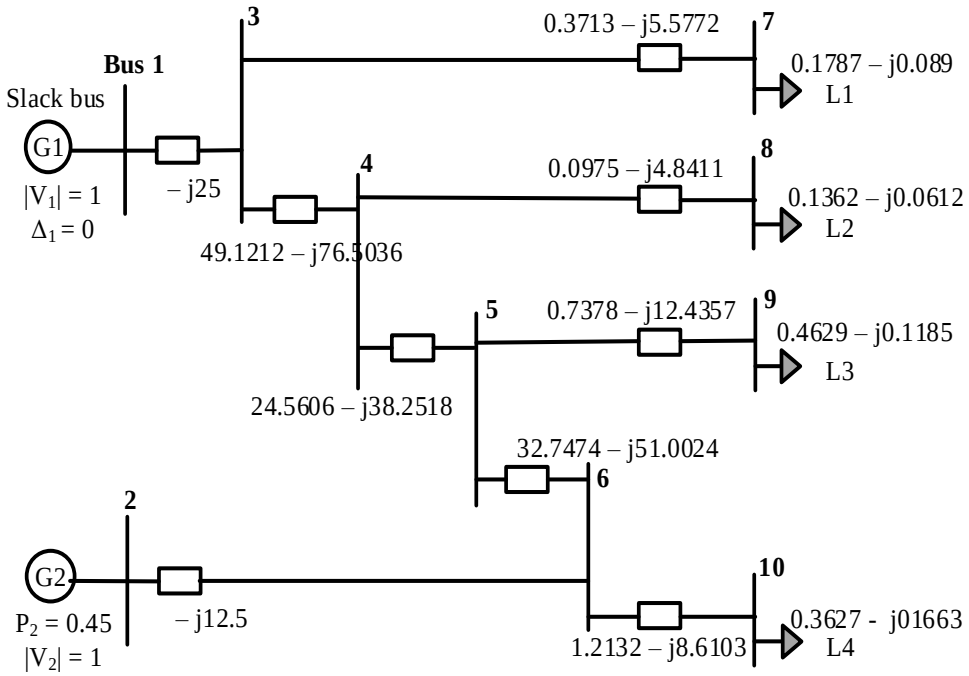

Figure 5.6 The modelled microgrid represented in pu system.

The power flow analysis is performed with a slack bus voltage set to $1\angle 0^{o}$ pu. During the experiment, around seven iterations were required for the Newton Raphson method to obtain a convergence result. Fig. 5.7 shows the power flow analysis result.

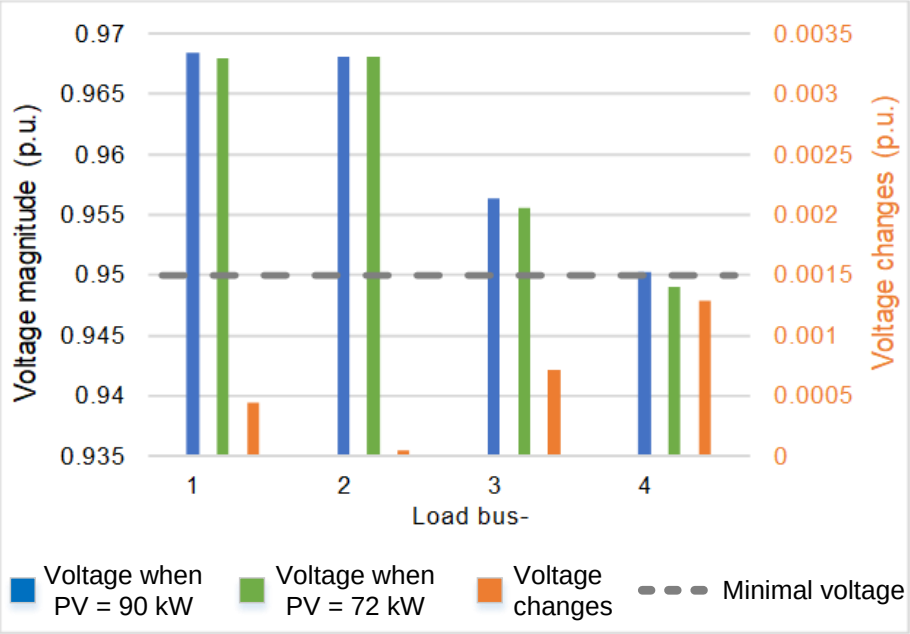

Figure 5.7 Load bus voltage when PV power is 90 and 72 kW.

When the injected power from the PV system is 90kW, all the load buses are within the allowed voltage magnitude. However, when the PV system's active power decreases to 72kW, only bus-L4 encounters under-voltage, i.e. 0.947 pu. It can be seen that bus-L4, the location of which is the farthest from the generation bus, suffers the biggest voltage reduction. On the other hand, bus-L2 encounter the smallest voltage drop because this bus is the nearest node, and it also has the smallest load' capacity; note that the power dissipated on the distribution network increases in proportion to its total line impedance and the current flows in it.

Let us consider that bus-L4 of the modelled microgrid needs to have a voltage magnitude of 0.955 pu. As shown in Fig. 5.7, that after the PV output power is decreased from 90 to 72 kW, load bus-4, the distance from the feeder bus is the farthest encountered under voltage. As mentioned before, line losses contribute to the voltage drop [140]; thus, the farther a load bus is located from the generation unit, the greater will be its drop in voltage.

In this thesis, by repeating the Newton-Raphson power flow analysis 15 times, and using the results as the input for the linear regression, the droop constant is determined. During the simulation, the PV system output power is set to 72kW while the capacity of the bus-L4 is decreased with each step to reduce the bus-L4 capacity by 0.2%. Results of this repetition are shown in Fig.5.8. Using equations (5.31) and (5.32), the intercept a and droop gain b are retrieved; a is 1.66E+06 and b is 1.67E+06.

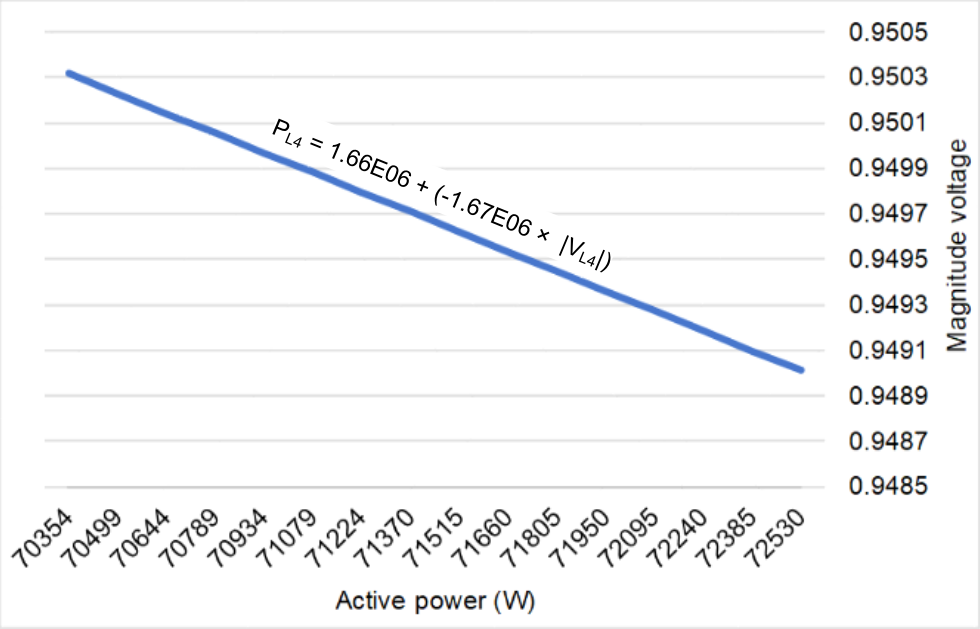

Figure 5.8 The L4-bus active power-voltage droop.

Further, let us consider that the desired adjusted magnitude voltage is 0.95 pu; then, using the retrieved a and b the load capacity of bus-L4 is adjusted from 72530 Watt and 33260 VAr to 70880 Watt and 32503 VAr. With this load adjustment and again using the Newton-Raphson method, the voltage magnitude is checked as shown in Fig. 5.9. This figure shows that the voltage is corrected to 0.95 pu as desired. Moreover, other load buses' voltage profiles are also improved.

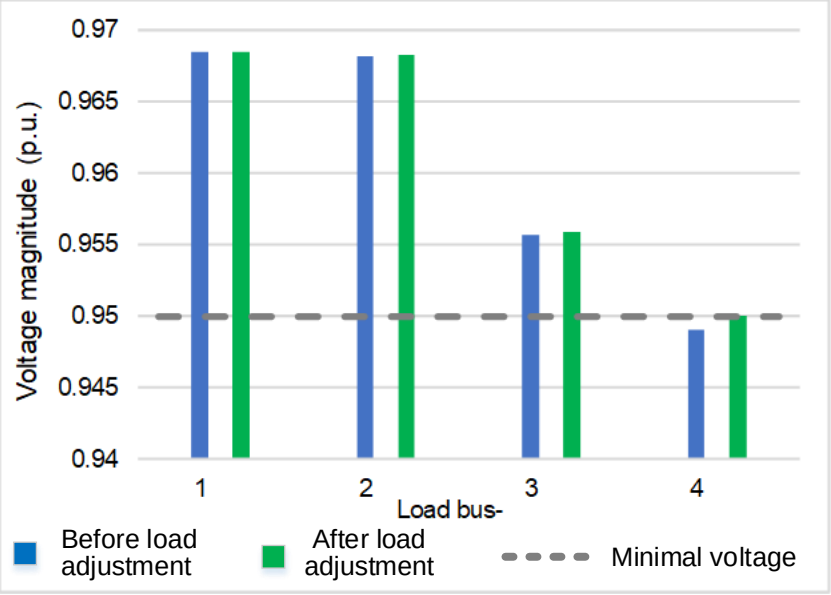

Figure 5.9 Buses' voltage before and after load adjustment.

5.2.2.3 Load-shedding optimization

Assumed that the desired adjusted magnitude voltage is 0.955 pu; then, using the proposed *P-V* droop control, it has resulted that the bus-L4 capacity should be adjusted to 64693 W and 29666 Var. This means that the bus-L4 capacity is reduced by 7837 W and 3594 Var. To simulate the GA optimisation in selecting the best combination of the shed loads, let us assumed that bus-L4 is supplying 40 loads as listed in Table 5.3.

In this study, the GA objective is to minimise the number of affected loads and meet the constraint of load adjustment capacity. The adjusted capacity must be bigger and as close as the targeted power to be reduced. Let us also assume that the upper bond of the adjusted power is 10% of the targeted power to be reduced. Minimising the number of affected loads is the highest priority for GA optimization to be fulfilled with the assumption that a smaller number of controlled loads means a faster restoration time. On the other hand, the reactive power constraint is the least priority, since a smaller reactive power will improve the system power factor.

Table 5.3 Bus-L4's loads.

Load no.	1	2	3	4	5	6	7	8	9	10
P (W)	680	2220	1590	360	4520	2350	3650	3740	520	2740
Q (Var)	230	1620	1160	310	2820	1150	1880	2230	140	1390
Load no.	11	12	13	14	15	16	17	18	19	20
P (W)	5400	1180	3250	1820	2270	1150	370	140	580	200
Q (Var)	3500	790	2240	830	1880	-480	190	0	40	0
Load no.	21	22	23	24	25	26	27	28	29	30
P (W)	360	210	2000	250	1300	3000	4500	5650	180	2220
Q (Var)	180	90	-420	70	0	2030	2050	3340	0	1790
Load no.	31	32	33	34	35	36	37	38	39	40
P (W)	1180	1650	730	2270	2360	600	860	1700	440	2340
Q (Var)	250	-460	240	-950	1060	270	230	150	0	1420

The chosen combinations of the shed loads are listed in Table 5.4. From this table, it can be seen that from the five attempts of GA optimization, the number of shed loads is minimised. The total capacity of the shed loads is also resulting in a value which is higher and close to the

amount of active and reactive power to be reduced. Table 5.4 also shows bus-L4's voltage after load adjustment. It is noted that the voltage of bus-L4 is around the desired voltage magnitude.

Table 5.4 Results of 5 attempts GA implementation.

No.	Total reduced P (W)	Total reduced Q (Var)	Index of the chosen loads	Voltage after load adjustment (pu)
	Target: 7837 W	Target: 3594 VAr		
	Upper bound: 8621	Upper bound: 3953		Target: 0.955
1.	7890	3780	8, 16, 26	0.955114
2.	8400	3650	11, 25, 38	0.955110
3.	7980	3650	12, 16, 28	0.955024
4.	8550	3660	7, 13, 32	0.955149
5.	7840	3940	8, 19, 31, 40	0.955238

5.3 Summary

This chapter has shown that demand response can improve the stability of microgrid. The studies show that by preserving the power of the grid-forming unit, the proposed load-shedding scheme, which is based on the BES's SoC level, can prolong the energy supply to the microgrid's critical loads. Furthermore, it is shown that the proposed *P-V* droop control method, which determines the amount of the adjusted capacity of the connected loads on a bus within a microgrid, can successfully restore the bus voltage. The studies have also shown that in order to minimise the number of affected loads as well as the demand response costs, a load with a higher capacity and discomfort tolerance level but small economic benefits can be controlled more often.

Chapter 6 Determining the Demand Response Incentive

In this chapter, an approach has been presented for determining the customer incentives that take into consideration of load' and customer' types to minimise the discomfort felt by the participants as well as maximise the microgrid owner's profit. The proposed demand response optimisation is simulated and evaluated in a modelled microgrid. Further, the incentives are calculated and used to analyse the feasibility of the demand response deployment in microgrids. The feasibility is examined in terms of the demand response project payback period. Moreover, sensitivity analysis is conducted to investigate the effect on the demand response feasibility of the allocated fund for incentives and the load variation.

6.1 The Concept

The development of demand response programs is relatively slow. First, both the microgrid operator and the customer have to purchase the demand response enabling technologies. The need for enabling technologies varies based on the automated level of the demand response program chosen by the customers. For example, a fully automated demand response program needs advanced software and hardware for its control mechanism, and the conventional load may need to change to smart load. Besides, the microgrid operator needs to provide incentives to compensate for the customers' demand response deployment costs and comfort reduction as a side effect of demand response execution.

The types of incentives presented in [141, 142] are:

- Indirect incentive: mostly for demand response program based on electricity price variation such as peak/off-peak, time of use, critical peak, and seasonal rate. The utility needs to send a signal price to the participants

- Upfront incentive: the incentive to install the meter and upgrade system and equipment. Mostly for the demand response program which requires a response, such as the DR program which is intended for frequency correction

- Fixed per period:
  - based on nominated capacity or number of events, regardless whether it is called during demand response events;
  - annually (kW-year), monthly (kW-month)

- Performance-based: based on the actual performance during demand response events, such as the total kWh reduction during demand response event and monthly performance ratio between the shed load (kW) and the nominated capacity (kW)

- Market program: through a bidding process in the real-time and day-ahead market. Participants are paid based on the clearing price. Include penalty for the non-performance of the nominated capacity.

- Special contract: available for industrial and commercial customers. The compensation varies, case-by-case per contract and may include a penalty for non-performance.

It is stated in [141, 143] that the demand response incentive should be efficient so that both the utility and the customers obtain high net profits. For example, the Hawai utility on its DLC program for commercial and industrial customers gives incentives of $5 - 10/kW-month of the nominated load and an additional $0.5/kWh for the reduction during shedding events. However, this incentive is considered inefficient because the cost of the incentive is higher than the cost of dispatching the high-cost peaking generation unit. Therefore, this study performs a feasibility study of demand response implementation in microgrid by comparing the ratio of demand response costs and the benefits to calculate the incentives that can/should be given to compensate the participants.

6.1.1 Demand Response Costs

To engage in the demand response program, customers need to have the appropriate enabling technologies such as smart meters, routers for communication and primary controllers for each controlled electric appliance. The costs for residential customers will be less than those

for commercial customers that may even need additional upgrading or retrofitting of their control systems. Meanwhile, the demand response aggregator incurs additional costs for the development of the demand response program to include extra communication and computation across the network.

A microgrid may already comprise some of the required demand response enabling technologies. One good example is the smart meters, as well as the communication technologies, up to a limit. However, additional costs may be needed for system upgrading to adjust the existing technologies to the requirements of the proposed demand response program. Therefore, the total initial costs for the demand response deployment can be formulated as

$$Cost_{\mathrm{int}} = Cost_{\mathrm{ET}} + Cost_{\mathrm{SU}} + Cost_{\mathrm{MA}} \tag{6.1}$$

where

$$\begin{aligned} Cost_{\mathrm{ET}} &= Cost_{\mathrm{ET}}^{\mathrm{res}} + Cost_{\mathrm{ET}}^{\mathrm{com}} \\ &= \sum_{i=1}^{N_{\mathrm{cus}}} (cost_{\mathrm{m}}^{i} + cost_{\mathrm{co}}^{i} + cost_{\mathrm{inst}}^{i} + cost_{\mathrm{up}}^{i}) \end{aligned} \tag{6.2}$$

$$Cost_{\mathrm{ma}} = r_{\mathrm{MA}} \times Profit_{\mathrm{DR}} \tag{6.3}$$

where $Cost_{int}$, $Cost_{et}$, $Cost_{su}$, and $Cost_{ma}$ are the initial, enabling technology, system upgrading, and marketing costs; superscripts *res* and *com* refer to the residential and commercial customers; $cost_m$, $cost_{co}$, $cost_{inst}$ and $cost_{up}$ are the cost for meters, communication technologies, installation, and upgrading equipment; r_{ma} is the percentage of the profit (denoted by $Profit_{DR}$, defined in below) used for marketing and k ($1 \leq k \leq N_{\mathrm{cus}}$) denotes the customer index.

6.1.2 Demand Response Benefits

Assuming a grid-connected microgrid, the first benefit of deploying the demand response program is a reduction of the cost of purchasing additional energy from the upstream grid. Moreover, with demand response shifting program, some of the loads which are usually operated during peak period can be shifted to non-peak periods when the electricity spot price is lower. In addition, a reduction in the amount of power consumed will indirectly reduce power loss in the distribution line, as well as CO_2 emissions. The benefits of CO_2 reduction can be

quantified based on the carbon tax policy and the CO_2 emission factor associated with electricity-producing [32].

The additional profits of demand response implementation (denoted by $Profit_{\mathrm{DR}}^{h}$)) are calculated as the difference between the microgrid's ongoing revenue and cost of energy before and after implementing the demand response program (respectively denoted by $Profit^{\mathrm{DR},h}$ and $Profit^{h}$); i.e.,

$$Profit_{\mathrm{DR}}^{h} = Profit^{\mathrm{DR},h} - Profit^{h} \tag{6.4}$$

where

$$Profit^{h} = Revenue^{h} - Cost_{\mathrm{ES}}^{h} - Cost_{\mathrm{CO_2}}^{h} \tag{6.5}$$

in which $Revenue^{h}$, $Cost_{\mathrm{ES}}^{h}$ and $Cost_{\mathrm{CO_2}}^{h}$ respectively denote the microgrid's income from supplying electricity to the customers, its cost of energy supply, and its carbon tax resulting from CO_2 emission, and h is the time index (e.g., in hours).

The $Revenue^{h}$ in (6.5) is calculated by considering the amount of power supplied to the loads (denoted by P_{load}^{h}), the energy tariff of the loads (denoted by $Tariff_{\mathrm{cus}}^{h}$) and the duration of the supply (denoted by T) from

$$Revenue^{h} = P_{\mathrm{load}}^{h} \times Tariff_{\mathrm{cus}}^{h} \times T \tag{6.6}$$

Again, in (6.5), $Cost_{\mathrm{ES}}^{h}$ can be defined based on the fuel cost of the generators owned and operated by the microgrid (denoted by $Cost_{\mathrm{fuel}}^{h}$), the energy transaction cost with the upstream grid (denoted by $Cost_{\mathrm{ET}}^{h}$) and the wear cost, if any, of the BES within the microgrid, (denoted by $Cost_{\mathrm{BES}}^{h}$) in the form of

$$Cost_{\mathrm{ES}}^{h} = Cost_{\mathrm{fuel}}^{h} + Cost_{\mathrm{BES}}^{h} + Cost_{\mathrm{ET}}^{h} \tag{6.7}$$

in which

$$Cost_{\mathrm{fuel}}^{h} = Fuel^{h} \times Tariff_{\mathrm{fuel}}^{h} \tag{6.8}$$

$$Cost_{\mathrm{BES}}^{h} = \frac{Cost_{\mathrm{BES}}^{\mathrm{rep}} \times \left|P_{\mathrm{BES}}^{h}\right| \times T}{E_{\mathrm{th}} \times \sqrt{\eta}} \tag{6.9}$$

$$Cost_{ET}^{h} = Cost_{\mathrm{imp}}^{h} - Revenue_{\mathrm{exp}}^{h} \tag{6.10}$$

where $Fuel^h$ and $Tariff^h_{\text{fuel}}$ are the amount of fuel consumption for the generators owned and operated within the microgrid and its unit purchase price, $Cost^{\text{rep}}_{\text{BES}}$, E_{th}, η and P^h_{BES} are the BES's replacement cost, throughput energy, round trip efficiency, and the discharging power; and $Cost^h_{\text{imp}}$ and $Revenue^h_{\text{exp}}$ are respectively the cost of importing a power of P^h_{imp} from the upstream grid and exporting P^h_{exp} to that, respectively at rates of $Tariff^h_{\text{imp}}$ and $Tariff^h_{\text{exp}}$, defined by

$$Cost^h_{\text{imp}} = P^h_{imp} \times Tariff^h_{\text{imp}} \times T \tag{6.11}$$

$$Revenue^h_{\text{exp}} = P^h_{\text{exp}} \times Tariff^h_{\text{exp}} \times T \tag{6.12}$$

The difference between the consumed and the generated power within a microgrid (denoted by P^h_{DCG}) can be calculated with

$$P^h_{\text{DCG}} = P^h_{\text{load}} + P^h_{\text{loss}} - P^h_{\text{BES}} - P^h_{\text{RES}} - P^h_{\text{Gen}} \tag{6.13}$$

where P^h_{loss} is the power loss in the microgrid's network, while P^h_{RES} and P^h_{Gen} are respectively the generated power by the renewable energy resources and the generated power by the generators owned and operated in the microgrid. If $P^h_{\text{DCG}} > 0$, then $P^h_{\text{imp}} = P^h_{\text{DCG}}$. However, if $P^h_{\text{DCG}} < 0$, $P^h_{\text{exp}} = P^h_{\text{DCG}}$. Note that, P^h_{BES} is positive during discharging and negative when charging.

Now, from (6.1) and (6.4), the NPV of deploying the demand response program over N years (i.e., the project lifetime) can be defined from

$$Profit^{\text{NPV}}_{\text{DR}} = \sum_{y=1}^{N_{\text{year}}} \frac{Profit^y_{\text{DR}}}{(1+RDR)^{y-1}} - Cost_{\text{int}} \tag{6.14}$$

where RDR is the real discount rate.

6.1.3 Microgrid Tariff

Large interconnected power systems usually have low-cost central generations; thus, their levelized cost of energy (LCOE) is usually cheaper than that of a microgrid. Moreover, electricity tariff structure in some countries may include subsidies so that the tariff does not reflect the actual cost of energy production. Thus, the microgrid operator may encounter financial loss if

offers the same tariff to its customers as that of the upstream grid. Hence, some studies such as [144, 145] have focused on determining the energy tariffs for the customers in a microgrid. With the discounted method in [146, 147], the microgrid LCOE can be calculated as

$$LCOE = \frac{\sum_{y=1}^{Y} \frac{Cost_{\text{invest}}^{y} + Cost_{\text{O\&M}}^{y} + Cost_{\text{fuel}}^{y} + Cost_{\text{ET}}^{y}}{(1+R_{\text{disc}})^{y}}}{\sum_{y=1}^{Y} \frac{\left(E_{G}^{y} + E_{\text{imp}}^{y}\right)}{(1+R_{\text{disc}})^{y}}} \quad (6.15)$$

where $Cost_{\text{invest}}$ is the investment costs for deploying the microgrid such as the cost for purchasing generator unit, renewable power plant, BES, and building the MG distribution network; while $Cost_{\text{O\&M}}$ is the microgrid operating and maintenance cost.

With the $LCOE$ defined in (6.15), the electricity tariff in the microgrid is formulated as

$$Tariff_{\text{cus}}^{\text{peak},h} = \left(1 + r_{\text{profit}}\right) \times LCOE \times r_{\text{peak}} \quad (6.16)$$

$$Tariff_{\text{cus}}^{\text{off-peak},h} = \left(1 + r_{\text{profit}}\right) \times LCOE \times r_{\text{off-peak}} \quad (6.17)$$

where r_{profit} is the ratio of the microgrid operators' desired profit versus the experienced LCOE while

$$r_{\text{peak}} = 1 + \frac{\sum_{y=1}^{N_{\text{year}}} E_{\text{imp}}^{y}}{\sum_{y=1}^{Y} E_{G}^{y} + \text{E}_{\text{imp}}^{y}} \quad (6.18)$$

$$r_{\text{off-peak}} = \frac{\sum_{y=1}^{N_{\text{year}}} E_{G}^{y} + E_{imp}^{y} + \left(E_{G}^{y}\right)^{2} - \left(E_{\text{imp}}^{y}\right)^{2}}{\sum_{y=1}^{N_{\text{year}}} \left(E_{G}^{y}\right)^{2} + E_{G}^{y} + E_{\text{imp}}^{y}} \quad (6.19)$$

in which E^{y} denotes the annual energy in year-*y*, and

$$E_{G}^{y} = E_{\text{Gen}}^{y} + E_{\text{RES}}^{y} + E_{\text{BES}}^{y} \quad (6.20)$$

6.1.4 Demand Response Incentives

Fig. 6.1. shows the flowchart of the proposed method for determining the demand response incentives. The microgrid operator gives incentives, as compensation, to the demand response participants. To ensure that the microgrid operator will not face financial loss by providing an incentive, a percentage of the profit obtained through demand response (denoted

by r_{inc}) is used as the total incentive (denoted by Inc_{NPV}), i.e.,

$$\mathrm{INC}_{NPV} = \mathrm{r_{inc}} \times \mathrm{Profit}_{DR}^{NPV} \tag{6.21}$$

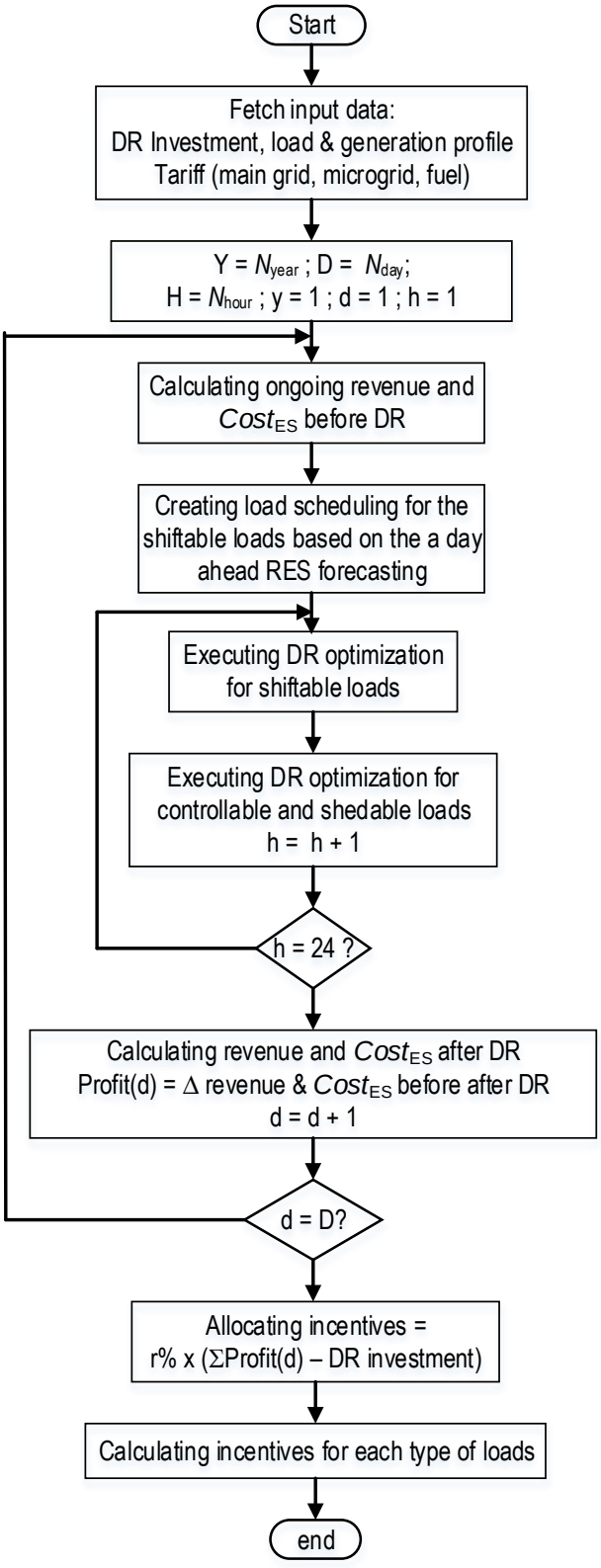

Figure 6.1 Flowchart of the demand response incentives calculation.

A demand response action in the form of load-shifting may provide more profit to the microgrid operator than a load-shaving action for controllable loads, as the microgrid operator will continue to receive revenue from selling electricity to the shifted loads later. On the other hand, even though the customers will benefit from bill reduction when some of their loads are shifted to the off-peak rate, this bill reduction may not be as great as when their loads are shaved.

Hence, in this thesis, the customers' discomfort level and the loads' economic value are taken into consideration when determining the percentage from the allocated incentives fund for each load type. Therefore, with the predefined loads weighting the incentive is defined as

$$INC_{\text{base}}^{y} = \frac{INC_{\text{NPV}} \times (1 + RDR)^{\text{y}-1} \times \left(E_{\text{load}}^{\text{DR,y}} - E_{\text{load}}^{\text{y}}\right)}{(E_{\text{shift}} + E_{\text{cont}} + E_{\text{shed}}) \times \sum_{y=1}^{N_{\text{year}}} E_{\text{load}}^{\text{DR},y} - E_{\text{load}}^{y}} \tag{6.22}$$

$$E_x = \sum_{h=1}^{8760} \sum_{n=1}^{N_{\text{load}}} P_n^h \times \omega_{x_1} \times EV_{x_2} \times T \tag{6.23}$$

where $x_1 \in \{\text{shift}, \text{cont}, \text{shed}\}$ and $x_2 \in \{\text{res}, \text{com}\}$ denote the load and customer type respectively, N_{load} is the number of loads for the customers participating in the demand response scheme, ω denotes the weighting of the load type, and EV is the economic value of the customers.

From (6.22), the demand response incentive offered to each load of a customer (in \$/kWh) can be defined from

$$INC_{x_1} = INC_{\text{base}} \times \omega_{x_1} \times EV_{x_2} \tag{6.24}$$

considering the load type and the customer's economic value. Note that, commercial customers are assumed to have a higher economic value than residential customers (i.e., $EV_{\text{com}} > EV_{\text{com}}$). This economic value is assumed the same for all residential customer but can be different for various commercial customers.

6.2 Mathematical Modelling for the Microgrid DERs

When analysing the effects of deploying a demand response program in the microgrid, either the cost and the output power of the microgrid DERs need to be represented in the related mathematical modelling. This section describes the mathematical modelling of the PV system

output power and its forecasting, the fuel used by the diesel generator, the BES charge and discharge process, and the power loss in the microgrid network.

6.2.1 PV Forecasting

Because the modelled microgrid consists of a PV system and the modelled shift-able loads have their preferred time to be shifted, in choosing the neighbourhood load's operating time, the PV output prediction is taken into consideration so that load-shifting will not create another peak load because of over-shifting. Solar insolation can be forecasted either using a stochastic, time series, or artificial intelligence method [148, 149].

As in this study, only a series of historical insolation data is available; thus, a time series method is used in predicting solar insolation. Seasonal auto-regressive integrating moving average (ARIMA) model is used with its seasonal *P* (regression), *D* (differencing), *Q* (moving average) order is 2, 1, 1. The S (seasonal) order is set to 24 as the model will predict a day-ahead (24 hours) solar insolation based on a series of hourly insolation data. Using the backshift operator (B), the model can be presented as

$$\varphi_P(B^S)(1-B^S)^D Z_h = \theta_Q(B^S)e_h \tag{6.25}$$

$$\varphi_3(B^{24})(1-B^{24})^1 Z_h = \theta_1(B^{24})e_h \tag{6.26}$$

$$\hat{Z}_h = (1+\varphi_1)Z_{h-24} + (\varphi_2-\varphi_1)Z_{h-48} + (\varphi_3-\varphi_2)Z_{h-72} - \varphi_3 Z_{h-96} - \theta_1 e_{h-24} + e_h \tag{6.27}$$

where Z_h and $\hat{Z}_h$ are respectively denote the measured and predicted insolation at hour *h*, while φ and θ are the constants for the auto-regressive (AR) and moving average (MA) operator (autocorrelation function) respectively.

Disregarding climatic variation, this study considers that every day, solar insolation will most likely have the same magnitude at the same hour of the day. Therefore, instead of using a single AR and MA operator through the whole 24 hours ahead prediction, this study uses difference AR and MA operator for each time of the day. These AR and MA operators are calculated using the first month series of insolation data. These AR and MA operators are estimated using auto-correlation function (ACF) as

$$\varphi_s = \frac{\text{covariance}(Z_h, Z_{h-s})}{\text{variance}(Z_h)} \tag{6.28}$$

$$\varphi_s = \frac{\sum_{h=1}^{N_{\text{hour}}}\left(Z_h - \overline{Z}\right)(Z_{h-s} - Z)}{\sum_{h=1}^{N_{\text{hour}}}\left(Z_h - \overline{Z}\right)^2} \tag{6.29}$$

where s is the seasonal range, i.e., 24 in this study and $\overline{Z}$ is the average value from the hourly insolation data. Meanwhile, to measure the performance of the proposed ARIMA model, this study considered the mean absolute error (MAE). MAE is one of the methods used to evaluate the accuracy of a prediction model. MAE is defined as

$$MAE = \frac{1}{N_{\text{hour}}}\sum_{h=1}^{N_{\text{hour}}}\left|Z_h - \hat{Z}_h\right| \tag{6.30}$$

As MAE calculates the average of the absolute difference between the predicted and the actual value, this means that all data is weighted equally. Fig. 6.2 shows the measured and predicted PV output power on two consecutive days. The MAE value calculated from the measured and predicted data of the PV output power over one year results in the MAE of 4.61 kW for a system with maximal PV output power of 100 kW.

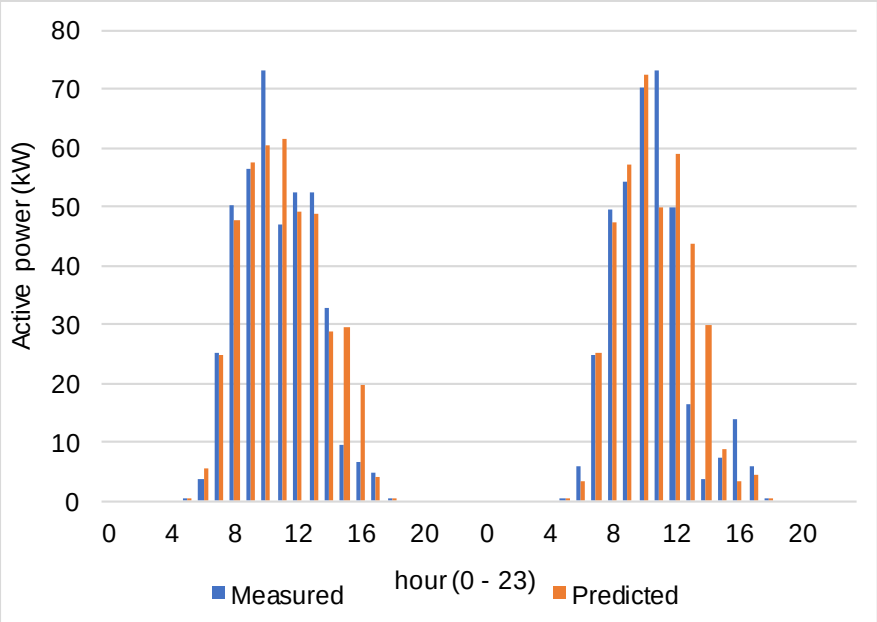

Figure 6.2 PV prediction in two consecutive days.

6.2.2 BES Utilisation

In the BES system modelling, this study uses an idealised BES model, which assumes that the BES voltage remains constant during the charge and discharge process. Therefore, the BES's SoC can be estimated using the coulomb counting method [150] as

$$SOC_h = SOC_{h-1} + \frac{I_h}{RC_{\mathrm{BES}}}\,\Delta h \tag{6.31}$$

where SOC_h and SOC_{h-1} are the BES SoC at the current and previous hour respectively, I_h is the discharge current at the current time step, RC_{BES} is the BES rated capacity, and Δh is the discharge hours.

Because the balanced parameter in this study is the microgrid's active power, where P_{BES}^{h} is the BES power at the current time step, the simplified SoC BES modelling will be calculated in kWh instead of Ah as

$$SOC_h = SOC_{h-1} + (P_{\mathrm{BES}}^{h} \times \Delta h) \tag{6.32}$$

The BES' charging and discharging processes are constrained by the BES' maximal and minimal SOC, and the BES' maximal charging and discharging power. If the remaining energy stored in the BES has reached its minimum SOC, then discharging cannot occur. Whereas, the charging process terminates when the BES has fully charged. Meanwhile, maximal charging ($P_{\mathrm{BES,charge}}^{\max}$) and discharging power ($P_{\mathrm{BES,discharge}}^{\max}$) are defined as

$$P_{\mathrm{BES,charge}}^{\max} = N_{\mathrm{BES}} \times V_{\mathrm{BES}} \times I_{\mathrm{BES,charge}}^{\max} \tag{6.33}$$

$$P_{\mathrm{BES,discharge}}^{\max} = N_{\mathrm{BES}} \times V_{\mathrm{BES}} \times I_{\mathrm{BES,discharge}}^{\max} \tag{6.34}$$

where N_{BES} is the number of batteries, V_B is the BES nominal voltage (Volt), and $I_{\mathrm{BES,charge}}^{\max}$ and $I_{\mathrm{BES,discharge}}^{\max}$ are respectively the maximal current charging and discharging (Ampere).

The lifetime of a BES is usually limited. In this study, the modelled BES lifetime is based on its life cycle. Therefore, the BES throughput is defined as the total energy from the BES charging and discharging throughout its lifetime; the BES energy throughput (E_{th}) is formulated as

$$E_{\mathrm{th}} = E_{\mathrm{BES}}^{\mathrm{rated}} \times BES_{lc} \times 2 \tag{6.35}$$

where $E_{\mathrm{BES}}^{\mathrm{rated}}$ is the BES energy rated capacity and BES_{lc} is the BES lifecycle which can be obtained in the BES datasheet. Meanwhile, as one cycle consists of charging and discharging, thus it is multiplied by "2".

In this study, it is assumed that the BES system experiences one cycle of charging and discharging per day. Thus, the BES is set to be charged during day-time when the PV system has high output power, and is allowed to discharge only during the night when the microgrid facing a power shortage and the upstream grid tariff is higher than the microgrid tariff. The depth of discharge is constrained to 80%; thus, the minimal SoC is 20%. Fig. 6.3 illustrates the charging and charging cycle of the BES.

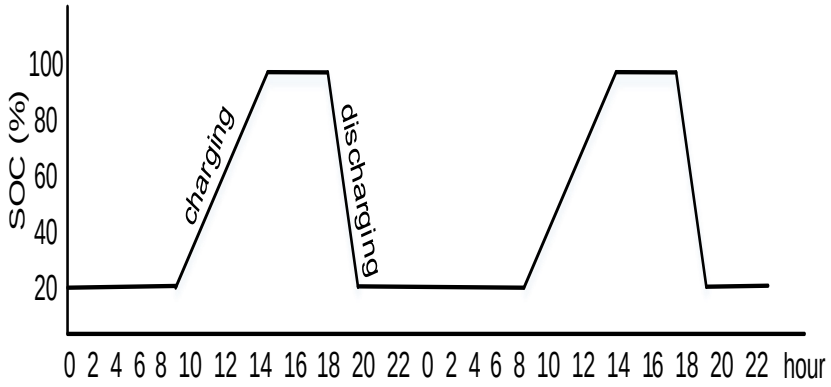

Figure 6.3 Charging and discharging cycle.

6.2.3 Fuel Used from Diesel Generation

A diesel generator will have better fuel efficiency when operated near its full load. In this paper, the diesel engine fuel curve is defined by linearising the fuel consumption data provided in its datasheet. The diesel fuel curve is formulated using a simple linear regression as

$$Fuel^h = a + \left(b \times P_{\mathrm{Gen}}^h\right) \tag{6.36}$$

$$a = \frac{\sum_{n=1}^{N_{\mathrm{DI}}} P_{\mathrm{Gen}}^n \times \sum_{n=1}^{N_{\mathrm{DI}}} (Fuel^n)^2 - \sum_{n=1}^{N_{\mathrm{DI}}} Fuel^n \times \sum_{n=1}^{N_{\mathrm{DI}}} P_{\mathrm{Gen}}^n \times Fuel^n}{N_{\mathrm{DI}} \times \sum_{n=1}^{N_{\mathrm{DI}}} (Fuel^n)^2 - \left(\sum_{n=1}^{N_{\mathrm{DI}}} Fuel^n\right)^2} \tag{6.37}$$

$$b = \frac{N_{\mathrm{DI}} \times \sum_{n=1}^{N_{\mathrm{DI}}} P_{\mathrm{Gen}}^n \times Fuel^n - \sum_{n=1}^{N_{\mathrm{DI}}} P_{\mathrm{Gen}}^n \times \sum_{n=1}^{N_{\mathrm{DI}}} Fuel^n}{N_{\mathrm{DI}} \times \sum_{n=1}^{N_{\mathrm{DI}}} (Fuel^n)^2 - \left(\sum_{n=1}^{N_{\mathrm{DI}}} Fuel^n\right)^2} \tag{6.38}$$

where a is the fuel curve intercept, b is the fuel curve slope, and N_{DI} is the number of data for the iteration which are provided in the generator's datasheet.

6.2.4 Line Losses

In this study, it is assumed that the system power factor is maintained near 1; thus, the value of reactive power is ignored. Line losses in the distribution network cause a voltage drop as

$$V_j = V_1 - I_i R_{1-j} \tag{6.39}$$

$$V_j = V_1 - \frac{P_{\text{load},j}}{V_j} R_{1-j} \tag{6.40}$$

$$V_j = \frac{V_1 + \sqrt{V_1 - (4 \times R_{1-j} \times P_{\text{load},j})}}{2} \tag{6.41}$$

$$I_j = \frac{P_{\text{load},j}}{V_j} \tag{6.42}$$

where V and I are respectively the voltage magnitude and current flows through a bus; i and j denote the index bus; V_1 is the voltage at the feeder which is assumed to be 1 pu, and R_{1-j} is the line resistance from feeder to the bus j. Therefore, the power dissipated through the transmission line is defined as

$$P_{\text{loss},j} = {I_j}^2 R_{1-j} \tag{6.43}$$

6.3 Study Case

Let us consider the microgrid system of Fig. 6.4 in the form of a radial system, consisting of a diesel generator (DG) of 450 kW, a PV system of 100 kWp, a BES of 20kWh, and two commercial buildings and 50 residential customers. Bus-1 represents the first 20 households, bus-2 supplies a commercial building, bus-3 is connected to a commercial building and 10 households, and bus-4 is connected to the 20 households.

There will be no curtailment of the power output by the PV system. Meanwhile, the DG is constrained to its minimum loading, i.e., 35% from its rated capacity. If the total amount of power consumed is lower than the DG minimum power, the microgrid will export the excess power to the upstream grid. On the other hand, prior to the implementation of the microgrid demand response program, if there is shortage power, at first the BES system will discharge its stored energy, and if the power deficiency persists, then the microgrid will import energy from the

upstream grid. On the other hand, if the microgrid has excess power, at first it will try to re-charging the BES storage, and then sell the remaining excess power to the upstream grid.

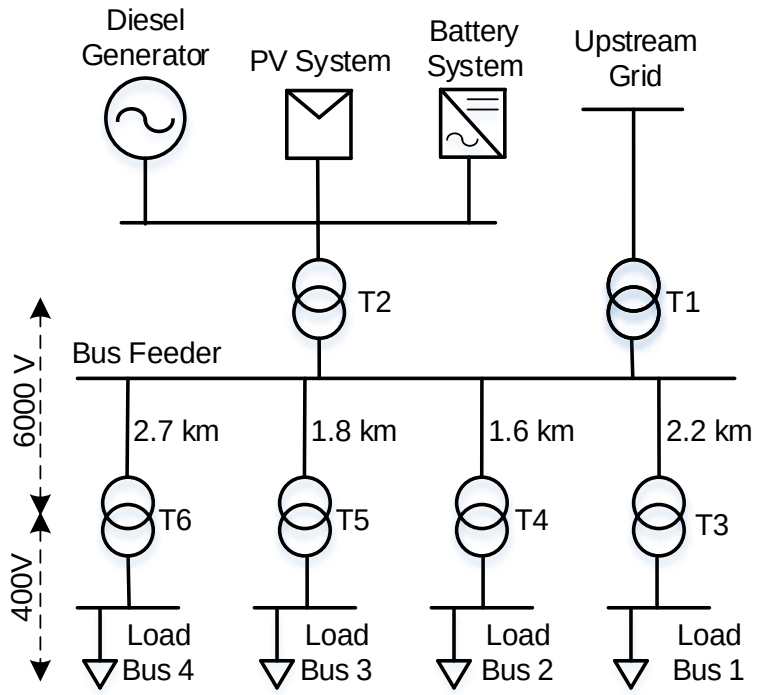

Figure 6.4 Grid-connected microgrid network under consideration.

Each customer's loads are profiled for one week on an hourly basis. The load's profile is assumed to be the same for each week. This one-week data is then extended to cover the lifetime of the program. However, the profile of solar insolation varies based on data taken from a pyranometer located in Jakarta, Indonesia; thus, demand response profit varies every day. Because the business activity in the commercial buildings takes place during weekdays only, there will be a significant difference between the load profiles for weekdays and weekends as shown in Fig. 6.5. This figure also shows the profiles of different types of loads such as shiftable, uninterruptable, controllable and shedable loads.

Fig. 6.6 illustrates typical demand and generation profiles for a typical day. The network peak period is assumed to be between 18:00 and 20:00. This figure also shows the profile of the power imported from the upstream grid. Furthermore, each load has specific information that is used to calculate the load's capacity and flexibility weighting.

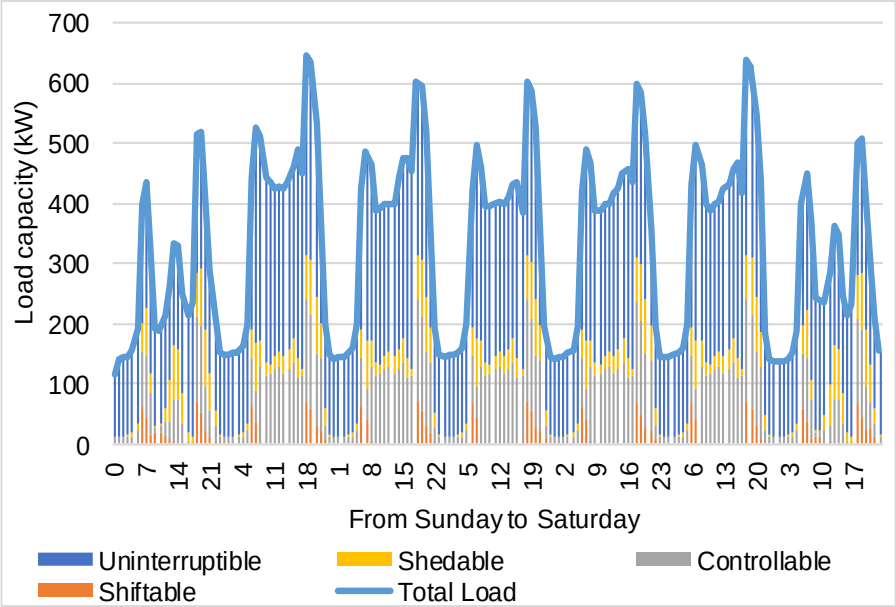

Figure 6.5 Profile of loads over one week.

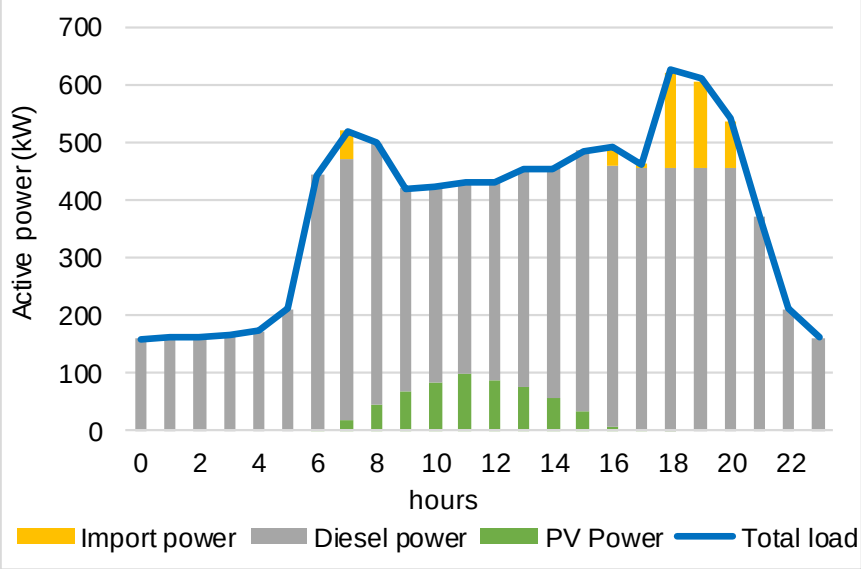

Figure 6.6 Load and generation profile in a typical day.

Table 6.1 presents the microgrid project's investment, as well as its periodic costs for the operation and maintenance (O&M) and part replacement costs. The cost of the fuel used by the diesel generator and the purchase of energy from the microgrid upstream grid in the first year of operation are also listed in Table 6.1. Note that the currency in this chapter is the Australian dollar.

Table 6.1 Microgrid development costs [42-27].

Initial costs	Price (AU$)	Annual costs	Price (AU$)
PV system (100 kWp)	157,400	PV System O&M	1,440
Diesel generator (560 kVA)	98,000	Distribution system O&M	20,238
BES (2 kWh)	14,800	Microgrid controller O&M	3,607
Network	407,690	DG maintenance	25,331
Control and protection	180,351	BES replacement	4,536
Installation and commissioning	125,867	Controller replacement	59,829
Other	188,000	Fuel used (1st year)	1,041,670
		Import energy (1st year)	67,760

The cash flow diagram in Fig. 6.7 depicts the periodic costs during the project's lifetime (25 years) with a 4% nominal discount rate and a 2% inflation rate [151, 152]. Based on the cash flow data, total capital expenditure is $1,172,108 while the NPV of total operating expenditure is $25,942,143; thus, the total cost of energy production is $\$27114251$. In this study, it is assumed that the demand profile will be the same every year; thus, the NPV of the total consumed energy is 62051837kWh. Therefore, the microgrid LCOE is:

$$LCOE = \frac{\text{NPV total cost}}{\text{total energy}} = \frac{\$27114251}{62051837\text{kWh}} = 0.436961\ \$/\text{kWh}$$

With the above LCOE and given the microgrid will earn a profit of 10%, $Tarif f_{\text{cus}}^{\text{peak},h}$ and $Tarif f_{\text{cus}}^{\text{off-peak},h}$ respectively become 0.512189 and 0.478302 $/kWh.

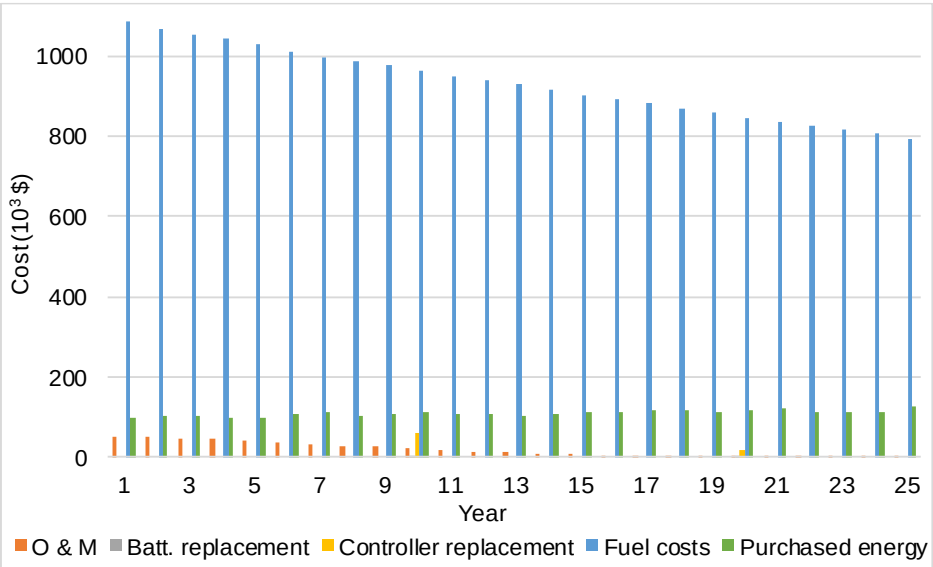

Figure 6.7 Cash flow diagram with the discounted method.

In this study, the upstream grid electricity price consists of three different tariffs for the off-peak, shoulder, and peak periods during weekdays [153]. On the other hand, in the microgrid, the peak period occurs twice a day; therefore, the microgrid tariff varies only in terms of off-peak and peak tariffs. As shown in Fig. 6.8, the upstream grid tariff is higher than the microgrid tariff from 15:00 to 21:00; hence, the microgrid may encounter losses during this period. Therefore, load-shifting, shaving, and shedding will be performed only within this time frame.

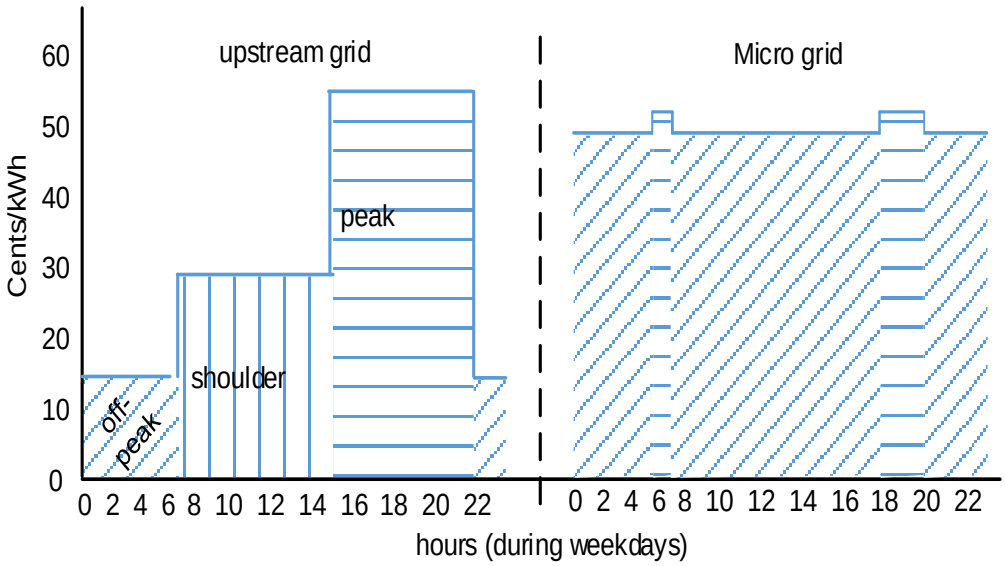

Figure 6.8 The microgrid and its upstream grid electricity tariff.

On the other hand, the demand response deployment costs are assumed as listed in Table .6.2 and Table .6.3. As reported in [154], Fort Irwin, a military installation, has been participating in the demand response program. At first, they implemented a manual demand response; however, this method did not produce the desired performance and result. Therefore, they then implemented an open automated demand response program. Therefore, in this thesis, it is assumed that the implemented demand response program is an automated demand response so that the periodic cost of demand response program management is assumed to be zero. Moreover, the periodic cost for data communication is also ignored in this study, as it is assumed that the microgrid already has a communication infrastructure.

Table 6.2 Assumed demand response deployment costs incurred at the user-end.

Item	Cost per unit ($)	Total cost ($)	Building 1	Building 2
Smart meter	330	16500	600	700
Programmable thermostat	50	2500	300	-
Switch Load control	40	2000	560	1440
Communication Module	70	3500	400	600
Installation & Commissioning	120	6000	600	1300
Miscellaneous	20	1000	300	500
smart plugin, dimmer			120	600
Energy Management System			1000	2000
Total		31500	3880	7140

Table 6.3 Assumed demand response deployment cost incurred to the microgrid operator.

Item	Cost ($)
Upgrading the billing & control system	8600
Marketing cost	1600
System developer	3400
Commissioning & installation	3800
Miscellaneous	1100
Total	18500

Tables 6.4, 6.5, and 6.6 show the examples of the loads' profile for the shiftable, controllable, and shedable loads, respectively. Each load type is represented with 10 loads. Note that customer type "1", "2", and "3" respectively denote residential, commercial-1, and commercial-2 customers and "tr" means that during the correlated day and time, the loads are being operated; while the operating day parameters from S to S denote the day from "Sunday" to "Saturday" in sequence. In the study, there are 218 shiftable loads, 155 controllable loads, and 104 shedable loads. Further, from these tables, the loads weighting capacity, flexibility, and economic value are derived.

Table 6.4 Example of shiftable loads.

No.	Appliances	Customer type	Customer index	Capacity	Operating hour	Normal operation		Allowed time		Discomfort		Operating Day						
						Start	End	Start	End	Start	End	S	M	T	W	T	F	S
1	Laundry	1	1	500	1	6	6	5	8	-1	2		*tr*	*tr*	*tr*	*tr*	*tr*	
2	Laundry	1	1	500	2	10	11	9	11	-1	0	*tr*						
3	Dryer	1	1	1500	1	7	7	9	11	2	4		*tr*	*tr*	*tr*	*tr*	*tr*	
4	Dryer	1	1	1500	2	12	13	9	11	-3	-2	*tr*						
5	Dishwasher	1	1	1800	2	21	22	5	9	-16	-13	*tr*	*tr*	*tr*	*tr*	*tr*		*tr*
6	water heater	1	1	4000	1	18	18	12	17	-6	-1	*tr*	*tr*	*tr*	*tr*	*tr*	*tr*	*tr*
7	water heater	1	1	4000	1	7	7	4	7	-3	0	*tr*	*tr*	*tr*	*tr*	*tr*	*tr*	*tr*
8	Laundry	1	2	500	1	6	6	5	8	-1	2		*tr*	*tr*	*tr*	*tr*	*tr*	
9	Laundry	1	2	500	2	7	8	7	11	0	3	*tr*						*tr*
10	water heater	1	2	3800	1	18	18	12	17	-6	-1	*tr*	*tr*	*tr*	*tr*	*tr*	*tr*	*tr*

Table 6.6 Example of controllable loads.

No	Appliances	C_{type}	C_{index}	Cap. (W)	*Flex*	ΔP_{load}	Operating Hour																						Operating Day						
							0	1	2	3	4	5	6	7	8	9	10	11	12	13	14	15	16	17	18	19	20	21	22	23	S	M	T	W	T	F	S
1	Air cond.	1	40	900	3	40								*tr*													*tr*	*tr*	*tr*		*tr*	*tr*	*tr*	*tr*	*tr*	*tr*	*tr*
2	Air cond.	1	40	1500	3	70								*tr*	*tr*				*tr*	*tr*	*tr*										*tr*						*tr*
3	water heater	1	40	3500	2	175							*tr*						*tr*						*tr*						*tr*	*tr*	*tr*	*tr*	*tr*	*tr*	*tr*
4	water heater	1	7	3800	3	190									*tr*					*tr*						*tr*	*tr*				*tr*						*tr*
5	Air cond.	1	8	1500	2	70																			*tr*	*tr*	*tr*				*tr*	*tr*	*tr*	*tr*	*tr*	*tr*	*tr*
6	Lighting	2	51	2000	4	100									*tr*	*tr*	*tr*	*tr*	*tr*	*tr*	*tr*	*tr*	*tr*	*tr*								*tr*	*tr*	*tr*	*tr*	*tr*	
7		2	51	600	3	50									*tr*	*tr*	*tr*	*tr*	*tr*	*tr*	*tr*	*tr*	*tr*	*tr*								*tr*	*tr*	*tr*	*tr*	*tr*	
8	Lighting	3	52	6000	6	300									*tr*	*tr*	*tr*	*tr*	*tr*	*tr*	*tr*	*tr*	*tr*	*tr*								*tr*	*tr*	*tr*	*tr*	*tr*	
9		3	52	8000	4	400																			*tr*	*tr*	*tr*	*tr*				*tr*	*tr*	*tr*	*tr*	*tr*	
10		3	52	8000	4	400																			*tr*	*tr*	*tr*	*tr*				*tr*	*tr*	*tr*	*tr*	*tr*	

Table 6.5 Example of shedable loads.

No.	Appliances	C_{type}	C_{index}	Cap. (W)	*Flex*	Operating Hour																							Operating Day						
						0	1	2	3	4	5	6	7	8	9	10	11	12	13	14	15	16	17	18	19	20	21	22	23	S	M	T	W	T	F	S
1	AirCond	1	37	2750	3								*tr*	*tr*											*tr*	*tr*	*tr*	*tr*	*tr*	*tr*	*tr*	*tr*	*tr*	*tr*	*tr*	*tr*	*tr*
2	AirCond	1	37	2750	2															*tr*	*tr*									*tr*						*tr*
3	Poolpump	1	39	1800	1					*tr*	*tr*	*tr*																		*tr*	*tr*	*tr*	*tr*	*tr*	*tr*	*tr*
4	Poolpump	1	39	1800	2																		*tr*	*tr*	*tr*	*tr*				*tr*	*tr*	*tr*	*tr*	*tr*	*tr*	*tr*
5	Miscellaneous	2	51	1500	1									*tr*	*tr*	*tr*	*tr*	*tr*	*tr*	*tr*	*tr*	*tr*									*tr*	*tr*	*tr*	*tr*	*tr*	
6	Miscellaneous	2	51	400	2									*tr*	*tr*	*tr*	*tr*	*tr*	*tr*	*tr*	*tr*	*tr*									*tr*	*tr*	*tr*	*tr*	*tr*	
7	Miscellaneous	3	52	490	10									*tr*	*tr*	*tr*	*tr*	*tr*	*tr*	*tr*	*tr*	*tr*	*tr*								*tr*	*tr*	*tr*	*tr*	*tr*	
8	Miscellaneous	3	52	500	3									*tr*	*tr*	*tr*	*tr*	*tr*	*tr*	*tr*	*tr*	*tr*									*tr*	*tr*	*tr*	*tr*	*tr*	
9	Miscellaneous	3	52	700	2									*tr*	*tr*	*tr*	*tr*	*tr*	*tr*	*tr*	*tr*	*tr*									*tr*	*tr*	*tr*	*tr*	*tr*	
10	Miscellaneous	3	52	1500	2									*tr*	*tr*	*tr*	*tr*	*tr*	*tr*	*tr*	*tr*	*tr*									*tr*	*tr*	*tr*	*tr*	*tr*	

Table 6.7 summarises the GA parameters used to optimize the proposed demand response program.

Table 6.7 GA parameters.

Parameter	Shiftable (daily)	Controllable (hourly)	Shedable (hourly)
Population size	$N_{\text{load}} \times 20$	$N_{\text{load}} \times Flex_{\text{cont}} \times 6$	$N_{\text{load}} \times 10$
Generation	15	26	20
Crossover probability	0.8	0.8	0.8
Mutation probability	0.02	0.01	0.02
Crossover point	random	random	random
Mutation point	random	predefined	predefined

6.3.1 Shiftable Loads

Because the output power from a PV system fluctuates depending on weather changes, one day ahead PV forecasting is used as a reference for performing load-shifting. In this study, it is assumed that loads from the commercial building cannot be shifted as this may affect business operations. In this study, it is assumed that some of the residential loads such as washing machine, dryer, and dishwasher that usually operate during peak load hours can be shifted from 5:00 am until 12:00 noon. It is also assumed that some of the households have a hot water tank; therefore, their water heater also can be shifted. However, with the consideration of heat losses, these loads can be shifted only close to their original operating time.

Fig. 6.9 and Fig. 6.10 show the results of the load-shifting under the demand response program in a day (during weekdays). Fig. 6.9 shows that some of the shiftable loads have been shifted from the peak to the off-peak period. The total amount of imported energy is reduced from 483 kWh to 388 kWh, while the total energy of the shifted load is 173 kWh. It can also be seen that as a result of load-shifting, the ongoing hourly cost and microgrid revenue have changed.

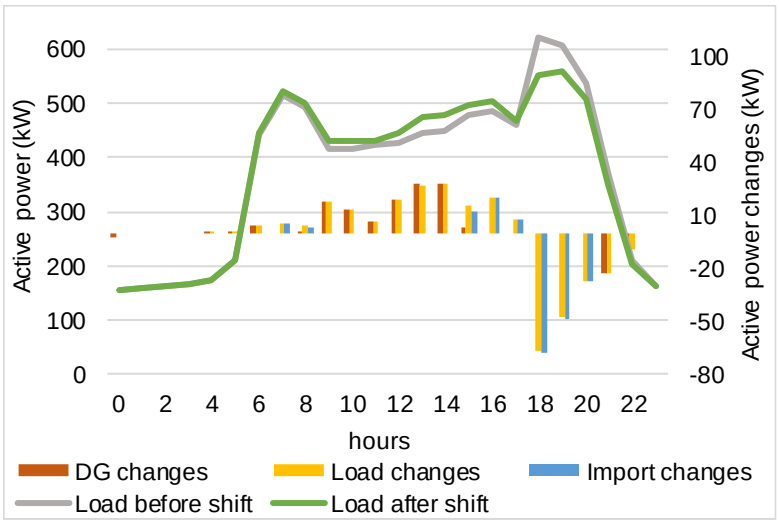

Figure 6.9 The consumed power changes after load-shifting.

Fig. 6.10 shows that the microgrid earns more profit (revenue – cost) mostly in every hour. However, during 15:00 – 17:00, the load-shifting program reduces the microgrid operator's profits because some of the water heaters were shifted to these hours when the upstream grid tariff is higher than the microgrid tariff. The microgrid operator's profit before deploying the demand response program is $1,043.24, increasing to $1,051.62 after load-shifting under the demand response program. Also, the total energy loss in the network lines has decreased from 84.8 to 83.3 kWh; as a result, the total amount of power generated to supply the microgrid is reduced. Therefore, the microgrid also earns profit from the carbon tax reduction of $0.029.

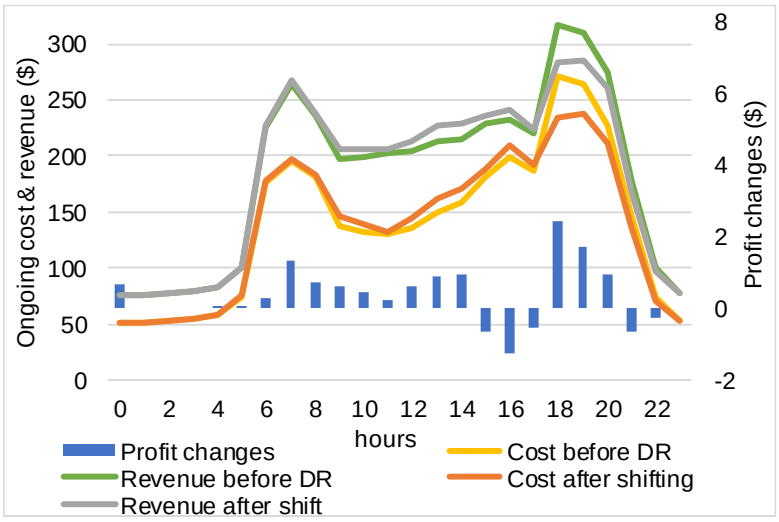

Figure 6.10 Microgrid operator's hourly cost and revenue changes after load-shifting.

Fig. 6.11 and Fig. 6.12 show the shifted load's profile. The loads that are depicted with a triangular shape are those that remain un-shifted during the demand response event. In the studied day, there are 53 available loads whose operating time can be shifted. It can be seen that, of the 53 loads, only four loads have not shifted as shown in Fig. 6.12. These four loads have 0 discomfort level. Of the 53 loads, 19 have different values of $\omega_{\text{flex}} \times \omega_{\text{cap}}$ and the four unshifted loads ranked at number 1 and 3 sorted from the smallest value. This result indicates that the proposed optimisation method has prioritised the loads which have higher capacity and flexibility to be chosen during demand response events.

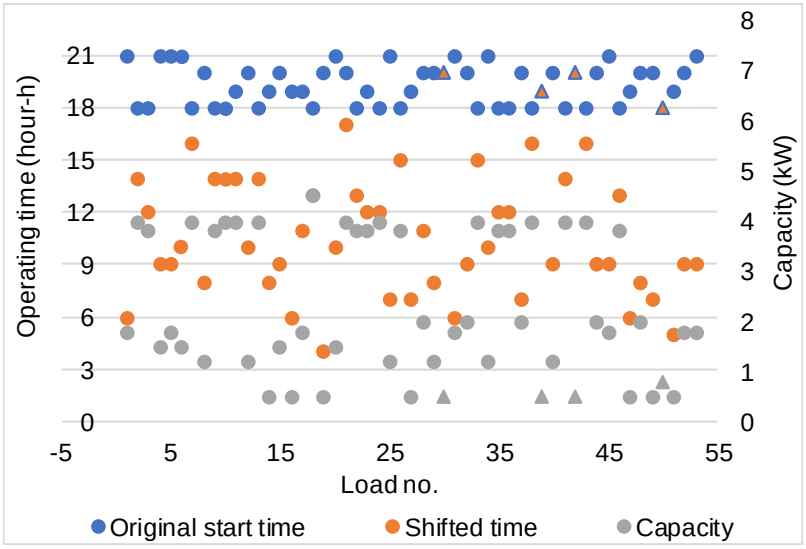

Figure 6.11 The loads' operation time before and after the load-shifting program.

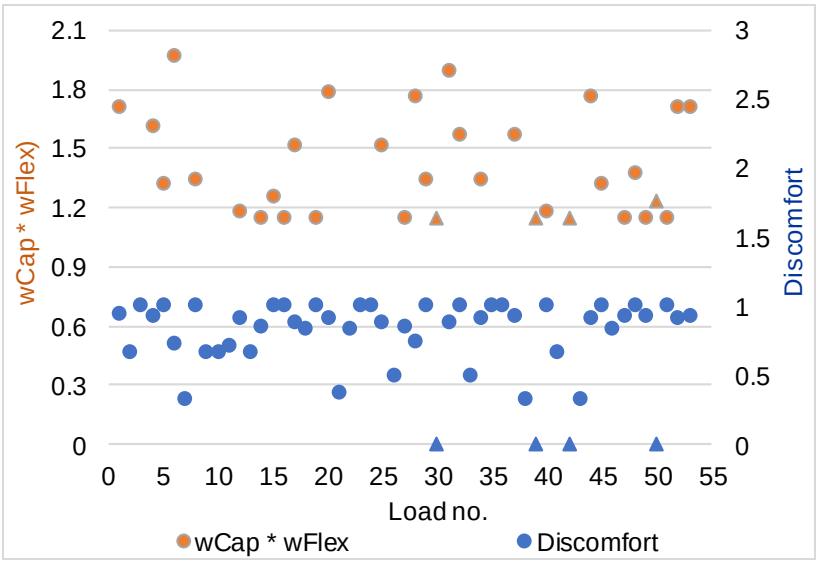

Figure 6.12 The weighting factor of the affected shiftable loads.

6.3.2 Controllable Loads

The demand response program for the group of controllable loads is executed when the microgrid is facing a power shortage when the upstream grid is at peak rate. Fig. 6.13 shows the result of demand response strategies for controllable loads. It can be seen that the total amount of power consumed from 15:00 to 21:00 has been reduced. This reduction results in additional profit to the microgrid as shown in Fig. 6.14 as it has reduced the imported power from the upstream grid at the expensive peak period tariff. The total controllable demand response profit for the simulated day is $5,45. Meanwhile, the reduction from line losses and the total energy consumed are 2.1 kWh and 105 kWh, respectively. Therefore, the additional profit from CO_2 reduction is $2.03.

If at hour h, the maximal available capacity that can be reduced from the controllable load is smaller than the targeted import power to be reduced, all the available controllable load will be controlled to the maximum allowed by the command to be applied; thus, all of these loads will encounter maximal discomfort. Meanwhile, if the targeted power to be shaved is smaller than the available power from controllable loads, the GA optimisation method will be carried out. Every demand response event which is affecting the controllable loads may cause discomfort to customers, which level of the discomfort varies from 0 to 1. Its shown in Fig. 6.13 that at hour 15:00 the targeted reduced power (12.02kW) is smaller than the maximal available load to be reduced (20.31kW).

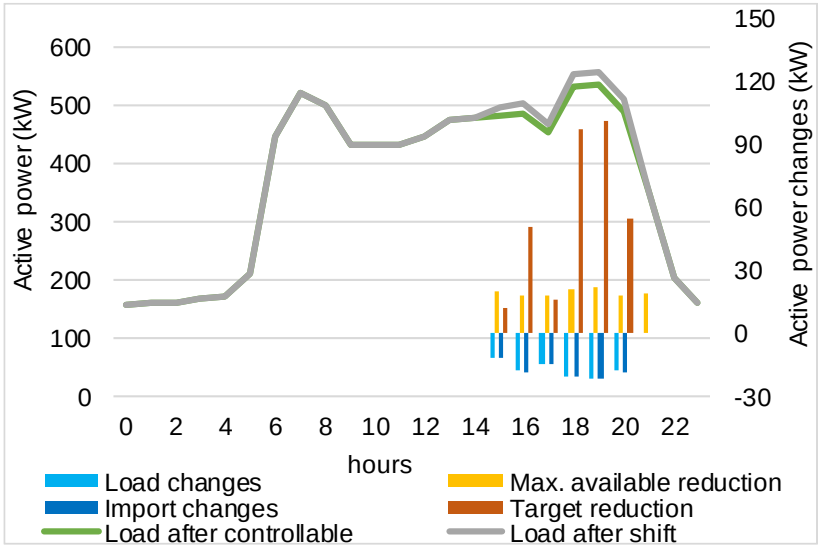

Figure 6.13 Consumed power changes with controllable demand response.

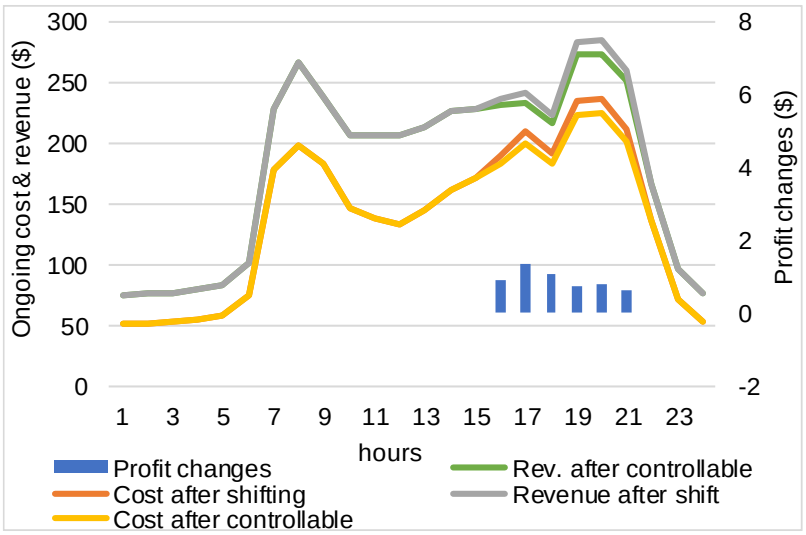

Figure 6.14 Profit from controlling the controllable loads under the demand response program.

The profile of the affected loads is shown in Fig. 6.15 and Fig. 6.16. During this hour, there are 12, two, and eight available loads from the residential, commercial building-1, and commercial building-2, respectively. Using GA optimisation, of the 22 available loads, only three loads have not had their power reduced. Sorting from the smallest to the largest value of $\omega_{\text{flex}} \times \omega_{\text{cap}}$, these three loads are ranked at 4.

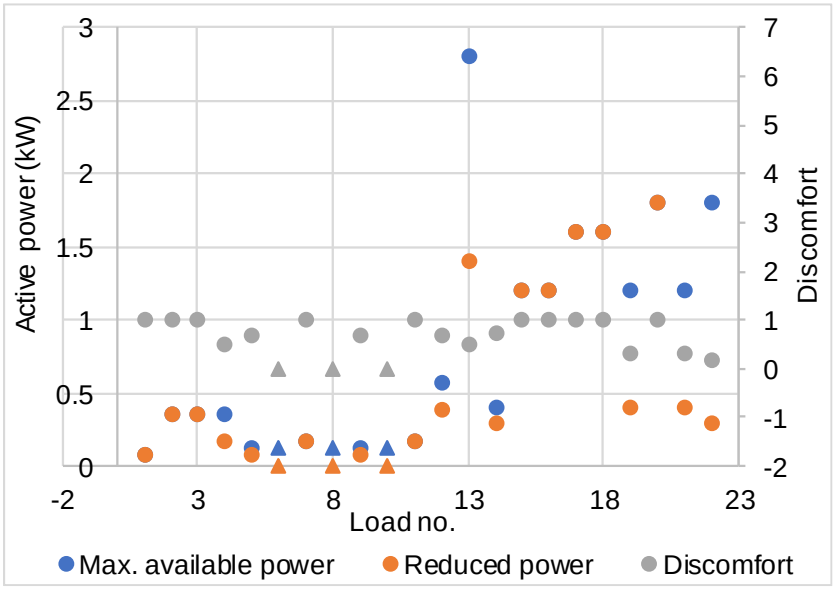

Figure 6.15 Power reduction from the controllable loads.

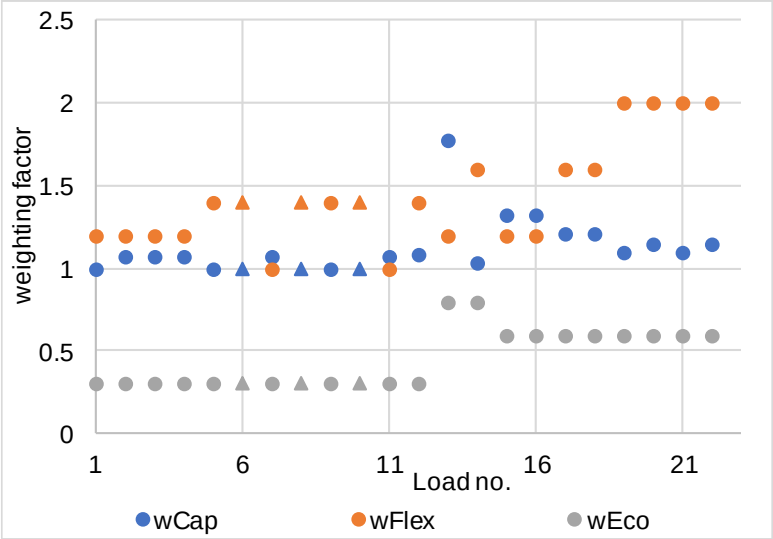

Figure 6.16 The weighting factor of the affected controllable loads.

6.3.3 Shedable Loads

If the microgrid still faces power deficiency, then it will begin to execute the load-shedding process. Similar to the strategy applied to the controllable loads, the GA optimisation will be executed when the available capacity from the shedable loads is higher than the capacity requiring to be reduced. Figs. 6.17 and 6.18 show the result of controlling the shedable loads under the demand response program. The total shedable demand response profit for a specific day is $7.95, and the total load and line losses reduction is 368 kWh; thus, the carbon tax reduction is $6.94.

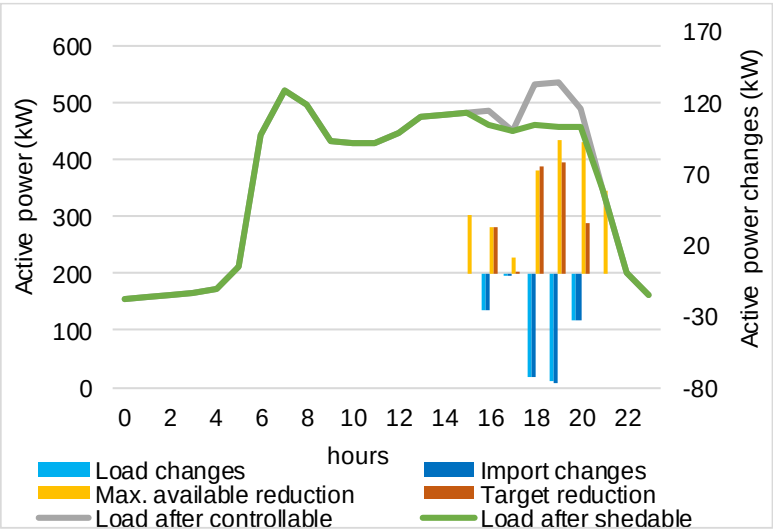

Figure 6.17 Consumed power changes from controlling the shedable loads under the demand response program.

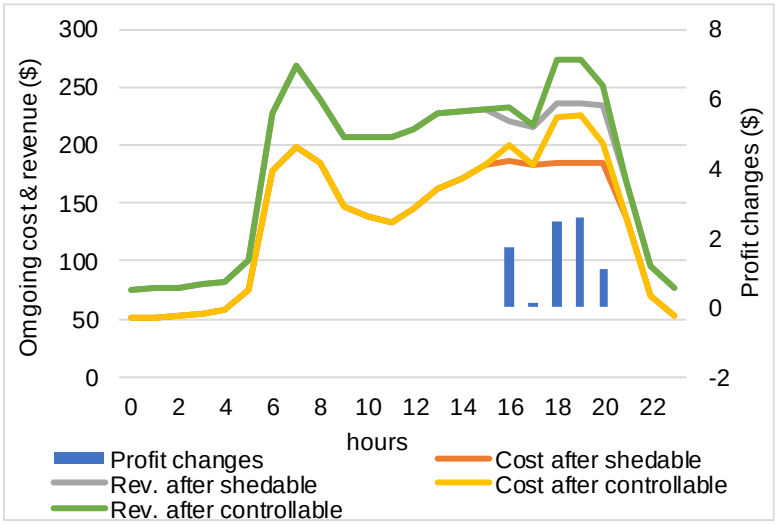

Figure 6.18 Profit from controlling the shedable loads under the demand response program.

To avoid the violation of set discomfort, each load has predefined information regarding the maximum number of shedding events per day. In every shedding event, the demand response optimisation memorises the discomfort level caused by each affected load. This discomfort level is then accumulated and reset every day. Fig. 6.19 shows that of the 31 available loads, only 12 loads have been disconnected. Moreover, loads with less flexibility, small capacity, and a high economic weighting factor are less likely to be controlled. Furthermore, Table 6.8 shows the discomfort caused by seven shedable loads which are running from 16:00 to 20:00; it can be seen that once the discomfort has reached its maximum level, the affected load can no longer be shed during the following operating hours.

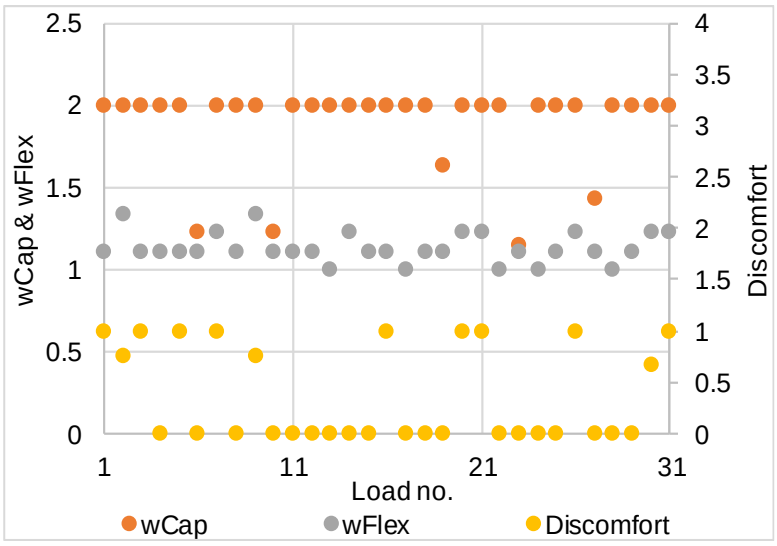

Figure 6.19 The shedable loads' weighting factor and the discomfort caused by the affected loads.

Table 6.8 Discomfort caused by the affected shedable loads'.

Maximum demand response event	Capacity	Operating hour (discomfort level)				
		16	17	18	19	20
4	2750			0.25	0.5	0.75
2	750	0.5	On	1	On	On
3	2750	0.33		0.67	1	On
2	550	On	On	0.5	1	On
2	1300			0.5	1	On
2	1100	0.5	On	1	On	
2	1800		On	0.5	1	On

note: ▮ indicate that load is not currently operated

Fig. 6.20 shows the total amount of affected energy, while Fig. 6.21 shows that the total demand response profit for one year is $9,857. It can be seen that the load-shifting program brings the largest profit because by implementing the load-shifting program, the total amount of energy sold to the customer remains the same while the cost of energy supply decreases. The smallest profit comes from controllable demand response because, in this study, the available capacity from the studied controllable loads was not as big as the available capacity from shedable loads. Assuming that there are no generation and consumption changes during the lifetime of the demand response project, the NPV profit over 10 years becomes $101,852.

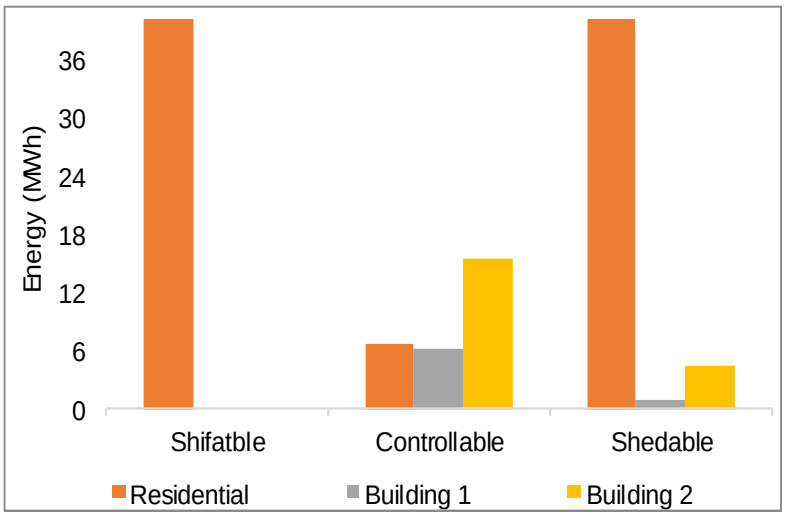

Figure 6.20 The affected energy supply to the customers in one year.

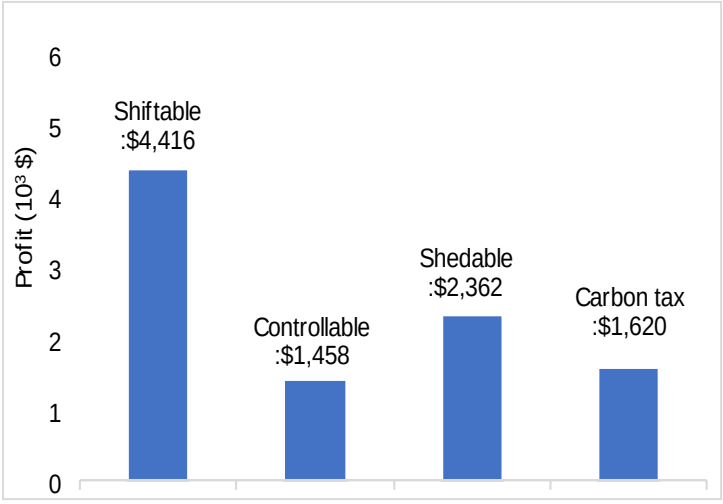

Figure 6.21 Profit of the demand response implementation in one year.

Assuming that there are no changes to generation and consumption during the lifetime of the demand response project, the additional revenue obtained by the microgrid from deploying demand response for 10 years is $101,852. Therefore, the NPV of the demand response profit is $40,832. As mentioned, it is assumed that 20% of the demand response profit is allocated for the customer incentive. Thus, the total amount allocated for the incentive is $8,166, resulting in an incentive of $790 for the first year. Given that ω_{Shift}, ω_{Cont} and ω_{Shed} are 0.3, 0.5, and 0.7 respectively, and EV_{res}, EV_{com1} and EV_{com2} are 0.3, 0.8, and 0.6 respectively, then the incentives are calculated as presented in Table 6.9, assuming that the microgrid operator has paid all the DR deployment costs.

Table 6.9 Demand response incentives per load types when all the deployment costs are paid by the microgrid operator.

Load type	Customer type		
	Residential (cents/kWh)	Commercial building 1 (cents/kWh)	Commercial building 2 (cents/kWh)
Shiftable	0.2822	-	-
Controllable	0.4704	1.2543	0.9407
Shedable	0.6585	1.756	1.317

Let us consider that the costs of enabling technologies at the end-user side are the participants' responsibility. In this case, the 10-year NPV of demand response profit becomes $83,352 and the first-year's allocated fund for incentive becomes $1613. Given this allocated

fund, the incentives for each type of load are shown in Table 6.9. Table 6.10 shows that, on average, the residential customers receive an incentive of $20.14 in one year. Meanwhile, commercial customers 1 and 2 receive $193 and $414 respectively.

Table 6.10 Demand response incentives per load types when the end-user deployment costs are paid by participants.

Load type	Customer type		
	Residential (cents/kWh)	Commercial building 1 (cents/kWh)	Commercial building 2 (cents/kWh)
Shiftable	0.5761	-	-
Controllable	0.9602	2.5604	1.9203
Shedable	1.3442	3.5846	2.6884

Fig.6.22 shows the incentive received by participants in one year. The NPV accumulation of the incentive through the demand response project lifetime is shown in Fig. 6.23. From these values, it can be deduced that the total amount of incentives received over 10 years is not enough to cover the end-users' demand response costs. The payback period for residential customers is 29 years on average while that for the commercial customers are 19 and 17 years. Fig. 6.23 shows the payback period for each customer type.

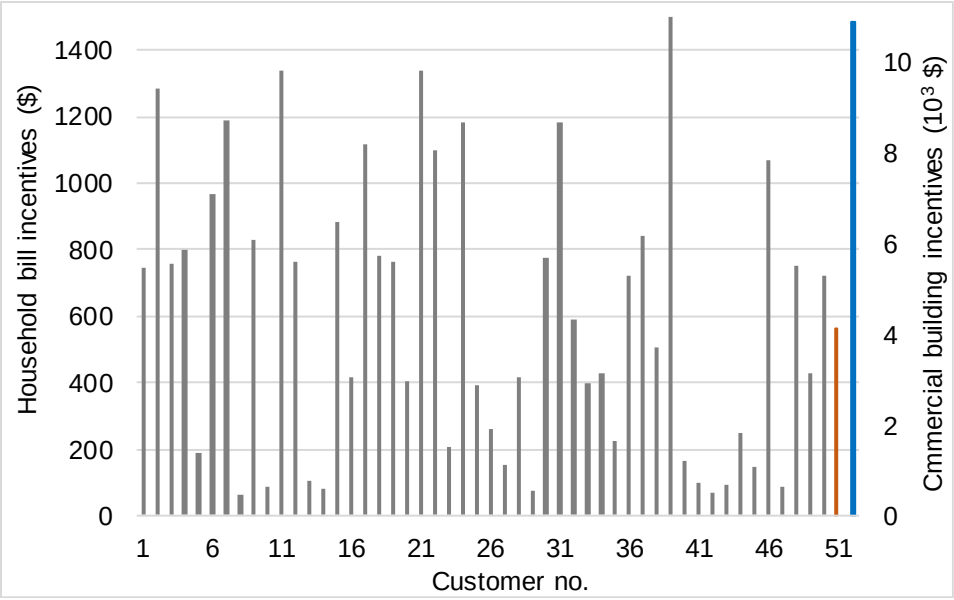

Figure 6.22 The incentives received by the demand response participants in one year.

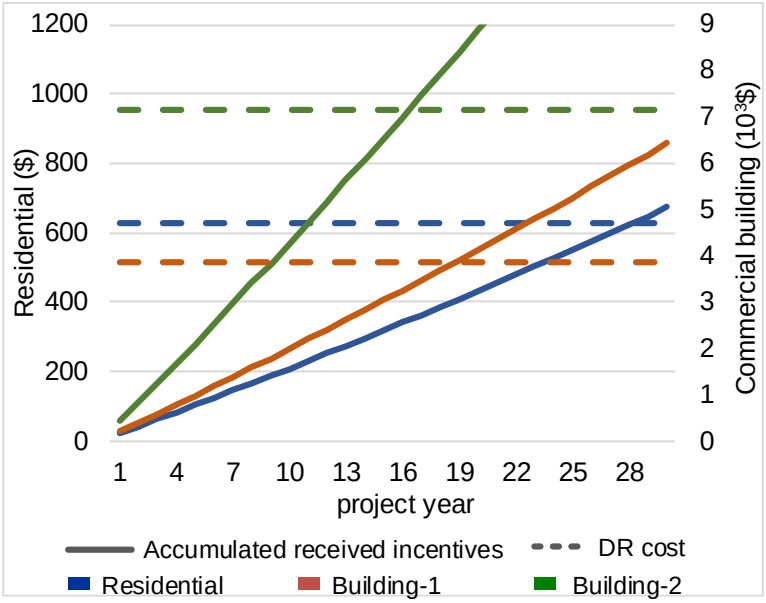

Figure 6.23 Payback period of the end-users' demand response deployment cost with the received incentive.

However, as each customer's total amount of consumed energy is reduced and some of their load are shifted to the microgrid off-peak tariff, besides receiving incentives, the customer will also earn indirect benefits from their electricity bill reduction. Fig. 6.24 shows customer bill reductions in a year. The household bill reduction varies from $54 to $1,573, and its average is $576.5. Meanwhile, commercial building 1 and building 2 receive bill reductions of $3,932 and $10,468 respectively. With the received incentive plus bill reduction, on average, the payback period for the end-user demand response deployment cost is in two years for a residential customer and one year for commercial customers as shown in Fig. 6.25.

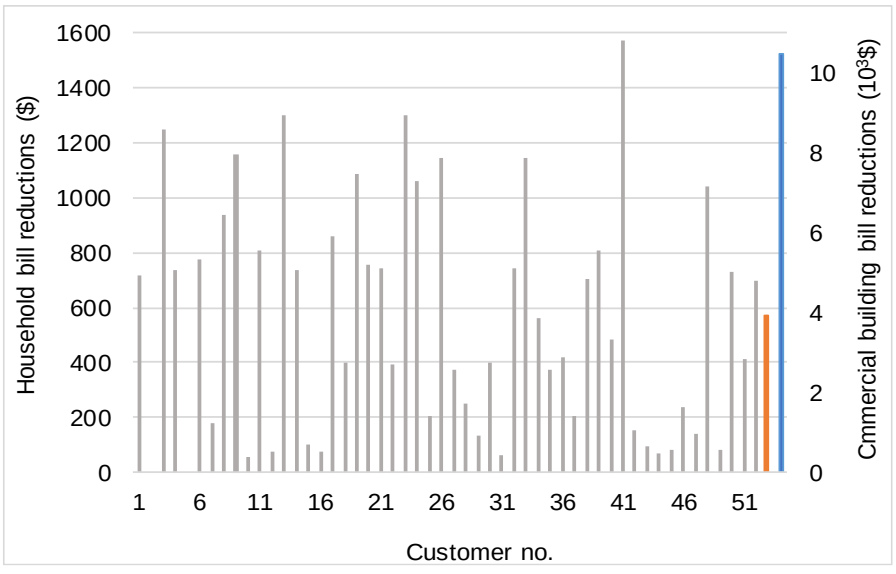

Figure 6.24 Customers' bill reduction in one year.

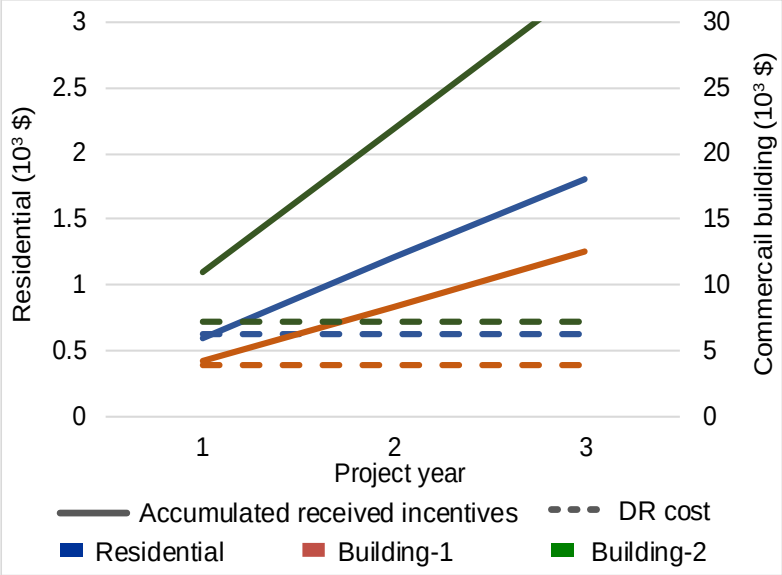

Figure 6.25 Payback period of the end-users' demand response deployment cost with the received incentive plus bill reduction.

6.4 Sensitivity Analysis

The following sections analyse the effect of the percentage variation in allocating the microgrid operator's profit of employing demand response for the participants' incentive toward the demand response deployment cost payback period. Furthermore, because energy demand is increasing every year, sensitivity analysis is also carried out by varying the microgrid loads.

6.4.1 Allocated Fund for Incentive

In the previous section, the allocated funds from the DR profits are set to 20% for the incentive. This is insufficient for both residential and commercial customers as they will not receive enough incentive to cover the cost of implementing the DR system. Therefore, a variation on the allocated fund is analysed to check its effects on the payback period. Fig. 6.26 shows the study result, indicating that at least 70% of the demand response profits needs to be reserved in order to pay the incentives so that the end-users' demand response deployment costs are reimbursed within the lifetime of the demand response project.

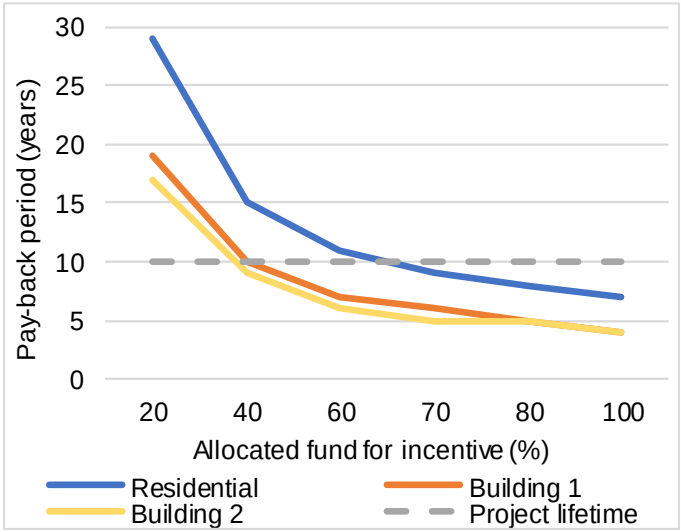

Figure 6.26 Payback period of the end-users' demand response deployment cost versus the percentage of profit allocated for incentive.

6.4.2 Load Variation

It is stated in [155] that the demand for energy is increasing year by year. Therefore, the sensitivity analysis of the variation in demand is simulated. In this study, the additional demand capacity is added to the group of uninterruptible loads, while the profile of other types of load which are the object of the demand response program remains the same. Fig. 6.27 and Fig. 6.28 show the comparison of microgrid's load, losses, import, and profit with and without demand response. Both figures indicate that the demand response achieves the most profit when the total microgrid demand is 80% of the previous modelled profile.

Fig. 6.27 shows that with 80% demand, the load reduction is much smaller compared to the import reduction, resulting in a smaller reduction in revenue compared to the reduction of energy production costs. This occurs as the load-shifting program does not allow additional energy to be imported to the shifted hours as the microgrid can supply the demand with the power generated by the microgrid's DERs. Furthermore, it can also be seen from both figures that with 90% to 120% load variations, the demand response profit is increasing. However, when the microgrid demand is 110% and 120%, the demand response profit changes modestly. This occurs because of the limited available capacity of the demand response loads.

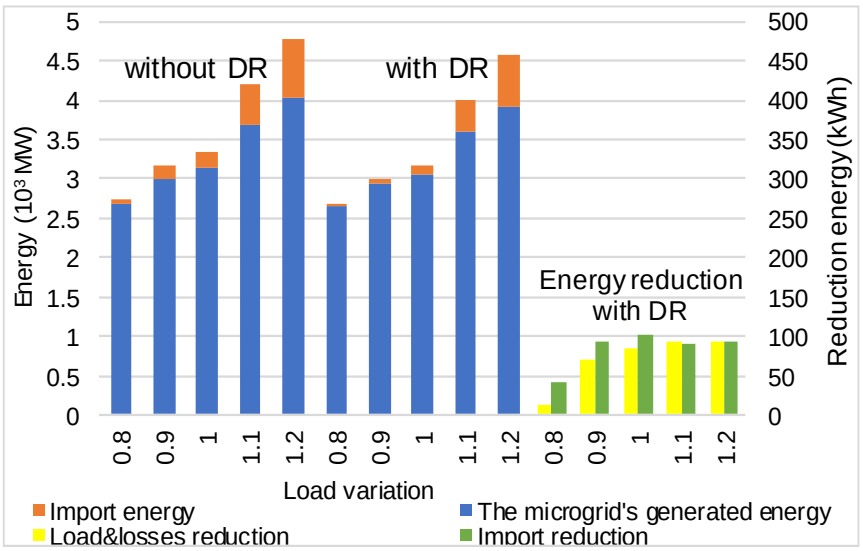

Figure 6.27 Load variation versus energy changes.

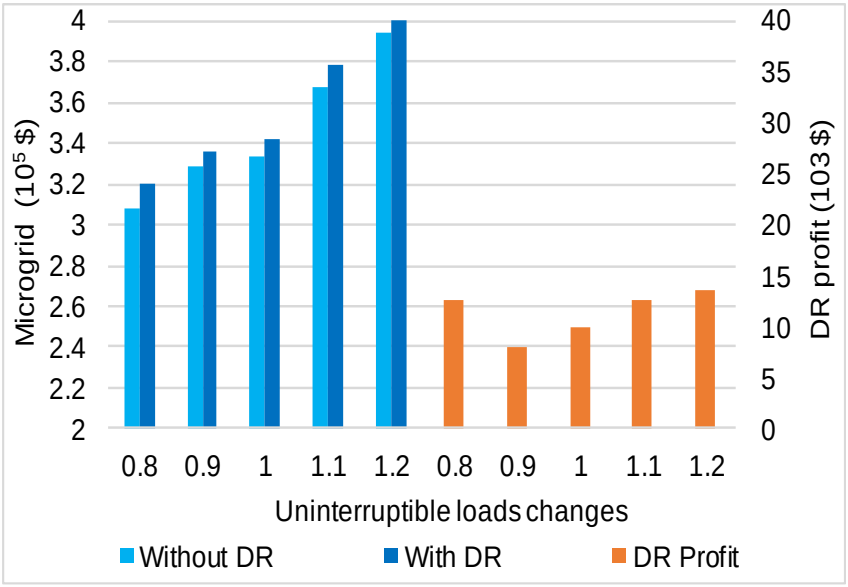

Figure 6.28 Load variation versus the microgrid operator's profit.

6.5 Summary

The study results show that under the proposed demand response scheme, a load with a higher capacity and greater flexibility tends to be chosen more to be controlled during the demand response events. Furthermore, the study results show that the microgrid operator benefits financially from the differences between the ongoing costs and revenues, and also from carbon tax reduction. Also, the results show that, if only 20% of the demand response profit is allocated for paying the participant incentive, and the end-user demand response cost is paid by the customer, the offered incentives are not enough to cover the demand response enabling

cost within the lifetime of the demand response project. However, the sensitivity analysis result of varying the percentage of demand response profit allocated for incentives shows that it is possible for the payback period to be within the lifetime of the demand response project. Moreover, the result shows that customers benefit from having bill reductions which will help to accelerate the rate of return and resulting in a one to two-year payback period.

Chapter 7 Conclusions and Recommendations

This chapter summarises the findings and the results of this study. Also, several recommendations are offered for future research related to this area of study.

7.1 Conclusions

The general conclusions of the thesis are:

- The studies have shown that the voltage and frequency of a microgrid, especially an inverter-based system operating in islanded mode, are prone to the fluctuation of RESs. The additional active power control, proposed for the inverters in the thesis, can stabilise the microgrid frequency and smooth its transition from the grid-connected to islanded mode.
- The algorithm developed for adjusting the demand capacity by determining the *P*-*V* droop constant for the individual bus can restore the bus voltage to the desired range of operation when the microgrid is overloaded. Meanwhile, the proposed load-shedding sequence based on the BES SoC can prolong the supply of energy to the microgrid's critical loads.
- To minimise the customer discomfort and maximise the microgrid operator's profit when employing the load-shedding approach, the proposed technique classifies the loads into shiftable, controllable, and shedable, in addition to differentiating the customers based on their economic value. Hence, the loads are then given weighted values that take into account each load's capacity, flexibility to withstand the demand response execution, and economic value. The study results show that the proposed load-shedding optimisation scheme for voltage correction has minimised the number of shed loads and reduced the demand.
- The thesis has determined the incentives that the microgrid operator will give to the customers participating in the demand response program as compensation for their discomfort. The study result indicates that the cost incurred by the end-user demand

response can be reimbursed within the project's lifetime. Moreover, customers benefit financially from reductions in their electricity bills.

7.2 Recommendations

Several areas in this thesis can be extended with future research as suggested below:

- The modelling of the loads' profile in this study did not involve the actual loads' characteristics. For example, a thermal load such as air conditioning has inertia characteristics that are affected by the ambient temperature, number of occupants, air ventilation, building materials, etc. Moreover, the loads are modelled on an hourly basis, so that the proposed demand response is executed hourly. However, in the real application of a demand response program, demand response events may need to be executed for only 15 minutes. Therefore, more detailed load profiles can be used in future research to yield more accurate results.
- This research has modelled only a PV system as the uncontrollable RES-based DERs; therefore, future research could focus on wind energy. Furthermore, various types of conventional fuel-based DERs can be used to simulate the cost optimisation problem.
- Nowadays, electric vehicles are gaining in popularity. Because they can be assumed to be both load and generation, it is believed that they have a bigger capability to stabilise the microgrid. On the other hand, the need to charge them quickly has raised a concern regarding the grid's stability. Moreover, as electric vehicles have mobility characteristics, the stability of the grid is unpredictable as it is demography dependent. Therefore, it would be a worthwhile issue to consider in future research, particularly when calculating the incentive for utilising them in a demand response program.
- In this thesis, the upstream grid electricity tariff was classified only as off-peak, shoulder, and peak rate. In future research, the feasibility of the demand response program can be investigated in terms of a dynamic real-time market price.

References

[1] C. Schwaegerl and L. Tao, "Quantification of Technical, Economic, Environmental and Social Benefits of Microgrid Operation," 1 ed. Chichester, United Kingdom: Wiley, 2013, pp. 275-313.

[2] T. L. Vandoorn, J. C. Vasquez, J. D. Kooning, J. M. Guerrero, and L. Vandevelde, "Microgrids: Hierarchical Control and an Overview of the Control and Reserve Management Strategies," *IEEE Industrial Electronics Magazine,* vol. 7, no. 4, pp. 42-55, 2013.

[3] A. Hirsch, Y. Parag, and J. Guerrero, "Microgrids: A review of technologies, key drivers, and outstanding issues," *Renewable and Sustainable Energy Reviews,* vol. 90, pp. 402-411, 2018/07/01/ 2018.

[4] M. S. Mahmoud, M. Saif Ur Rahman, and F. M. A.L.-Sunni, "Review of microgrid architectures – a system of systems perspective," *IET Renewable Power Generation,* vol. 9, no. 8, pp. 1064-1078, 2015.

[5] R. Zamora and A. K. Srivastava, "Controls for microgrids with storage: Review, challenges, and research needs," *Renewable and Sustainable Energy Reviews,* vol. 14, no. 7, pp. 2009-2018, 2010.

[6] J. I. Giraldez Miner, F. Flores-Espino, S. MacAlpine, P. Asmus, and G. C. O. National Renewable Energy Lab, "Phase I Microgrid Cost Study: Data Collection and Analysis of Microgrid Costs in the United States," United States 2018. [Online] Available: https://www.nrel.gov/docs/fy19osti/67821.pdf.

[7] F. Farzan, S. Lahiri, M. Kleinberg, K. Gharieh, F. Farzan, and M. Jafari, "Microgrids for Fun and Profit: The Economics of Installation Investments and Operations," *IEEE Power and Energy Magazine,* vol. 11, no. 4, pp. 52-58, 2013.

[8] M. Harper and B. C. A. Lawrence Berkeley National Lab, "Review of Strategies and Technologies for Demand-Side Management on Isolated Mini-Grids," United States. March. 2013. [Online] Available: https://www.osti.gov/servlets/purl/1171615.,

[9] C. Bergaentzlé, C. Clastres, and H. Khalfallah, "Demand-side management and European environmental and energy goals: An optimal complementary approach," *Energy Policy,* vol. 67, pp. 858-869, 2014/04/01/ 2014.

[10] Energy Information Administration, "U.S. Electric Utility Demand-Side Management 2000," Jan. 2002. [Online] Available: https://www.eia.gov/electricity/data/eia861/dsm/058900.pdf.

[11] P. Cappers, C. Goldman, and D. Kathan, "Demand response in U.S. electricity markets: Empirical evidence," *Energy,* vol. 35, no. 4, pp. 1526-1535, 2010/04/01/ 2010.

[12] U.S. Department of Energy, "Benefits of Demand Response in Electricity Markets and Recommendations for Achieveing Them," Feb. 2006. [Online] Available: https://eetd.lbl.gov/sites/all/files/publications/report-lbnl-1252d.pdf.

[13] M. A. Piette, S. Kiliccote, G. Ghatikar, and B. C. A. Ernest Orlando Lawrence Berkeley National Laboratory, "Design and Implementation of an Open, Interoperable Automated Demand Response Infrastructure," United States, 2007. [Online] Available: https://www.osti.gov/servlets/purl/928026.

[14] P. Bradley, M. Leach, and J. Torriti, "A review of the costs and benefits of demand response for electricity in the UK," *Energy Policy,* vol. 52, no. 1, pp. 312-327, 2013.

[15] P. Cappers, J. MacDonald, J. Page, J. Potter, and E. Stewart, "Future Opportunities and Challenges as a Resources in Distribution System and Planning Activities," Lawrence Berkeley National LaboratoryJan. 2016. [Online] Available: https://emp.lbl.gov/sites/all/files/lbnl-1003951.pdf.

[16] P. Guo, V. O. K. Li, and J. C. K. Lam, "Smart demand response in China: Challenges and drivers," *Energy Policy,* vol. 107, pp. 1-10, 2017.

[17] C. Bartusch, F. Wallin, M. Odlare, I. Vassileva, and L. Wester, "Introducing a demand-based electricity distribution tariff in the residential sector: Demand response and customer perception," *Energy Policy,* vol. 39, no. 9, pp. 5008-5025, 2011/09/01/ 2011.

[18] M. Hosseini Imani, P. Niknejad, and M. R. Barzegaran, "The impact of customers' participation level and various incentive values on implementing emergency demand response program in microgrid operation," *International Journal of Electrical Power & Energy Systems,* vol. 96, pp. 114-125, 2018/03/01/ 2018.

[19] R. N. Boisvert and B. F. Neenan, "Social Welfare implications of demand response programs in competitive electricity markets," Lawrence Berkeley National Lab, Berkeley

C. A., United States, Report. 2003. [Online] Available: https://www.osti.gov/servlets/purl/816220.

[20] S. Nolan and M. O'Malley, "Challenges and barriers to demand response deployment and evaluation," *Applied Energy,* vol. 152, pp. 1-10, 2015.

[21] L. Bird, J. Cochran, and X. Wang, "Wind and Solar Energy Curtailment: Experience and Practices in the United States," National Renewable Energy Laboratory (NREL), March. 2014. [Online] Available: https://www.nrel.gov/docs/fy14osti/60983.pdf.

[22] H. Schermeyer, C. Vergara, and W. Fichtner, "Renewable energy curtailment: A case study on today's and tomorrow's congestion management," *Energy Policy,* vol. 112, pp. 427-436, 2018/01/01/ 2018.

[23] R. Hasan, S. Mekhilef, M. Seyedmahmoudian, and B. Horan, "Grid-connected isolated PV microinverters: A review," *Renewable and Sustainable Energy Reviews,* vol. 67, pp. 1065-1080, 2017/01/01/ 2017.

[24] D. E. Olivares *et al.*, "Trends in Microgrid Control," *IEEE Transactions on Smart Grid,* vol. 5, no. 4, pp. 1905-1919, 2014.

[25] A. M. Bollman, "An Experimental Study of Frequency Droop Control in a Low-inertia Microgrid," Master Thesis, 2009. [Online] Available: https://pdfs.semanticscholar.org/4089/67e64989fdef82828b6bc21ebfb391ae4ac0.pdf.

[26] J. Liu, Y. Miura, and T. Ise, "Comparison of Dynamic Characteristics Between Virtual Synchronous Generator and Droop Control in Inverter-Based Distributed Generators," *IEEE Transactions on Power Electronics,* vol. 31, no. 5, pp. 3600-3611, 2016.

[27] Y. Liu, Q. Zhang, C. Wang, and N. Wang, "A control strategy for microgrid inverters based on adaptive three-order sliding mode and optimized droop controls," *Electric Power Systems Research,* vol. 117, pp. 192-201, 2014/12/01/ 2014.

[28] N. Hajilu, G. B. Gharehpetian, S. H. Hosseinian, M. R. Poursistani, and M. Kohansal, "Power control strategy in islanded microgrids based on VF and PQ theory using droop control of inverters," pp. 37-42: IEEE.

[29] K. S. Rajesh, S. S. Dash, R. Rajagopal, and R. Sridhar, "A review on control of ac microgrid," *Renewable and Sustainable Energy Reviews,* vol. 71, pp. 814-819, 2017.

[30] W. Alharbi and K. Bhattacharya, "Demand response and energy storage in MV islanded microgrids for high penetration of renewables," pp. 1-6: IEEE.

[31] K. Cavanagh *et al.*, "Electrical Energy Storage: Technology Overview and Applications," CSIRO, Australia,EP154168, 2015. [Online] Avialable:

https://www.aemc.gov.au/sites/default/files/content/7ff2f36d-f56d-4ee4-a27b-b53e01ee322c/CSIRO-Energy-Storage-Technology-Overview.pdf.

[32] T. Kerdphol, Y. Qudaih, and Y. Mitani, "Optimum battery energy storage system using PSO considering dynamic demand response for microgrids," *International Journal of Electrical Power and Energy Systems,* vol. 83, pp. 58-66, 2016.

[33] T. Ma, H. Yang, and L. Lu, "Feasibility study and economic analysis of pumped hydro storage and battery storage for a renewable energy powered island," *Energy Conversion and Management,* vol. 79, pp. 387-397, 2014.

[34] M. Farina, A. Guagliardi, F. Mariani, C. Sandroni, and R. Scattolini, "Model predictive control of voltage profiles in MV networks with distributed generation," *Control Engineering Practice,* vol. 34, pp. 18-29, 2015.

[35] F. Yang, Q. Sun, Q.-L. Han, and Z. Wu, "Cooperative Model Predictive Control for Distributed Photovoltaic Power Generation Systems," *IEEE Journal of Emerging and Selected Topics in Power Electronics,* vol. 4, no. 2, pp. 414-420, 2016.

[36] N. Kazemzadeh, S. M. Ryan, and M. Hamzeei, "Robust optimization vs. stochastic programming incorporating risk measures for unit commitment with uncertain variable renewable generation," *Energy Systems,* vol. 10, no. 3, pp. 517-541, 2019.

[37] Q. P. Zheng, J. Wang, A. L. Liu, and A. I. L. Argonne National Lab, "Stochastic Optimization for Unit Commitment-A Review," *IEEE Transactions on Power Systems,* vol. 30, no. 4, pp. 1913-1924, 2015.

[38] M. H. Elkazaz, A. A. Hoballah, and A. M. Azmy, "Operation optimization of distributed generation using artificial intelligent techniques," *Ain Shams Engineering Journal,* vol. 7, no. 2, pp. 855-866, 2016.

[39] B. Ramachandran, S. K. Srivastava, and D. A. Cartes, "Intelligent power management in micro grids with EV penetration," *Expert Systems With Applications,* vol. 40, no. 16, pp. 6631-6640, 2013.

[40] S. H. Hong, M. Yu, and X. Huang, "A real-time demand response algorithm for heterogeneous devices in buildings and homes," *Energy,* vol. 80, pp. 123-132, 2015.

[41] A. Malik and J. Ravishankar, "A review of demand response techniques in smart grids," in *2016 IEEE Electrical Power and Energy Conference (EPEC)*, 2016, pp. 1-6.

[42] A. M. Ibrahim, M. A. Attia, M. M. Othman, and A. A. Y., "A Survey on Demand Side Management in Electrical Power Systems," *I-Manager's Journal on Power Systems Engineering,* vol. 5, no. 1, pp. 40-50, 2017.

[43] D. Q. Oliveira, A. C. Zambroni de Souza, M. V. Santos, A. B. Almeida, B. I. L. Lopes, and O. R. Saavedra, "A fuzzy-based approach for microgrids islanded operation," *Electric Power Systems Research,* vol. 149, pp. 178-189, 2017.

[44] M. Majidi and K. Zare, "Integration of Smart Energy Hubs in Distribution Networks Under Uncertainties and Demand Response Concept," *IEEE Transactions on Power Systems,* vol. 34, no. 1, pp. 566-574, 2019.

[45] A. A. Khan, A. Khan, S. Razzaq, F. Khursheed, and Owais, "HEMSs and enabled demand response in electricity market: An overview," *Renewable and Sustainable Energy Reviews,* vol. 42, pp. 773-785, 2015.

[46] J. Potter and P. Cappers, "Demand Response Advanced Controls Framework and Assessment of Enabling Technology Costs," Lawrence Berkeley National Laboratory. August 2017. [Online] Available: https://emp.lbl.gov/sites/default/files/demand_response_advanced_controls_framework_and_cost_assessment_final_published.pdf.

[47] G. Derakhshan, H. A. Shayanfar, and A. Kazemi, "The optimization of demand response programs in smart grids," *Energy Policy,* vol. 94, pp. 295-306, 2016/07/01/ 2016.

[48] Federal Energy Regulatory Commission, "Assessment of Demand Response & Smart Metering: Staff Report," Dec. 2016. [Online] Available: https://www.ferc.gov/legal/staff-reports/2016/DR-AM-Report2016.pdf.

[49] H. Shareef, M. S. Ahmed, A. Mohamed, and E. A. Hassan, "Review on Home Energy Management System Considering Demand Responses, Smart Technologies, and Intelligent Controllers," *IEEE Access,* vol. 6, pp. 24498-24509, 2018.

[50] P. Siano, "Demand response and smart grids—A survey," *Renewable and Sustainable Energy Reviews,* vol. 30, pp. 461-478, 2014/02/01/ 2014.

[51] F. Gianelloni, L. Camara, A. Leite, and J. F. C. M. Mathias, "Demand Response: a survey on Challenges and Opportunities," Accessed on: 8 August 2019

[52] A. Losi, P. Mancarella, and A. Vicino, *Integration of Demand Response into the Electricity Chain : Challenges, Opportunities and Smart Grid Solutions*. New York, UNITED STATES: John Wiley & Sons, Incorporated, 2015.

[53] C. Hawk and A. Kaushiva, "Cybersecurity and the Smarter Grid," *The Electricity Journal,* vol. 27, no. 8, pp. 84-95, 2014/10/01/ 2014.

[54] B. J. Murrill, E. C. Liu, and R. M. Thompson, "Smart meter data: Privacy and cybersecurity," 2013.

[55] P. V. Dievel, K. D. Vos, and R. Belmans, "Demand response in electricity distribution grids: Regulatory framework and barriers," in *11th International Conference on the European Energy Market (EEM14)*, 2014, pp. 1-5.

[56] N. O'Connell, P. Pinson, H. Madsen, and M. O'Malley, "Benefits and challenges of electrical demand response: A critical review," *Renewable and Sustainable Energy Reviews,* vol. 39, pp. 686-699, 2014.

[57] A. S. Chuang, "Demand-side Integration for System Reliability," in *2007 IEEE Lausanne Power Tech*, 2007, pp. 1617-1622.

[58] D. Jang, J. Eom, M. Jae Park, and J. Jeung Rho, "Variability of electricity load patterns and its effect on demand response: A critical peak pricing experiment on Korean commercial and industrial customers," *Energy Policy,* vol. 88, pp. 11-26, 2016.

[59] S. R. Konda, A. S. Al-Sumaiti, L. Panwar, B. K. Panigrahi, and R. Kumar, "Impact of Load Profile on Dynamic Interactions Between Energy Markets: A Case Study of Power Exchange and Demand Response Exchange," *IEEE Transactions on Industrial Informatics,* pp. 1-1, 2019.

[60] L. Liu, H. Matayoshi, M. E. Lotfy, M. Datta, and T. Senjyu, "Load frequency control using demand response and storage battery by considering renewable energy sources," *Energies,* vol. 11, no. 12, p. 3412, 2018.

[61] M. Donnelly, D. Trudnowski, S. Mattix, and J. Dagle, "Autonomous Demand Response for Primary Frequency Regulation," Pacific Nortwest National LaboratoryJan. 2012. [Online] Available: https://www.pnnl.gov/main/publications/external/technical_reports/PNNL-21152.pdf.

[62] Y. He and M. Petit, "Valorization of demand response for voltage control in MV distribution grids with distributed generation," pp. 1-6: IEEE.

[63] M. M. Rahman, A. Arefi, G. M. Shafiullah, and S. Hettiwatte, "A new approach to voltage management in unbalanced low voltage networks using demand response and OLTC considering consumer preference," *International Journal of Electrical Power and Energy Systems,* vol. 99, pp. 11-27, 2018.

[64] Australian Energy Market Operator (AEMO), "Guide to Ancillary Services in The National Electricity Market," April 2015. [Online] Available; https://www.aemo.com.au/-/media/Files/PDF/Guide-to-Ancillary-Services-in-the-National-Electricity-Market.pdf.

[65] O. Ma *et al.*, "Demand Response for Ancillary Services," *IEEE Transactions on Smart Grid,* vol. 4, no. 4, pp. 1988-1995, 2013.

[66] S. P. Meyn, P. Barooah, A. Busic, Y. Chen, and J. Ehren, "Ancillary Service to the Grid Using Intelligent Deferrable Loads," *IEEE Transactions on Automatic Control,* vol. 60, no. 11, pp. 2847-2862, 2015.

[67] S. Chen, "Demand-side Management for Ancillary Services Provision in Smart Grid," Dissertation/Thesis, ProQuest Dissertations Publishing, 2017.

[68] A. Abiri-Jahromi and F. Bouffard, "Contingency-Type Reserve Leveraged Through Aggregated Thermostatically-Controlled Loads—Part I: Characterization and Control," *IEEE Transactions on Power Systems,* vol. 31, no. 3, pp. 1972-1980, 2016.

[69] M. Humayun, A. Safdarian, M. Z. Degefa, and M. Lehtonen, "Demand Response for Operational Life Extension and Efficient Capacity Utilization of Power Transformers During Contingencies," *IEEE Transactions on Power Systems,* vol. 30, no. 4, pp. 2160-2169, 2015.

[70] C. L. Floch, F. Belletti, S. Saxena, A. M. Bayen, and S. Moura, "Distributed optimal charging of electric vehicles for demand response and load shaping," in *2015 54th IEEE Conference on Decision and Control (CDC)*, 2015, pp. 6570-6576.

[71] S. Shao, M. Pipattanasomporn, and S. Rahman, "Demand Response as a Load Shaping Tool in an Intelligent Grid With Electric Vehicles," *IEEE Transactions on Smart Grid,* vol. 2, no. 4, pp. 624-631, 2011.

[72] T. Jiang, Y. Cao, L. Yu, and Z. Wang, "Load Shaping Strategy Based on Energy Storage and Dynamic Pricing in Smart Grid," *IEEE Transactions on Smart Grid,* vol. 5, no. 6, pp. 2868-2876, 2014.

[73] S. Kakran, S. Chanana, and N. I. o. T. K. Department of Electrical Engineering, "Energy Scheduling of Residential Appliances by a Pigeon-Inspired Algorithm under a Load Shaping Demand Response Program," *International Journal on Electrical Engineering and Informatics,* vol. 11, no. 1, pp. 18-34, 2019.

[74] Y. Liu, R. Fan, and V. Terzija, "Power system restoration: a literature review from 2006 to 2016," *Journal of Modern Power Systems and Clean Energy,* vol. 4, no. 3, pp. 332-341, 2016.

[75] J. V. Jonnalagedda, "Integration of Singer-Link Emulator with enhanced digital power system simulator for system blackstart," Dissertation/Thesis, ProQuest Dissertations Publishing, 1997.

[76] M. H. Albadi and E. F. El-Saadany, "A summary of demand response in electricity markets," *Electric Power Systems Research,* vol. 78, no. 11, pp. 1989-1996, 2008.

[77] The Brattle Group, "Quantifying Demand Response Benefits In PJM," Jan. 2007. [Online] Available: http://brattle.com/system/publications/pdfs/000/004/917/original/Quantifying_Demand_Response_Benefits_in_PJM_Jan_29_2007.pdf?1379343092.

[78] A. Whitfield, A. Kemp, and B. Quach, "Cost Benefit Analysis of Smart Metering and Direct Load Control Overview," NERA Economic Consulting report for Ministerial Council on Energy. 2008, Available: https://apo.org.au/node/2985

[79] V. Fusco, G. K. Venayagamoorthy, S. Squartini, and F. Piazza, "Smart AMI based demand-response management in a micro-grid environment," pp. 1-8: IEEE.

[80] A. Rieger, R. Thummert, G. Fridgen, M. Kahlen, and W. Ketter, "Estimating the benefits of cooperation in a residential microgrid: A data-driven approach," *Applied Energy,* vol. 180, no. Supplement C, pp. 130-141, 2016/10/15/ 2016.

[81] H. Ardeshiri, S. M. Barakati, and K. Ranjbar, "Using improved time of use demand response in optimal operation of microgrid," pp. 117-122: IEEE.

[82] P. Bradley, M. Leach, and J. Torriti, "A Review of Current and Future and Benefits of Demand Response for Electricity," Nov. 2011. [Online] Available: https://www.surrey.ac.uk/ces/files/pdf/1011_WP_Bradley_et_al_DemandResponse_3.pdf, Accessed on: 9 August 2019.

[83] G. Strbac, "Demand side management: Benefits and challenges," *Energy Policy,* vol. 36, no. 12, pp. 4419-4426, 2008.

[84] G. G. M. A Piette, S. Kiliccote, D. Watson, E. Koch, and D. Hennage, "Design and operation of an open, interoperable, automated demand response infrastructure for commercial buildings," LBNL-2340E, JCISE, Vol. 9, Issue 2, June 2009.

[85] L. Park, Y. Jang, H. Bae, J. Lee, C. Y. Park, and S. Cho, "Automated energy scheduling algorithms for residential demand response systems," *Energies,* vol. 10, no. 9, p. 1326, 2017.

[86] K. Vanthournout, B. Dupont, W. Foubert, C. Stuckens, and S. Claessens, "An automated residential demand response pilot experiment, based on day-ahead dynamic pricing," *Applied Energy,* vol. 155, pp. 195-203, 2015.

[87] M. A. Piette, O. Schetrit, S. Kiliccote, I. Cheung, and B. Z. Li, "Costs to Automate Demand Response-Taxonomy and Results from Field Studies and Programs," Lawrence Berkeley National Laboratory. California Energy Commision.2015. [Online] Available: https://gig.lbl.gov/sites/all/files/drrc_final_report_taxonomy.lbnl-1003924.pdf.

[88] M. Kuzlu, M. Pipattanasomporn, and S. Rahman, "Communication network requirements for major smart grid applications in HAN, NAN and WAN," *Computer Networks,* vol. 67, pp. 74-88, 2014.

[89] L. Kreuder, A. Gruber, and S. v. Roon, "Quantifying the costs of Demand Response for industrial businesses," in *IECON 2013 - 39th Annual Conference of the IEEE Industrial Electronics Society*, 2013, pp. 8046-8051.

[90] W. Shi, N. Li, C. C. Chu, and R. Gadh, "Real-Time Energy Management in Microgrids," *IEEE Transactions on Smart Grid,* vol. 8, no. 1, pp. 228-238, 2017.

[91] G. Brusco *et al.*, "A Smartbox as a low-cost home automation solution for prosumers with a battery storage system in a demand response program," pp. 1-6: IEEE.

[92] M. F. Zia, E. Elbouchikhi, and M. Benbouzid, "Optimal operational planning of scalable DC microgrid with demand response, islanding, and battery degradation cost considerations," *Applied Energy,* vol. 237, pp. 695-707, 2019.

[93] *How HOMER Calculates the PV Array Power Output*. Available: https://www.homerenergy.com/support/docs/3.10/how_homer_calculates_the_pv_array_power_output.html

[94] Canadian Solar, "Quartech CS6P-260 | 265P," Datasheet ed, 2015. [Online] Available: https://www.canadiansolar.com/downloads/datasheets/na/canadian_solar-datasheet-cs6pp_quartech-v5.3_na.pdf.

[95] Bank Sentral Republik Indonesia. *Data BI Rate*. Available: [Online] Available: https://www.bi.go.id/id/moneter/bi-rate/data/Default.aspx

[96] R. Fu, D. Feldman, R. Margolis, M. Woodhouse, and K. Ardani, "U.S. Solar Photovoltaic System Cost Benchmark: Q1 2017," National Renewable Energy Laboratory, Technical Report NREL/TP-6A20-68925, Aug. 2017. [Online] Available: https://www.nrel.gov/docs/fy17osti/68925.pdf.

[97] *Penetapan tarif Tenaga Listrik (Tariff Adjustment) Bulan April - Juni 2018*, 2018. [Online] Available: http://www.pln.co.id/statics/uploads/2018/05/Tariff-Adjustment-April-Juni-2018-1.jpg.

[98] Indonesian Ministry of Energy and Mineral Resources. Regulation No.50/2017 Regarding The Utilization of Renewable Energy for Electricity Production [Online]. Available: http://jdih.esdm.go.id/peraturan/PerMen%20ESDM%20NO.%2050%20TAHUN%202017.pdf

[99] Indonesian Ministry of Energy and Mineral Resources. Regulation No.27/2017 Regarding The Quality of Service and Costs Associated with The Electricity Distribution by PT Perusahaan Listrik Negara (Persero). [Online]. Available: http://jdih.esdm.go.id/peraturan/Permen%20ESDM%20No.%2027%20Thn%202017%20ttg%20Standar%20Mutu.pdf

[100] G. B. C. W. Y. Morris. On the Benefits and Costs of Microgrids [Online]. Available: http://digitool.library.mcgill.ca/webclient/StreamGate?folder_id=0&dvs=1527486755099~593

[101] Appendix Decision of The Director General of Electricity Regarding PT. PLN Quality of Service Standard 2017 of West Java Regional [Online]. Available: http://www.djk.esdm.go.id/pdf/Mutu%20Pelayanan%20PLN/2017/Regional%20Jawa%20Bagian%20Barat.pdf

[102] M. Martha. (April 2019. [Online] Available: http://www.thejakartapost.com/news/2014/04/29/carbon-tax-indonesia-time-act-now.html). *Carbon tax for Indonesia: Time to act now*.

[103] Directorat General of Electricity of Indonesian Ministry of Energy and Mineral Resources. GHG Emission Factor Electrical Power Interconnection System [Online]. Available: http://www.djk.esdm.go.id/pdf/Faktor%20Emisi%20Gas%20Rumah%20Kaca/Faktor%20Emisi%20GRK%20Tahun%202016.pdf

[104] Bank Sentral Republik Indonesia. *Data Inflasi*. Available: https://www.bi.go.id/id/moneter/inflasi/data/Default.aspx

[105] O. M. Longe, K. Ouahada, S. Rimer, A. N. Harutyunyan, and H. C. Ferreira, "Distributed demand side management with battery storage for smart home energy scheduling," *Sustainability (Switzerland),* vol. 9, no. 1, p. 120, 2017.

[106] M. T. Arif, A. M. T. Oo, A. S. Ali, and G. Shafiullah, "Impacts of storage and solar photovoltaic on the distribution network," pp. 1-6: IEEE.

[107] L. E. Luna-Ramírez, H. Torres-Sánchez, and F. A. Pavas-Martínez, "Spinning reserve analysis in a microgrid," *DYNA,* vol. 82, no. 192, pp. 85-93, 2015.

[108] F. Shahnia, "Stability and eigenanalysis of a sustainable remote area microgrid with a transforming structure," *Sustainable Energy, Grids and Networks,* vol. 8, pp. 37-50, 2016.

[109] K. Eger *et al.*, "Microgrid functional architecture description," Siemens AG, Grenoble INP, Iberdrola S.A., Orange Labs, Synelixis Thales on FINSENY projectMarch 2013. [Online]

Available: http://www.fi-ppp-finseny.eu/wp-content/uploads/2013/04/FINSENY_D3-3_Microgrid_Functional_Architecture_v1_0_March_2013.pdf.

[110] Minister of Energy and Mineral Resources of Replubilic Indonesia, "The Regulation of Minister of Energy and Mineral Resources No. 3 Year 2007 regarding Jawa – Bali Grid Code," 2007. [Online] Available: https://www.minerba.esdm.go.id/library/sijh/permen-esdm-03-2007.pdf.

[111] SMA, "Sunny Tripower 5000TL – 12000TL," Datasheet ed, 2017. [Online] Available: http://files.sma.de/dl/17781/stp12000tl-den1723-v10web.pdf.

[112] M. Balamurugan, S. K. Sahoo, and S. Sukchai, "Application of soft computing methods for grid connected PV system: A technological and status review," *Renewable and Sustainable Energy Reviews,* vol. 75, pp. 1493-1508, 2017/08/01/ 2017.

[113] SMA. Sunny Tripower Core1-US Grid Support Utility Interactive Inverters [Online]. Available: http://files.sma.de/dl/29422/stp50-us-40-gridservices-ti-en-10.pdf

[114] SMA. PV Grid Integration [Online]. Available: http://files.sma.de/dl/10040/pv-netzint-aen123016w.pdf

[115] North American Electric Reliability Corporation, "2011 Demand response Availability Report," March 2013. [Online] Available: http://www.nerc.com/docs/pc/dadswg/2011%20DADS%20Report.pdf.

[116] M. Ali, J. Jokisalo, K. Siren, A. Safdarian, and M. Lehtonen, "A User-centric Demand Response Framework for Residential Heating, Ventilation, and Air-conditioning Load Management," *Electric Power Components and Systems,* vol. 44, no. 1, pp. 99-109, 2016.

[117] S. A. Pourmousavi, S. N. Patrick, and M. H. Nehrir, "Real-Time Demand Response Through Aggregate Electric Water Heaters for Load Shifting and Balancing Wind Generation," *IEEE Transactions on Smart Grid,* vol. 5, no. 2, pp. 769-778, 2014.

[118] F. Zhang, R. de Dear, and C. Candido, "Thermal comfort during temperature cycles induced by direct load control strategies of peak electricity demand management," *Building and Environment,* vol. 103, pp. 9-20, 2016.

[119] F. Shahnia, M. T. Wishart, and A. Ghosh, "On-line demand management of low voltage residential distribution networks in smart grids," vol. 540, pp. 293-328.

[120] F. Shahnia, M. T. Wishart, and A. Ghosh, "Voltage regulation, power balancing and battery storage discharge control by smart demand side management and multi-objective decision making."

[121] F. Shahnia, M. T. Wishart, A. Ghosh, G. Ledwich, and F. Zare, "Smart demand side management of low-voltage distribution networks using multi-objective decision making," *IET GENERATION TRANSMISSION & DISTRIBUTION,* vol. 6, no. 10, pp. 986-1000, 2012.

[122] M. T. Wishart, F. Shahnia, A. Ghosh, and G. Ledwich, "Multi objective decision making method for demand side management of LV residential distribution networks with plug-in electric vehicles," pp. 1-8: IEEE.

[123] M. Kuzlu, "Score-based intelligent home energy management (HEM) algorithm for demand response applications and impact of HEM operation on customer comfort," *IET Generation, Transmission & Distribution,* vol. 9, no. 7, pp. 627-635, 2015.

[124] A. C. Roussac, J. Steinfeld, and R. de Dear, "A preliminary evaluation of two strategies for raising indoor air temperature setpoints in office buildings," *Architectural Science Review,* vol. 54, no. 2, pp. 148-156, 2011.

[125] A. Surendran and P. Samuel, "Evolution or revolution: the critical need in genetic algorithm based testing," *Artificial Intelligence Review,* vol. 48, no. 3, pp. 349-395, 2017.

[126] A. Alajmi and J. Wright, "Selecting the most efficient genetic algorithm sets in solving unconstrained building optimization problem," *International Journal of Sustainable Built Environment,* vol. 3, no. 1, pp. 18-26, 2014.

[127] M. Vannucci and V. Colla, "Fuzzy adaptation of crossover and mutation rates in genetic algorithms based on population performance," *Journal of Intelligent and Fuzzy Systems,* vol. 28, no. 4, pp. 1805-1818, 2015.

[128] A. Konak, D. W. Coit, and A. E. Smith, "Multi-objective optimization using genetic algorithms: A tutorial," *Reliability Engineering & System Safety,* vol. 91, no. 9, pp. 992-1007, 2006/09/01/ 2006.

[129] J. P. Rivera-Barrera, N. Muñoz-Galeano, and H. O. Sarmiento-Maldonado, "Soc estimation for lithium-ion batteries: Review and future challenges," *Electronics (Switzerland),* vol. 6, no. 4, p. 102, 2017.

[130] "IEEE Recommended Practice for Voltage Sag and Short Interruption Ride-Through Testing for End-Use Electrical Equipment Rated Less than 1000 V," *IEEE Std 1668-2017 (Revision of IEEE Std 1668-2014),* pp. 1-85, 2017.

[131] S. Hardi and I. Daut, "Sensitivity of low voltage consumer equipment to voltage sags," pp. 396-401: IEEE.

[132] A. Honrubia-Escribano, E. Gómez-Lázaro, A. Molina-García, and J. A. Fuentes, "Influence of voltage dips on industrial equipment: Analysis and assessment," *International Journal of Electrical Power and Energy Systems,* vol. 41, no. 1, pp. 87-95, 2012.

[133] S. Ouyang, P. Liu, L. Liu, and X. Li, "Test and analysis on sensitivity of low-voltage releases to voltage sags," *IET Generation, Transmission & Distribution,* vol. 9, no. 16, pp. 2664-2671, 2015.

[134] F. Capitanescu, "Critical review of recent advances and further developments needed in AC optimal power flow," *Electric Power Systems Research,* vol. 136, pp. 57-68, 2016/07/01/ 2016.

[135] B. Hayes, I. Hernando-Gil, A. Collin, G. Harrison, and S. a. Djokić, "Optimal Power Flow for Maximizing Network Benefits From Demand-Side Management," *IEEE Transactions on Power Systems,* vol. 29, no. 4, pp. 1739-1747, 2014.

[136] H. Abdi, S. D. Beigvand, and M. L. Scala, "A review of optimal power flow studies applied to smart grids and microgrids," *Renewable and Sustainable Energy Reviews,* vol. 71, pp. 742-766, 2017/05/01/ 2017.

[137] J. A. Momoh, M. E. El-Hawary, and R. Adapa, "A review of selected optimal power flow literature to 1993. II. Newton, linear programming and interior point methods," *IEEE Transactions on Power Systems,* vol. 14, no. 1, pp. 105-111, 1999.

[138] H. Saadat, *Power system analysis*, 2nd ed. (no. Book, Whole). Sydney;Boston;: McGraw-Hill Primis Custom, 2002.

[139] B. M. Weedy, *Electric power systems*, 5th;5. Aufl.; ed. (no. Book, Whole). Chichester, West Sussex, UK: Wiley, 2012.

[140] S. Houndedako, A. H. C, G. J. Aredjodoun, and C. Espanet, "Reduction of on-line losses and voltage drops in an electrical grid low voltage," in *2015 International Conference and Workshop on Computing and Communication (IEMCON)*, 2015, pp. 1-5.

[141] D. A. Gagne, D. E. Settle, A. Y. Aznar, and R. Bracho, "Demand Response Compensation Methodologies: Case Studies for Mexico," National Renewable Energy Lab, Golden C. O., United States 2018. [Online] Available: https://doi.org/10.2172/1452706.

[142] Z. Liu, W. Cui, R. Shen, Y. Hu, H. Wu, and C. Ye, "Design of capacity incentive and energy compensation for demand response programs," vol. 121, p. 52059.

[143] Australian Renewable Energy Agency, "Demand Management Incentives Review," June 2017. [Online] Available: https://arena.gov.au/assets/2017/06/20170628-DMIR-Report-Final.pdf.

[144] G. Fridgen, M. Kahlen, W. Ketter, A. Rieger, and M. Thimmel, "One rate does not fit all: An empirical analysis of electricity tariffs for residential microgrids," *Applied Energy,* vol. 210, pp. 800-814, 2018.

[145] T. J. Reber, S. S. Booth, D. S. Cutler, X. Li, J. A. Salasovich, and G. C. O. National Renewable Energy Lab, "Tariff Considerations for Micro-Grids in Sub-Saharan Africa," United States Feb. 2018. [Online] Available: https://www.nrel.gov/docs/fy18osti/69044.pdf.

[146] D. G. Newman, T. G. Eschenbach, and J. P. Lavelle, *Engineering Economic Analysis*, 9 ed. New York: Oxford University Press, 2004.

[147] F. Shahnia, M. Moghbel, A. Arefi, G. M. Shafiullah, M. Anda, and A. Vahidnia, "Levelized cost of energy and cash flow for a hybrid solar-wind-diesel microgrid on Rottnest island," vol. 2017-, pp. 1-6: IEEE.

[148] R. H. Inman, H. T. C. Pedro, and C. F. M. Coimbra, "Solar forecasting methods for renewable energy integration," *Progress in Energy and Combustion Science,* vol. 39, no. 6, pp. 535-576, 2013.

[149] M. Q. Raza, M. Nadarajah, and C. Ekanayake, "On recent advances in PV output power forecast," *Solar Energy,* vol. 136, pp. 125-144, 2016/10/15/ 2016.

[150] G. Fathoni, S. A. Widayat, P. A. Topan, A. Jalil, A. I. Cahyadi, and O. Wahyunggoro, "Comparison of State-of-Charge (SOC) estimation performance based on three popular methods: Coulomb counting, open circuit voltage, and Kalman filter," in *2017 2nd International Conference on Automation, Cognitive Science, Optics, Micro Electro-Mechanical System, and Information Technology (ICACOMIT)* Jakarta, 2017, pp. 70-74: IEEE.

[151] Reserve Bank Of Australia, "Reserve Bank of Australia Annual Report," Aug. 2018. [Online] Available: https://www.rba.gov.au/publications/annual-reports/rba/2018/pdf/2018-report.pdf.

[152] M. Terrill and H. Batrouney, "Unfreezing discount rates Transport infrastructure for tomorrow," GRATTAN Institute, Australia. Feb. 2018. [Online] Available: https://grattan.edu.au/wp-content/uploads/2018/02/900-unfreezing-discount-rates.pdf.

[153] Synergy, "Standard Electricity Prices and Charges," ed, 2018. [Online] Available: https://www.synergy.net.au/-/.../Standard_Electricity_Prices_Charges_brochure.PDF.

[154] S. Gabel, "Automated Demand Response for Energy Sustainability Cost and Performance Report," Sep. 2015. [Online] Available: https://apps.dtic.mil/dtic/tr/fulltext/u2/1000199.pdf.

[155] U.S. Energy Information Administration, "Annual Energy Outlook 2019," Jan. 2019. [Online] Available: https://www.eia.gov/outlooks/aeo/pdf/aeo2019.pdf.